# Poly(vinyl alcohol) for Biomedical Applications

Dissertation

zur Erlangung des akademischen Grades
Doktor-Ingenieur (Dr. -Ing.)

vorgelegt dem

Zentrum für Ingenieurwissenschaften
der Martin-Luther-Universität Halle-Wittenberg
als organisatorische Grundeinheit für Forschung und Lehre im Range einer Fakultät
(§75 Abs. 1 HAG LSA, §19 Abs. 1 Grundordnung)

von Frau Yanjiao Jiang

geb. am 05.12.1978 in Nei Mongol, China

Gutachter:

1. Prof. Dr. J. Kressler
2. Prof. Dr. K. F. Arndt

Halle (Saale), den 16. April 2009

**Dedicated to My Loving Parents**

# Acknowledgement

First of all, I would like to express my sincere thanks to my advisor Prof. Dr. Jörg Kressler for offering me the opportunity to do research in this friendly group, for his valuable suggestions, discussions and continued encouragement during this period.

I would like to acknowledge the company - Aesculap AG & CO.KG for offering this very interesting research theme and financial support of this work. I would sincerely appreciate Dr. Erich K. Odermatt (Aesculap AG & CO.KG, Tuttlingen) and Dr. Christine Weis (Aesculap AG & CO.KG, Tuttlingen) for their valuable suggestions and friendly cooperation.

I would also like to thank Dr. Frank Heyroth, Dr. Klaus Schröter, Dr. Wolfgang Schmitt, Ms. Isolde Trümper and Ms. Ingrid Otten for their help and cooperation during the course of my work in their laboratories.

I am grateful to all colleagues for their cooperation and help, special thanks to Dr. Karsten Busse, Dr. Henning Kausche, Dr. Zofia Funke, Samuel Kyerematen, and Hangsheng Li for sharing their knowledge related to my research work.

Finally, I would like to appreciate all my loving family members and kind friends for their encouragement and supports throughout my studies in Germany.

**Yanjiao Jiang**

**Publications:**

Jiang Y., Kressler J., Weis C., Odermatt E. K., **Poly(vinyl alcohol) based materials for postoperative adhesion prevention in surgery.** Polymer Preprints (American Chemical Society, Division of Polymer Chemistry) (2008), 49, (2), 463-464.

Jiang Y., Schädlich A., Kressler J., Weis C., Odermatt E. K., ***In vivo*** **studies on intraperitoneally administered poly(vinyl alcohol).** J Biomed. Mat. Res., Part B: Appl. Biom., in preparation.

**Patent application:**

Jiang Y., Kressler J., Weis C., Odermatt E. K., **PVA Hydrogel with Nucleation agents**, Aesculap AG & CO.KG

**Contents**

**1 Introduction** 1

1.1 Poly(vinyl alcohol) ... 1
1.2 Poly(vinyl alcohol) cryogel ... 2
1.3 Applications of poly(vinyl alcohol) in biomedical engineering ... 3

**2 Study of aging behavior in poly(vinyl alcohol) aqueous solution** 5

2.1 Introduction ... 5
2.2 Experimental section ... 6
2.2.1 Materials ... 6
2.2.2 Experimental methods ... 6
2.3 Results and discussion ... 8
2.3.1 The aging process of poly(vinyl alcohol) aqueous solution ... 8
2.3.1.1 Aged poly(vinyl alcohol) aqueous solutions ... 9
2.3.1.2 Diluted aged poly(vinyl alcohol) aqueous solutions ... 11
2.3.1.3 Thermal stability of aged poly(vinyl alcohol) aqueous solutions ... 15
2.3.2 Rheological characterization of aged poly(vinyl alcohol) aqueous solutions ... 16
2.3.3 Water crystallization in aged poly(vinyl alcohol) aqueous solutions ... 19
2.4 Conclusion ... 22

**3 Poly(vinyl alcohol) cryogel – a potential postoperative anti-adhesion agent** 23

3.1 Introduction ... 23
3.1.1 General introduction ... 23
3.1.2 PVA cryogel near gel point ... 24
3.1.3 Supercooling and ice nucleation agents ... 26
3.1.3.1 Thermodynamic theory of heterogeneous nucleation ... 27
3.1.3.2 Ice nucleation agents ... 29
3.2 Experimental section ... 30
3.2.1 Materials ... 30

3.2.2 Preparation of poly(vinyl alcohol) cryogel by using different freezing temperatures and freezing times ... 30
3.3 Experimental methods ... 31
3.3.1 $^{1}$H pulse NMR spectroscopy ... 31
3.3.2 Rheological measurements ... 31
3.3.3 Differential scanning calorimetry measurements ... 33
3.3.4 Scanning electron microscope ... 34
3.4 Results and discussion ... 34
3.4.1 PVA cryogel produced by repeated freeze/thawing ... 34
3.4.2 Effective ice nucleation agents applied for production of PVA cryogel ... 39
3.4.2.1 Water crystallization temperature of PVA aqueous solutions ... 39
3.4.2.2 Water crystallization ability of ice nucleation agents in PVA aqueous solution ... 40
3.4.2.3 Critical concentration of L-aspartic acid as ice nucleation agent ... 42
3.4.3 PVA cryogel near gel point ... 42
3.4.3.1 PVA cryogel produced in dry ice/ethanol bath ... 43
3.4.3.2 PVA cryogel produced by adding ice nucleation agent ... 46
3.5 Conclusion ... 52

**4 Preparation of micro-size and nano-size poly(vinyl alcohol) particulate powder using the emulsion-diffusion method** 55

4.1 Introduction ... 55
4.1.1 General introduction ... 55
4.1.2 The formation of PVA particulate powder by emulsion-diffusion method ... 56
4.2 Experimental section ... 57
4.2.1 Materials ... 57
4.2.2 Preparation of PVA particulate powder ... 57
4.2.3 Experimental techniques ... 58
4.3 Results and discussion ... 60
4.3.1 Selection of an efficient surfactant for PVA/MCT oil emulsions ... 60
4.3.2 Morphology and size distribution of PVA powder ... 63
4.3.2.1 Surface morphology of PVA particles ... 63
4.3.2.2 Size distribution of PVA particles ... 63
4.3.2.3 Investigation of PVA powder in water ... 68

4.4 Conclusion ..... 70

**5 *In vivo* studies on intraperitoneally administered poly(vinyl alcohol)** 71

5.1 Introduction ..... 71
5.2 Experimental section ..... 73
5.2.1 Materials ..... 73
5.2.2 Dialysis and precipitation of urinary excreted polymer ..... 74
5.2.3 Experimental methods ..... 75
5.2.3.1 Gel Permeation Chromatography (GPC) ..... 75
5.2.3.2 $^{1}$H-NMR spectroscopy ..... 75
5.2.3.3 Thermal gravimetric analysis and FT-IR spectroscopy ..... 75
5.2.3.4 Histological test ..... 75
5.3 Results and discussion ..... 77
5.3.1 Characterization of dialyzed-precipitated polymer ..... 77
5.3.2 Histological tests ..... 85
5.4 Conclusion ..... 92

**6 Summary** 93

**7 Zusammenfassung** 97

**Literature** 102

**Resume** 114

## Abbreviations and symbols

| | |
|---|---|
| AgI | Silver iodine |
| Cont. | Concentration |
| $C_{agg}$ | Minimum aggregation concentration |
| $C_{gel}$ | Critical concentration of sol-gel transition |
| D | Diffusion coefficient |
| DLS | Dynamic light scattering |
| DMSO | Dimethylsulfoxid |
| DSC | Differential scanning calorimetry |
| DTG | Differential thermogravimetry |
| ESEM | Environmental scanning electron microscopy |
| $f$ | Frequency |
| FT-IR | Fourier transform infrared |
| G | Germ |
| G´ | Storage modulus |
| G´´ | Loss modulus |
| G* | Complex modulus |
| $\Delta G^*$ | Critical free energy to nucleation |
| $\Delta G^*_{homo}$ | Homogeneous nucleation energy barrier |
| GPC | Gel permeation chromatography |
| H&E | Hematoxylin and eosin |
| HLB | Hydrophile-lipophile balance |
| i.p | Intraperitoneal |
| i.m | Intramuscular |
| k | Boltzmann constant |
| L | Length of bob |
| L | Liquid phase |
| MCT | Medium-chain triglyceride |
| MWCO | Molecular weight cut off |
| NMR | Nuclear magnetic resonance |
| PVA | Poly(vinyl alcohol) |
| PVA-195k | Poly(vinyl alcohol) $M_w$ 195,000 g/mol |
| PVA- 26k | Poly(vinyl alcohol) $M_w$ 26,000 g/mol |

| | |
|---|---|
| PVAc | Poly(vinyl acetate) |
| PTFE | Polytetrafluorethylen |
| $r_c$ | Critical radius |
| $R_h$ | Hydrodynamic radius |
| $R_i$ | Radius of bob |
| $R_o$ | Radius of cup |
| S | Substrate |
| SANS | Small angle neutron scattering |
| s.c | Subcutaneous |
| SEM | Scanning electron microscopy |
| Tan δ | Loss tangent |
| $T_2$ | Spin–spin relaxation time |
| TGA | Thermal gravimetric analysis |
| $\sigma_0$ | Stress amplitude, |
| $\gamma_0$ | Strain amplitude, |
| δ | Phase lag |
| η* | Complex viscosity |
| α | Opening angle |
| η | Viscosity |
| γ; | Shear rate |
| σ | Shear stress |
| $\omega_o$ | Motor angular velocity |
| τ | Applied stress |
| θ | Contact angle |
| $\gamma_{SL}$ | Substrate /liquid interfacial energy |
| $\gamma_{SG}$ | Substrate /germ interfacial energy |
| $\gamma_{GL}$ | Germ/liquid interfacial energy |

# Chapter 1

# 1 Introduction

## *1.1 Poly(vinyl alcohol)*

Poly(vinyl alcohol) (PVA), a polyhydroxy polymer, is one of the largest, water-soluble synthetic polymer based on volume. The first discovery of PVA dates back to 1924, PVA solution was obtained by saponifying poly(vinyl ester) with caustic soda solution.[1-3] Since monomeric vinyl alcohol cannot be achieved in quantities and purity, PVA can be produced by converting poly(vinyl acetate) (PVAc) to PVA by transesterification, hydrolysis, or aminolysis.[4] The transesterification is commonly used in industry, where PVAc is hydrolyzed by treating an alcoholic solution of PVAc with aqueous acid or alkali. Figure 1.1 gives the main chemical reactions of PVA production: polymerization of vinyl acetate to PVAc and hydrolysis of PVAc to PVA.

.

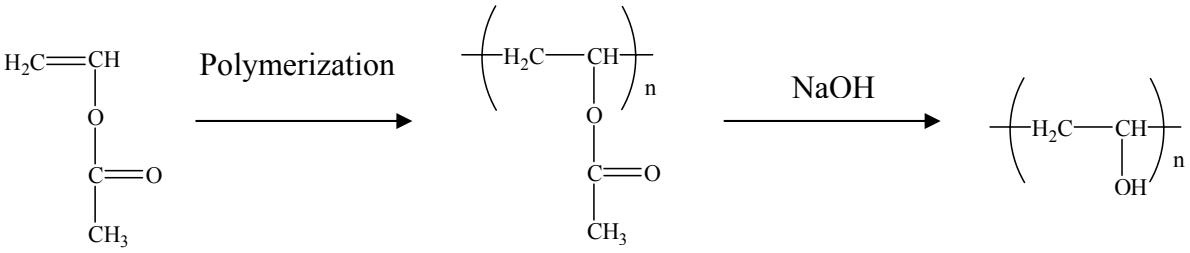


Figure 1.1: Chemical reactions for the preparation of poly(vinyl alcohol) - polymerization of vinyl acetate and hydrolysis of poly(vinyl acetate) to poly(vinyl alcohol)

**Physical properties of poly(vinyl alcohol)**

The basic properties of PVA depend on its degree of polymerization, degree of hydrolysis, and distribution of the degree of hydrolysis.[5] In terms of degree of hydrolysis, the principal grades of PVA produced can be classified as fully hydrolyzed (97.5-99.5 percent degree of hydrolysis) and partially hydrolyzed which can be considered as the mixture of polymer of vinyl alcohol and vinyl acetate. PVA is used mainly in aqueous solutions. The degree of hydrolysis has the most significant effect on the solubility. The more hydroxyl groups cause strong hydrogen bonding between the intra- and intermolecular hydroxyl groups, greatly decreasing its solubility in water. The amount of crystallization depends on the degree of hydrolysis, which can induce a decrease in solubility.[6] Aqueous solutions of PVA with a high

degree of hydrolysis increase in viscosity with time and concentration, and may finally gel. The higher the concentration and the higher the degree of polymerization the lower is the viscosity stability of aqueous solutions.[7, 8] PVA has a melting point of 230 °C and 180–190 °C for the fully hydrolyzed and partially hydrolyzed grades, respectively. The thermal degradation of PVA usually starts at about 150 °C or above, depending upon the PVA grade.

**Chemical reactions of poly(vinyl alcohol)**

Poly(vinyl alcohol) reacts in a manner similar to other secondary alcohols.[9] Acetalization, esterification and etherification reactions of poly(vinyl alcohol) can be carried out with a number of compounds.[10] PVA is crosslinkable through their secondary hydroxyl functionality. Cross-linked PVAs are very important commercially products which can be formed by reaction with aldehydes (e.g. formaldehyde, glyoxal or glutaraldehyde),[11, 12] dicarboxylic acids (e.g. citric acid)[13] and inorganic compounds (e.g. boric acid),[14] or by radiation and photo-cross-linking reaction,[15] or by physical cross-linking using cyclic freezing and thawing of aqueous PVA solutions.[16, 17]

PVA has outstanding resistance to oil, grease, and solvents, plus high tensile strength, flexibility, high oxygen barrier and biodegradability by microorganisms in the environment.[18] The main use of PVA is in textile wrap sizing, adhesive, paper sizing agent, ceramic binder, fiber, emulsion polymerization and also extensively in cosmetics, pharmacy and electronic industry. As an important industrial and commercial product, PVA is valued for its solubility and environmental biodegradability. Several microorganisms have been identified which are able to degrade PVA through enzymatic processes to contribute to very low environmental pollutions.

## *1.2 Poly(vinyl alcohol) cryogel*

The physical cross-linked PVA gel is obtained by cryogenic treatments of aqueous poly(vinyl alcohol) (PVA) solutions which has been well-known since the 1970s.[19-21] The cryogenic treatment basically consists of freezing an initially homogeneous polymer solution at low temperatures, storing it in the frozen state for a definite time, followed by thawing. The gel obtained through such cryogenic treatment is named as ‘cryogel’ (from the Greek *κριοσ* (kryos) meaning frost or ice).[22] This cryogenic method results in a physically cross-linked PVA cryogel, whose macroporous structure is mainly imprinted by formation of ice crystals within the homogenous aqueous PVA system during the freezing step. Ice crystals expel amorphous polymer segments that finally separate the initial PVA aqueous solution into

polymer-rich parts and polymer-poor parts of a porous polymer network. Polymer chain-folded microcrystallites are formed in polymer-rich phases as network junctions in physical PVA cryogels.[23-25] Figure 1.2 gives the schematic representation of PVA cryogel formation by freeze/thawing.

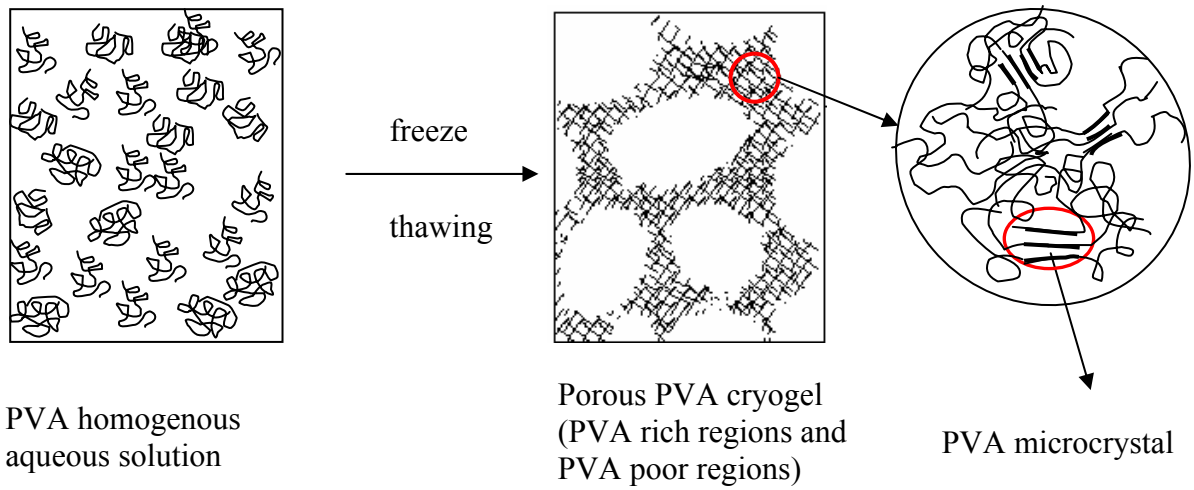


Figure 1.2: Model PVA hydrogels obtained by freeze-thawing cycles with a PVA-rich phase and a PVA-poor phase.

PVA cryogel is thermoreversible and stable up to temperatures of 70-90 °C.[26] Properties of PVA cryogel are dependent on molecular weight of the polymer, temperature and duration of freezing, rate of thawing, and the number of refreezing cycles.[27, 28] The freeze/thawing method for PVA cryogel preparation offers several advantages with respect to chemical or radiation-induced cross-linking: it is simply controlled, does not require any additional chemicals, and does not need high temperatures. The good biocompatibility of PVA cryogel attracts interest in biotechnology (carriers of immobilized enzymes, antibodies, whole cells),[29, 30] in medicine (drug delivery systems, artificial cartilage tissue, materials for ophthalmology, etc.),[31, 32] and in materials science (gel basis of chemomechanical actuators).[33]

## *1.3 Applications of poly(vinyl alcohol) in biomedical engineering*

Poly(vinyl alcohol) is a hydrophilic polymer with a simple chemical structure, high hydroxyl group contents provide PVA and PVA-based materials many desired properties (biocompatible, nontoxic, non-carcinogenic, non-immunogenic and inert in body fluids) suitable for biomedical applications.[34-37] As a promising biomaterial, several studies have focused on the application of PVA in biomedical and pharmaceutical fields.[38-41] Because of

its high water content, high oxygen permeability, high optical clarity, and low protein adsorption, PVA hydrogel finds new applications in the manufacturing of soft contact lenses.[42, 43, 44] High mechanical strength, rubber-like elasticity and no adhesion to surrounding tissue make PVA gels potential materials for soft tissue replacements,[45] artificial cartilage,[46] intervertabrate disc nuclei,[47] and other artificial organs.[48, 49] PVA gels with unique semi-crystalline structure exhibit controlled dissolution behavior of durgs.[50] Based on this property, PVA as drug-delivery system was studied extensively for pharmaceutical applications.[51-54] Mucoadhesive and non-immunogenic characteristics of PVA gels were investigated for accelerating wound healing and anti-postoperative adhesion.[55, 56] Sponge-like PVA cryogel contains macropores in size of tens or hundreds to a few micrometers, which makes PVA cryogel a promising material for chromatographic matrices and scaffolds for tissue engineering in immobilizing of molecules and cells.[57, 58]

# Chapter 2

# 2 Study of aging behavior in poly(vinyl alcohol) aqueous solution

## *2.1 Introduction*

Poly(vinyl alcohol) (PVA) is a semi-crystalline polymer having hydroxyl groups which give many unique properties due to the inter- and intra-molecular hydrogen bonding, e.g. physical gelation of PVA.[59, 60] PVA is a highly hydrophilic and water-soluble polymer and the phase diagram of the PVA/water binary system shows an upper critical solution temperature.[61] It is well known that the freshly prepared PVA solution is metastable and concentrated PVA aqueous solutions experience the sol-gel phase transition with increasing aging time - the viscosity of the solution increases progressively with time and finally a gel is formed, which is also called a physical aging process.[62-64] Frisch and Simha reported that the dynamic behavior of polymer solutions can be classified into several regions using the semi-empirical rules according to the interaction degree of the polymer with its environment. According to their classification the effects of change in concentration are usually separated into four different concentration regions, i.e. the infinite dilution limit, the hydrodynamic screening limit, the polymer–polymer contact region and the polymer chain entanglement region.[65] The aging of PVA aqueous solutions has been studied for several decades.[66-68] The process of aging cannot be interpreted simply by entanglement of polymer chains. The formation of supermolecular structures or microgel particles was found to play an important roll in the gelation process of the aging poly(vinyl alcohol) aqueous solution with time.[69-71] These supermolecular structures are regarded as thermostable paracrystalline PVA, which contains an amorphous and a crystalline phase[72] and the tendency to form stable paracrystal structures is affected by the polymer molar mass, hydrolysis degree, concentration, tacticity of polymer and temperature.[73, 74] The paracrystal structure in aged PVA solutions may be attributed to the hydrogen bonds formed by the hydroxyl groups in aggregated polymer chains. Fully hydrolyzed PVA contains high amounts of hydroxyl groups, which provides the good biocompatibility for biomedical applications. The kinetics of the formation process of the supermolecular structures in aged aqueous solutions of fully hydrolyzed PVA with different molar masses is studied in the present work by dynamic light scattering and rheological tests.

The paracrystalline model assumes microcrystalline grains surrounded by fully amorphous material, which has a higher energy state than the continuous random network model. The

important distinction between this model and the microcrystalline phases are the lack of defined grain boundaries and highly strained lattice parameters. These paracrystal structures formed in aged PVA solutions are expected to have the property of ice nucleation agent.[75, 76] The supercooling points of aged PVA aqueous solutions are determined by differential scanning calorimetry (DSC) to investigate if these have the positive effect on ice nucleation during the PVA cryogel formation.

## *2.2 Experimental section*

### 2.2.1 Materials

98 % hydrolyzed poly(vinyl alcohol), Mowiol 4-98 with $M_w$ 26,000 g/mol (PVA-26k) and Mowiol 56-98 with $M_w$ 195,000 g/mol (PVA-195k) manufactured by Kuraray, Japan, were used in this study. 1-5 wt-% PVA solutions were prepared by heating in an oven at 98 °C for 4 h with stirring. The flakes of PVA were swollen to form a transparent gel and then gradually passed into a visually homogenous solution. Prepared PVA solutions were under static condition to age at ~22 °C. The solvent is bi-distilled water, which is purified by filtration by using a 0.02 μm Teflon filter for removing dust before use. The solutions with various polymer concentrations were filtered by using 1.0 μm Millipore filters directly into both a light scattering cell and sealed test tubes, respectively. Aged PVA aqueous solutions were diluted to 1 wt-% prior to DLS measurement by bi-distilled water.

.

### 2.2.2 Experimental methods

The kinetic aggregation of aged aqueous solutions of fully hydrolyzed PVA with different molar masses was investigated under different conditions of thermal treatment. The variation of hydrodynamic radius ($R_h$) and dynamic rheological character of PVA solutions were determined by dynamic light scattering and viscoelastic shear measurement.

Dynamic light scattering (DLS)

DLS measurements were performed with an ALV-5000 goniometer equipped with a Nd/YAG DPSS-200 laser at a wavelength of 532 nm. The intensity time-correlation function $g^2(\tau)$ was recorded with an ALV-5000E multiple-taudigital autocorrellator. Measurements were made at

multi-angles (from 30 - 140°, in intervals of 10°). The correlation functions from dynamic light scattering were analyzed by the CONTIN method. The data measured in a dynamic light scattering (DLS) experiment result in the correlation curve. The correlation curve contains all of the information regarding the diffusion of particles within the sample being measured. The diffusion coefficient D is calculated by fitting the correlation curve to an exponential function, with D being proportional to the lifetime of the exponential decay. The hydrodynamic radius $R_h$ is then calculated from the diffusion coefficient using the Stokes-Einstein equation, $R_h = kT/6\pi\eta D$, where k is the Boltzmann constant, T is the temperature, η is the medium viscosity. The temperature of the bath was set at 25 °C. The signals are observed only in a vertical distribution at all angels, which can be used to determine the average radii of polymer chains.

Original aged PVA aqueous solutions and dilute aged PVA aqueous solutions were used for DLS measurements to characterize the PVA aqueous system. Dilute PVA aqueous solutions were prepared by adding bi-distilled water to 1 wt-% of the polymer prior to DLS measurement. The whole aging process has been studied until 41 days. The aged PVA aqueous systems were measured in intervals of 1 to 5 days.

Rheological measurements

The measurements were performed using the fluid spectrometer RFSII equipped with the Couette geometry by steady rate sweep test at 25 °C. Steady testing uses continuous rotation to provide a constant shear rate. In steady shear testing, the test sample is placed in rotational shear at a given shear rate and the resulting shear stresses were measured by the instrument transducer.

In the Couette (diameter of cup 34 mm and diameter of bob 32 mm) geometry (Fig. 2.1) chosen for this study, the shear rate, $\dot{\gamma}$, is chosen in the range of 0.1 to 100 $s^{-1}$. The rheometer measures the shear stress, σ, using a torque gauge (producing measurement of applied stress, τ). The computer generates viscosity, η, and data using equations 2.1, 2.2, and 2.3.

$$\dot{\gamma} = \frac{2\omega_o R_o^2}{R_o^2 - R_i^2} \tag{2.1}$$

$$\sigma = \frac{\tau}{2\pi L R_i^2} \tag{2.2}$$

$$\eta = \frac{\sigma}{\dot{\gamma}} \tag{2.3}$$

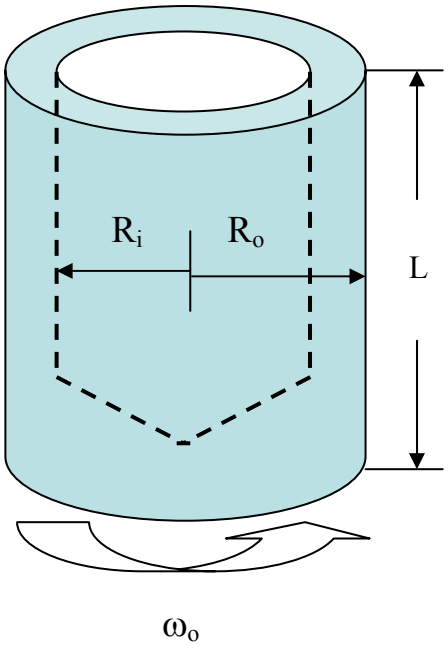


Figure 2.1: Couette geometry for rheometry (L - length of bob, $R_i$ – radius of bob, $R_o$ – radius of cup, $\omega_o$ – motor angular velocity).

Differential scanning calorimetry (DSC)

DSC experiments were carried out with DSC 822e (Mettler Toledo, Greifensee, Switzerland) to evaluate freezing points ($T_f$) of aged PVA solutions. The DSC was calibrated with In and Pb standards. Fresh prepared and aged PVA solutions were filled into pans for DSC measurements. The cooling rate was -1 °C/min to –25 °C.

.

## *2.3 Results and discussion*

### 2.3.1 The aging process of poly(vinyl alcohol) aqueous solution

DLS is an effective tool for probing the dynamic behavior of polymer chains, on different length and time scales, in a wide range of polymer concentrations. The temporal intensity fluctuations caused by the movement of the particles in the suspension are analyzed for the determination of the particle size distribution. The aggregation behavior of PVA aqueous solutions is investigated from dilute to concentrated solutions through DLS analyses. The presence of supermolecular particles (aggregates) is sensitively recorded by the light scattering method.

### 2.3.1.1 Aged poly(vinyl alcohol) aqueous solutions

Two relaxation modes in multi-angle DLS, i.e. fast mode and slow mode were observed in 3, 4, 5 wt-% PVA-195k aqueous solutions and 2, 3, 4, 5 wt-% PVA-26k with different aging time (Fig. 2.3, 2.5). Fast modes were from small particles, which appeared in all PVA aqueous solutions and exhibited no remarkable change with concentration. It represents the hydrodynamic behaviour of single chains of PVA in water system.[77] $R_h$ of a single polymer chain of PVA-195k is 13.5 ± 1.6 nm (Fig. 2.10). $R_h$ of a single polymer chain of PVA-26k is 6.5 ± 1.9 nm (Fig. 2.11). Slow modes were from large particles, which appeared dependent on the molecular weight, concentration and aging time of PVA aqueous solutions. Slow modes denoted as the formation of supermolecular aggregates in aged PVA solutions, which are cohesional entanglements of the polymer chains and formed easier and faster in higher concentration and lower molar mass PVA aqueous solutions, but the formation of supermoleuclar aggregates in PVA-26k system is much smaller than for PVA-195k systems. When the concentrations reached the critical concentration of aggregation, the size of supermolecular formations increased with increasing concentration of PVA. High molar mass PVA exhibited high minimum aggregation concentration (Fig. 2.2, 2.4). The minimum aggregation concentration of high molar mass PVA-195k was between 2 ~ 3 wt-%. The minimum aggregation concentration of low molar mass PVA-26k was between 1 ~ 2 wt-%.

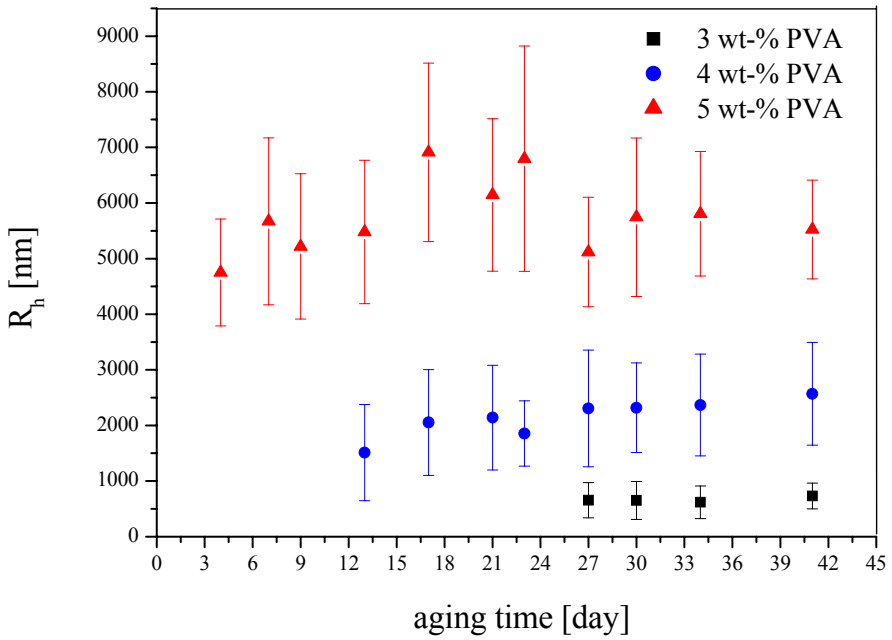


Figure 2.2: $R_h$ as a function of aging time for PVA-195k aqueous solution with different concentrations (slow mode can be detected in 3, 4, 5 wt-% PVA solution by DLS).

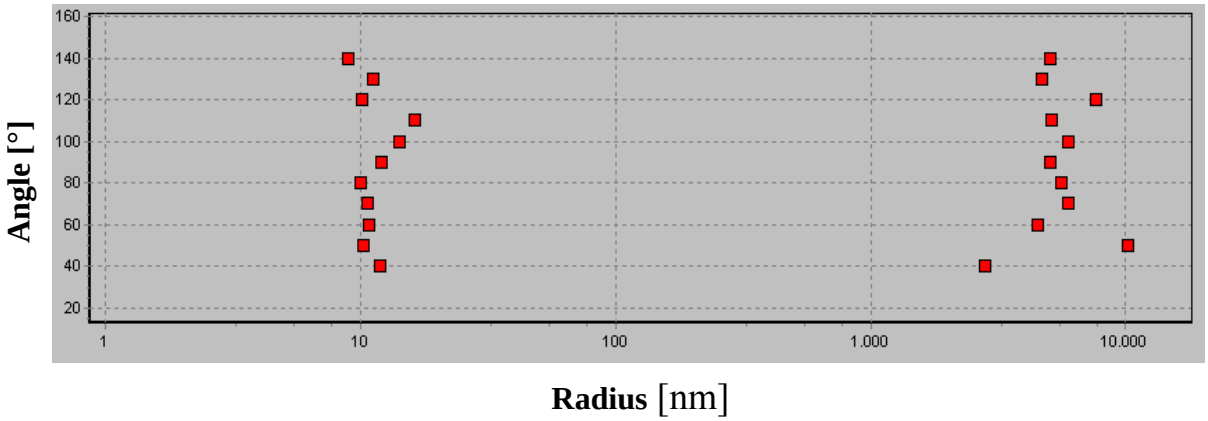


Figure 2.3: $R_h$ distribution of 40 days aged 5 wt-% PVA-195k aqueous solutions (multi-angle DLS 30 -140° using Contin method).

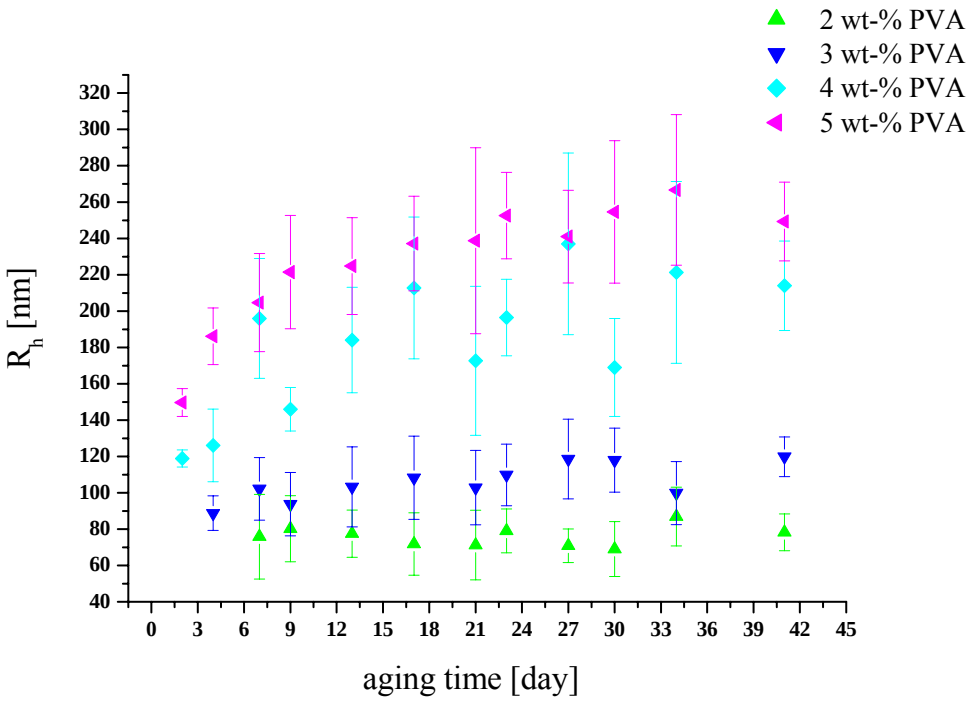


Figure 2.4: $R_h$ as a function of aging time for PVA-26k aqueous solution with different concentrations (slow mode can be detected in 2, 3, 4, 5 wt-% PVA solutions by DLS)

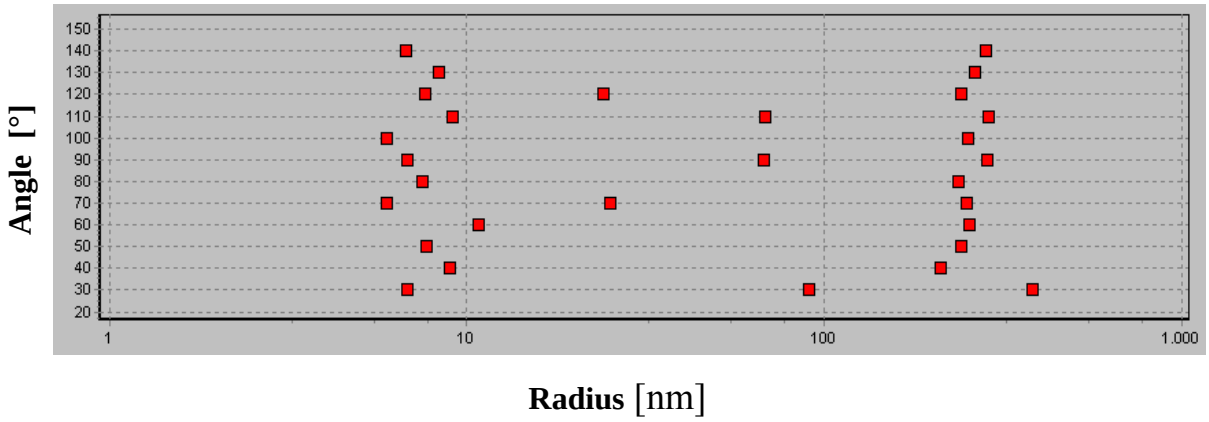


Figure 2.5: $R_h$ distribution of 40 days aged 5 wt-% PVA-26 k aqueous solution (multi-angle DLS 30 -140° using Contin method)

### 2.3.1.2 Diluted aged poly(vinyl alcohol) aqueous solutions

Aged PVA aqueous solutions were diluted to 1 wt-% with bi-distilled water prior to DLS measurements. Two relaxation modes, i.e. fast modes and slow modes were still observed in these diluted PVA systems as in the original aged PVA systems, but the slow modes detected in diluted PVA solutions were different from the slow modes detected in original aged PVA solutions (Fig. 2.2, 2.4, 2.6, and 2.8). The slow modes here exhibited much smaller $R_h$ values than the respective original PVA solutions and several times larger than the size of single PVA chains (Fig. 2.3, 2.5, 2.7, and 2.9). Fast modes had no big difference to the original aged PVA systems (Fig. 2.3, 2.4). The smaller aggregates in diluted PVA systems indicated that the aging process of PVA aqueous systems is not only simple aggregations of polymer chains, but also some more stable clusters formed in the PVA aggregates. The disappearance of the slow mode in the diluted 3 wt-% PVA-195k sample indicated that the formation of the smaller stable clusters was based on the aggregation of polymer chains. These supermolecular aggregates in original PVA systems were assumed as the intermolecular aggregation through entanglements, while they can be destroyed easily by dilution. The stable smaller clusters could be the paracrystal structures formed by ordered intra- and intermolecular hydrogen bonds in aggregates with time. Paracrystal structures exhibited lower threshold concentration of the formation in aged low molar mass PVA solutions. The size of paracrystal structures was dependent on the molar mass of PVA solutions (Fig. 2.6 and 2.8).

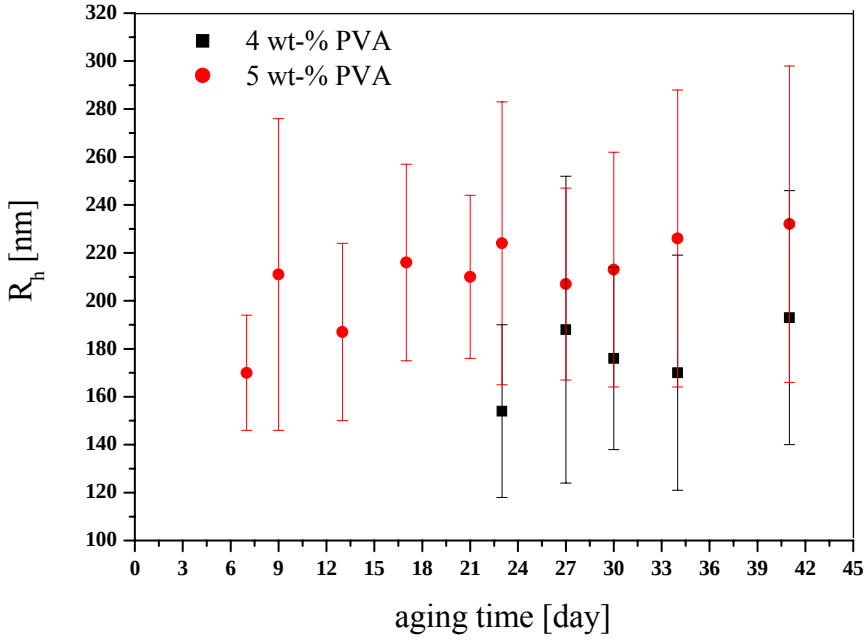


Figure 2.6: $R_h$ as a function of aging time for diluted aged PVA-195k aqueous solution with different concentrations (slow mode can be detected in 4, 5 wt-% PVA solutions by DLS).

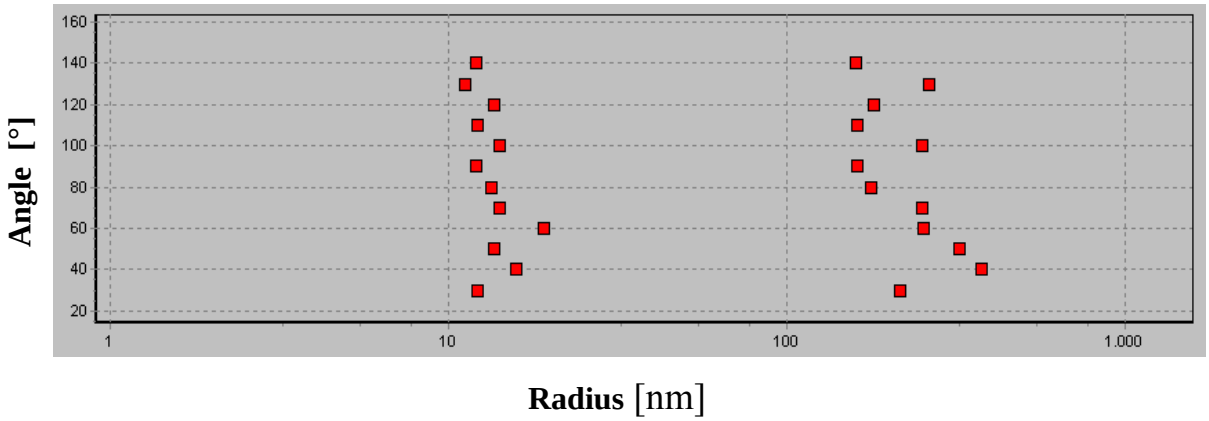


Figure 2.7: $R_h$ distribution of diluted 40 days aged 5 wt-% PVA-195k aqueous solution (multi-angle DLS 30 -140° by Contin method).

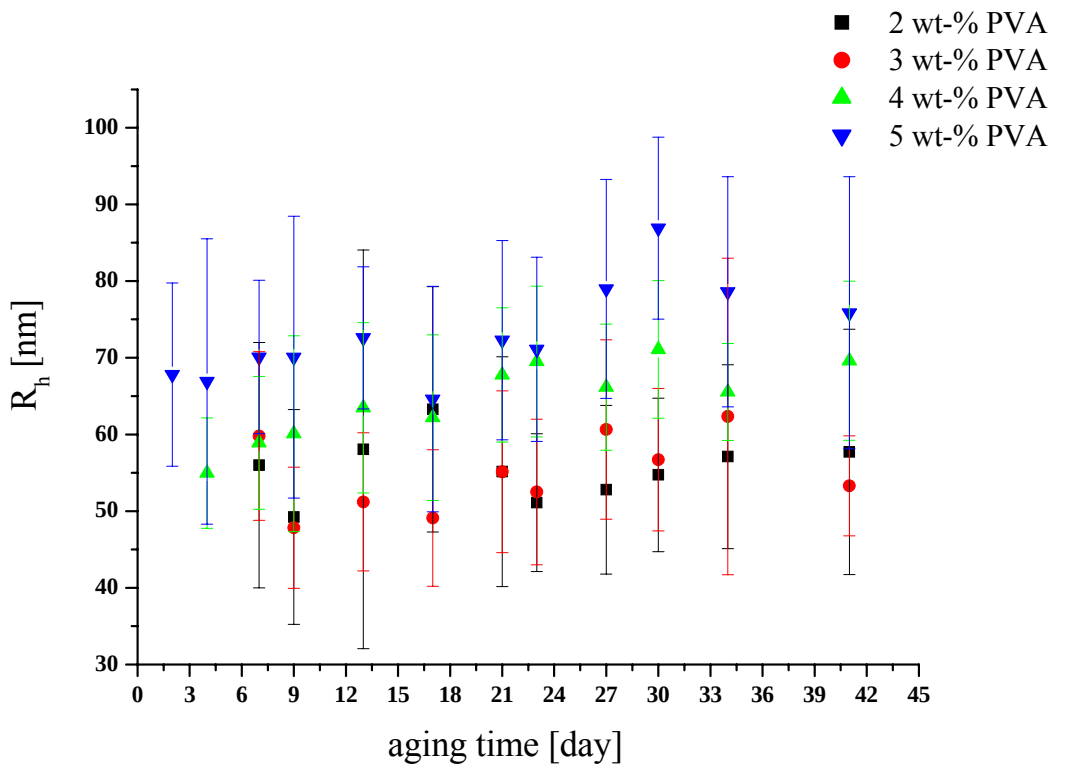


Figure 2.8: $R_h$ as a function of aging time for diluted aged PVA-26k aqueous solutions with different concentration (slow mode can be detected in 2, 3, 4, 5 wt-% PVA solutions by DLS).

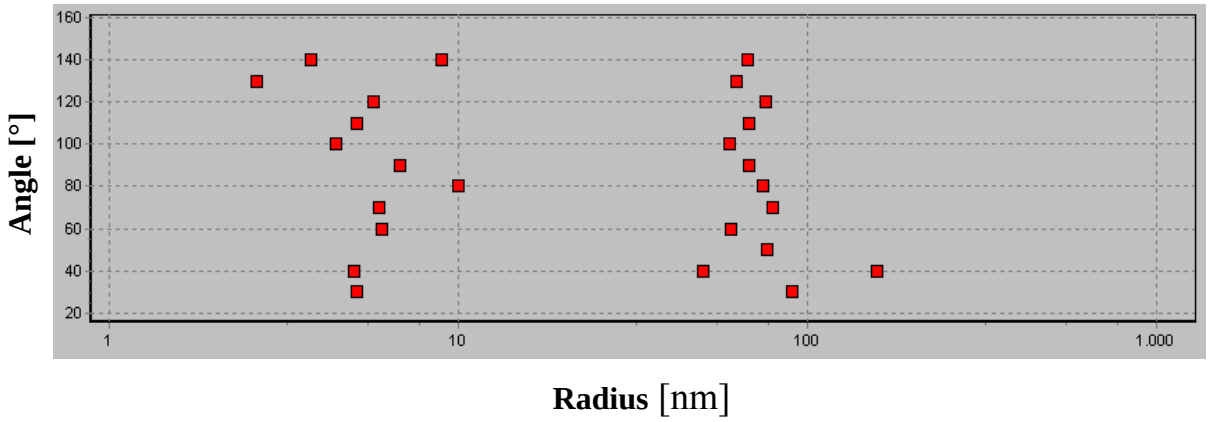


Figure 2.9: $R_h$ distribution of diluted 40 days aged 5 wt-% PVA-26k aqueous solution (multi-angle DLS 30 -140° using Contin method).

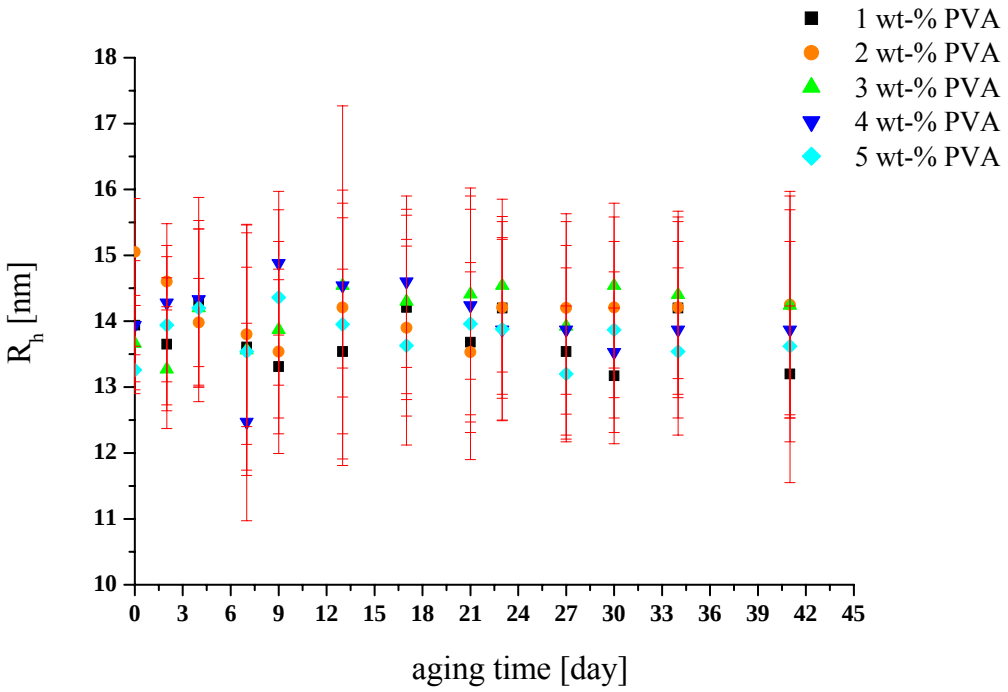


Figure 2.10: $R_h$ of a single polymer chain in aged PVA-195k aqueous solution (fast mode detected by DLS).

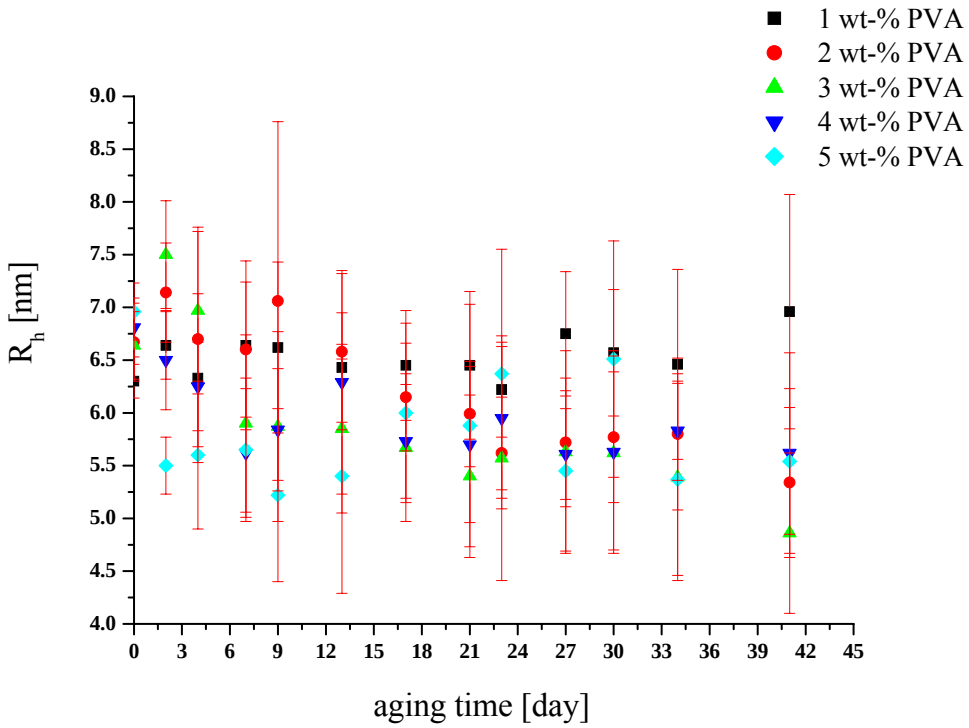


Figure 2.11: $R_h$ of single polymer chain in aged PVA-26k aqueous solution (fast mode detected by DLS).

### 2.3.1.3 Thermal stability of aged poly(vinyl alcohol) aqueous solutions

The relationship between stability of the supermolecular aggregates and concentration and molar mass of PVA solutions was investigated by DLS. The diluted 1 wt-% aged PVA samples were thermally treated at different temperatures for 3 h. The stable smaller clusters formed in aged PVA solutions can still be detected, when the thermal treatment was lower than 60 °C. With increasing temperature the size of clusters decreased slightly.(Tab. 2.1) Until the thermal energy is high enough to break the strong bonding of the clusters, the aged PVA aqueous solution were reversed to molecularly dispersed PVA chains.

Table 2.1: Variation the size of stable clusters in diluted 180 days aged PVA aqueous solutions after thermal treatments (fast modes and slow modes (green marked) detected by DLS, PVA-195k).

| $R_h$(nm) / Original Conc. (wt-%) | Diluted to1 wt-% PVA solution after thermal treatment | | | | | |
|---|---|---|---|---|---|---|
| | 25 °C | 40 °C | 50 °C | 60 °C | 70 °C | 80 °C |
| 1 | 13.72 | 14.24 | 13.98 | 13.08 | 15.12 | 12.38 |
| 4 | 13.58<br>144.4 | 12.99<br>176.4 | 13.7<br>135.9 | 12.23 | 14.57 | 14.22 |
| 6 | 14.16<br>183.4 | 11.91<br>187.3 | 12.73<br>172 | 12.79<br>120.3 | 12.68 | 13.07 |
| 7 | 12.34<br>190.9 | 12.34<br>190.9 | 13.54<br>150.3 | 13.07<br>100 | 14.58 | 13.43 |
| 9 | 12.77<br>203.4 | 11.71<br>172.4 | 12.49<br>162.6 | 12.79<br>96.4 | 14.45 | 13.48 |

The size of stable clusters formed in aged PVA solutions increased with increasing molar mass and concentration of PVA. The thermal stability of clusters formed in aged PVA solutions with different molar mass PVA behaved similar, which indicated the thermal stability of clusters could be related to the hydrolysis degree of PVA and less affected by the size of cluster. Both kinds of PVAs have the same hydrolysis degree - 98 mol-% (Table 2.2). High hydrolysis degree of PVA contains high amount of hydroxyl groups, which are attributed to the formation of the stable clusters - paracrystal structures by tight hydrogen bonding. Their existence is connected with the considerable crystallization capacity of PVA.

Table 2.2: Size of stable clusters in aged PVA solutions after thermal treatments (fast modes and slow modes (green marked) detected by DLS).

| $R_h$ (nm) / Aging time (day) | Diluted to1 wt-% PVA-26k | | | Diluted to 1 wt-% PVA-195k | | |
|---|---|---|---|---|---|---|
| | 1wt-% | 5 wt-% | 10 wt-% | 1 wt-% | 5 wt-% | 10 wt-% |
| freshly prepared | 8.91 | 7.12 | 6.46 | 14.26 | 14.92 | 14.58 |
| 5 | 7.59<br>25.57 | 5.5<br>56.27 | 5.5<br>87.12 | 14.99 | 13.25<br>154.2 | 13.88<br>287.4 |
| 12 | 7.09<br>27.25 | 5.65<br>66.94 | 6.11<br>91.94 | 13.55 | 13.87<br>197.3 | 14.94<br>288 |
| 20 | 6.64<br>25.27 | 5.54<br>60.05 | 6.52<br>96.98 | 13.2 | 13.16<br>210.8 | 14.57<br>244.7 |
| 20<br>Heated at 50 °C | 7.19<br>24.3 | 7.03<br>57.8 | 6.87<br>87.5 | 13.98 | 13.65<br>140.6 | 14.12<br>238.7 |
| 20<br>Heated at 60 °C | 8.09 | 7.26 | 7.28 | 14.21 | 14.65 | 14.59 |

### 2.3.2 Rheological characterization of aged poly(vinyl alcohol) aqueous solutions

As a continuation of this study into the aging behavior of poly(vinyl alcohol) solutions, the effect of increasing concentration on the rheological behavior of this fully hydrolyzed PVA was studied. The experiments using the rheometer provided viscosity data at different shear rates. The data collected from these experiments provided insight into the relationship between viscosity and aging of PVA solutions. As the polymer concentration was increased, the different molar mass PVAs had very different viscosities. The viscosity of low molar mass PVA-26k increased slightly with increasing concentrations. High molar mass PVA-195k showed a sharp viscosity increase in a concentration range of over 8 wt-%. (Fig. 2.12) This obvious increase in viscosity is typical for the rheology of PVA solutions, when it was close to the critical state of sol-gel transition. Supermolecular aggregates and stable paracrystal structures were detected in aged PVA solutions according to above investigations. Supermolecular structures are formed in solutions which increasingly influence its intrinsic viscosity. Influences of supermolecules on shear viscosity were investigated by steady shear testing on the fresh and 40 day aged PVA solutions (1 - 5 wt-% PVA-26k and PVA-195k). The shear viscosities of PVA solutions showed Newtonian behavior in the shear rate range between 1 and 100 $s^{-1}$. The obvious changes of shear viscosities were not observed with the aging process of PVA solutions, when the PVA solutions were below the critical concentration of gelation (Fig. 2.13 a, b). Below the critical concentration of sol-gel phase

transition in aged PVA solutions, the formation of supermolecular aggregates had no influence on the shear viscosity of PVA. The entanglements between the supermolecular aggregates can be easily broken down by agitation. It is assumed that an important factor on the viscosity is the size of paracrystal structures of aged PVA solutions, which grow with increasing concentration and molar mass. The structures of paracrystalline PVA were formed by hydrogen bonding, and exhibit a higher stability than the supermolecular aggregates. When the volume fraction and size of paracrystalline PVA are sufficient to connect each other to form the matrix in aged PVA solutions leading to gelation, apparent molar mass of aged PVA solution became infinite and the sol-gel phase transition takes place under this situation.

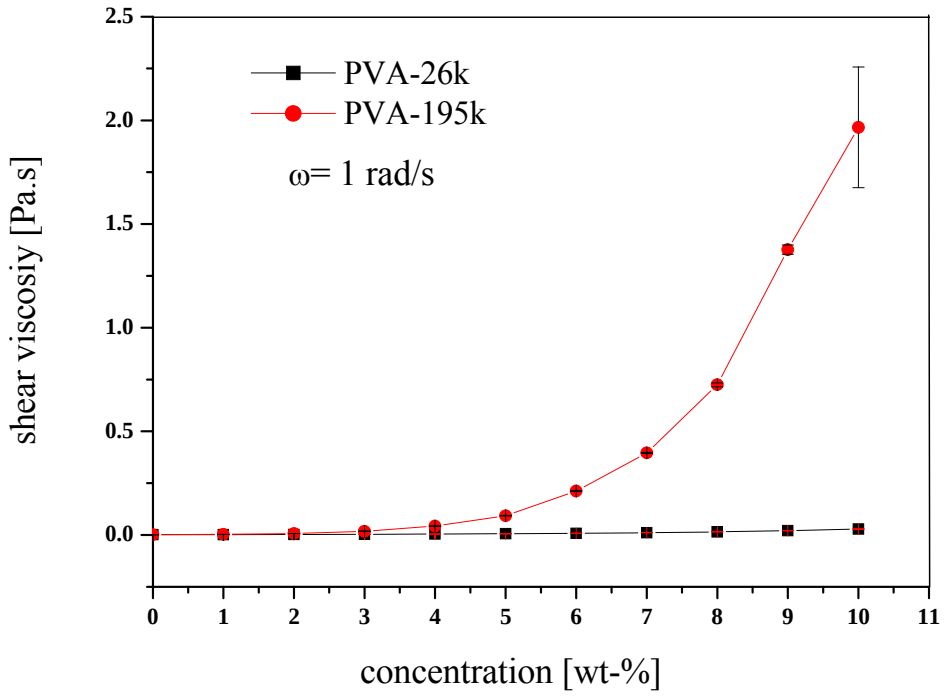


Figure 2.12: Average shear viscosity versus the concentration of poly(vinyl alcohol) aqueous solutions (steady shear rate 0.1 to 100 $s^{-1}$, 25 °C).

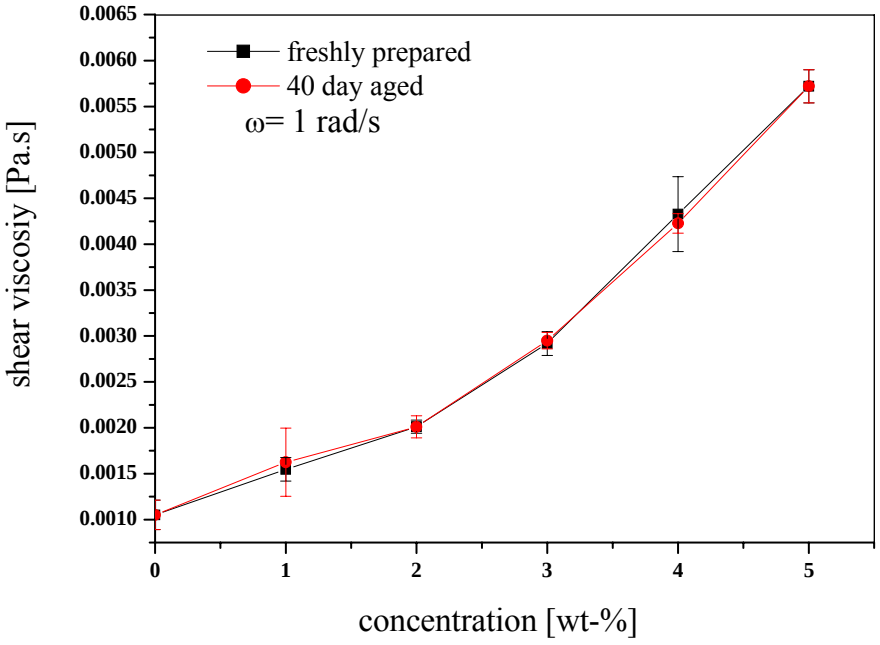


(a)

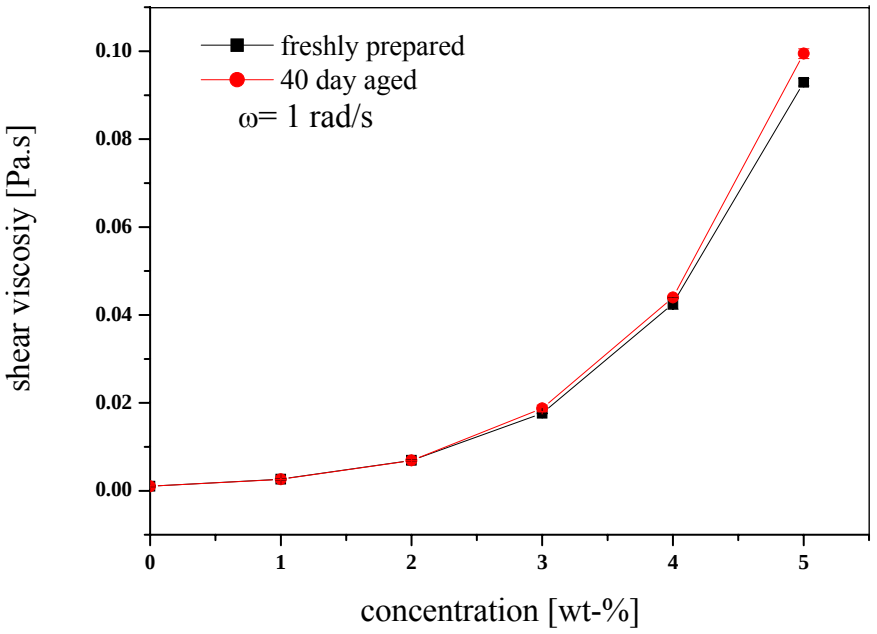


(b)

Figure 2.13: Average shear viscosities as a function of concentration for fresh and 40 day aged PVA aqueous solutions (a) PVA -26k, (b) PVA-195k (steady shear rate 0.1 to 100 $s^{-1}$, 25 °C).

### 2.3.3 Water crystallization in aged poly(vinyl alcohol) aqueous solutions

Solutions may be supercooled over a wide temperature range. The temperature of crystallization of pure water in the laboratory is around – 40 °C. Some kinds of aliphatic long-chain alcohols can promote the ice nucleation between –1 and –10 °C.[78] DSC measurements detected the temperature of water crystallization – the onsets of freezing points of fresh and aged PVA aqueous solutions under cooling treatment. The temperature of crystallization of bi-distilled water used for preparation of PVA aqueous solutions is usually at ~ -20 °C. The water crystallizations of PVA aqueous solutions were independent on the concentrations in the range of 1 to 5 wt-%, molar mass and aging time. (Fig. 2.14 and 2.15) The paracrystalline structures in aged PVA solutions did not promote the ice nucleation, which might be caused by the poor lattice fit to ice.

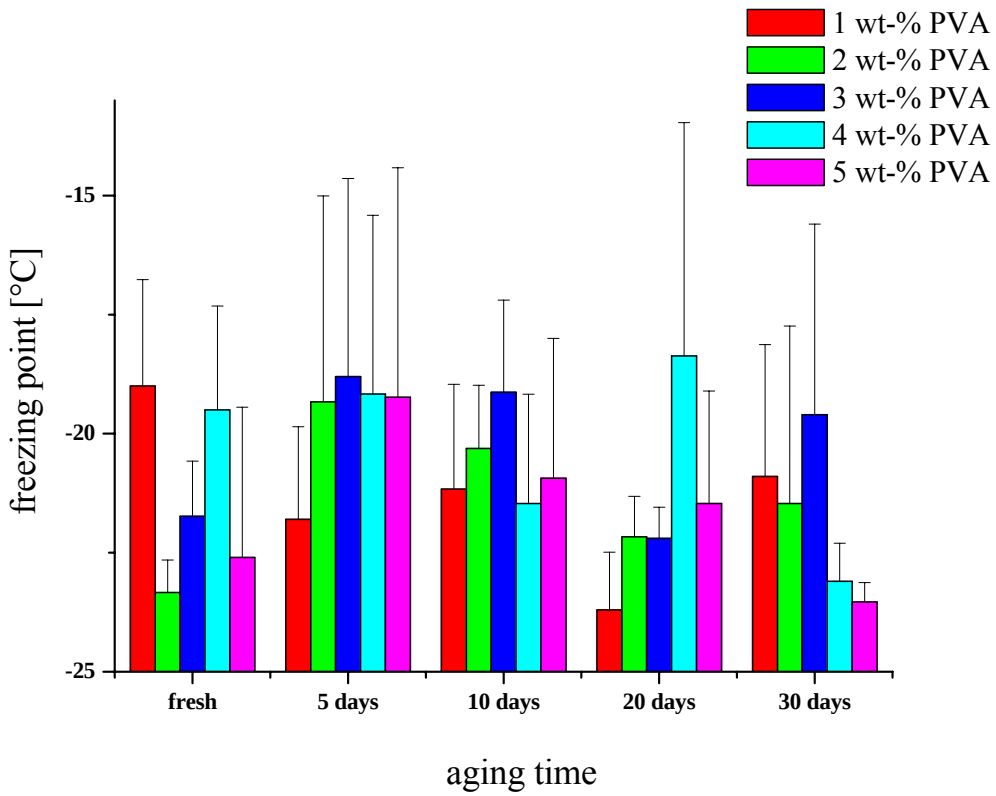


Figure 2.14: Freezing points distribution of aged 1 – 5 wt-% PVA-26k solutions (detected by DSC, cooling rate -1 °C/min, to -25 °C).

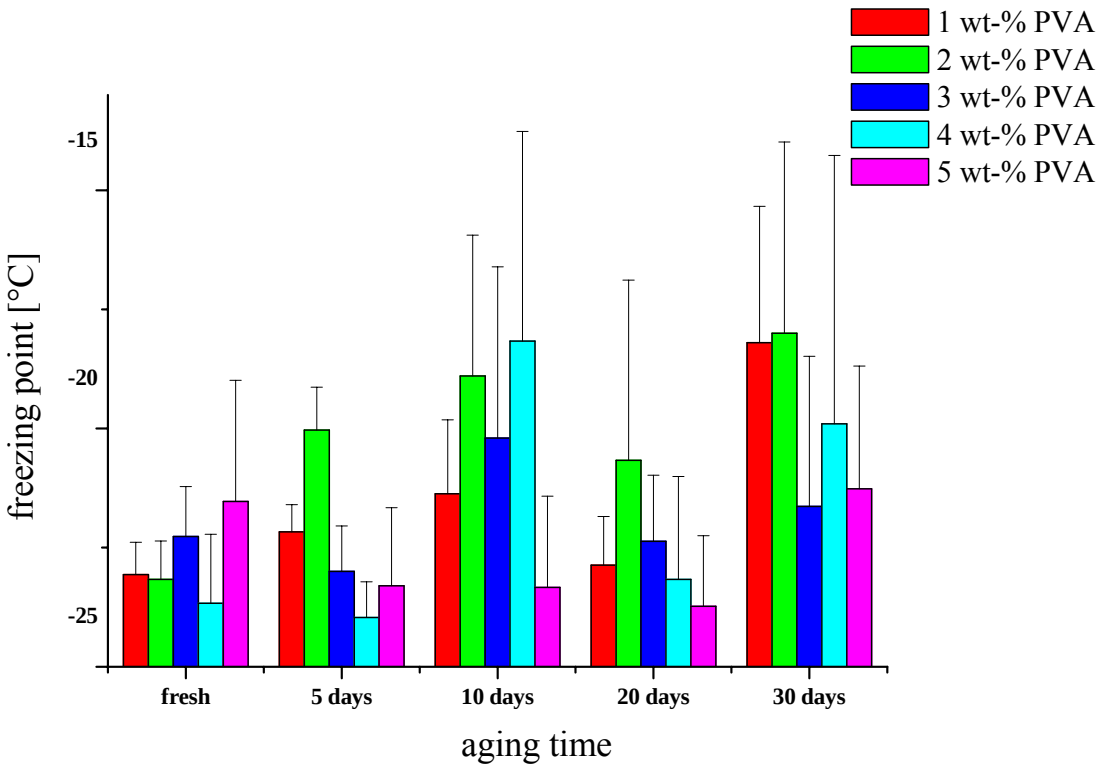


Figure 2.15: Freezing points distribution of aged 1 – 5 wt-% PVA-195k solution (detected by DSC, cooling rate -1 °C/min, to -25 °C).

The aging process of PVA aqueous solutions was investigated by DLS and rheological measurements. Fast modes of DLS were detected in all original and diluted aged PVA solutions, which indicated that the main part of the single polymer chains remained in solution in the non-aggregated form below the concentration of gelation (Fig. 2.8 and 2.10). Two different kinds of slow modes indicated two different aggregating behaviors in aged PVA solution (Fig. 2.7 and 2.9). The supermolecular aggregates detected only in original PVA solutions were self-assembled pseudo-micellar structures driven by e.g. van der Waals forces, electrostatic attractions or hydrogen bonding. These supermolecular aggregates were weakly bounded polymer coils, which can be eliminated easily by dilution and agitation. The investigation of rheological properties showed a very small influence of the supermolecular aggregates on the shear viscosity. The smaller clusters detected in diluted PVA solutions were thermostable paracrystal structures, which can be destroyed by heating at 60 °C. These aggregates were caused by strong intramolecular and intermolecular hydrogen bonding in PVA solutions.[79] The mean size of paracrystal structure increased during aging, and after some time they become joined and formed a strong gel network. The dynamic light scattering results indicate that the dynamic behavior of PVA solutions can be classified into three

regions by increasing the concentration of PVA. The schematic illustration of the aging process of PVA aqueous solution is given in Figure 2.16. Two critical concentrations affected the aging behaviour of PVA solutions: minimum aggregation concentration ($C_{agg.}$) - below a certain concentration all polymer chains act as isolated coils, no intensive formation of supermolecular structures can be detected under the threshold concentration. DLS results exhibit a single relaxation mode related to the individual PVA coil; the critical concentration of sol-gel transition ($C_{gel}$) - at concentrations lower than the critical concentration, the PVA solutions are liquid, but clusters are formed by molecular aggregates. When the concentration is higher than $C_{gel}$, the paracrystal aggregates become dominant, and form a strongly joined matrix of PVA gel. In the range of these two critical concentrations, the fraction of aggregated PVA chains increased with increasing concentration. DLS results exhibit two relaxation modes denoted as the fast and slow modes from the individual PVA coils and chain aggregates.

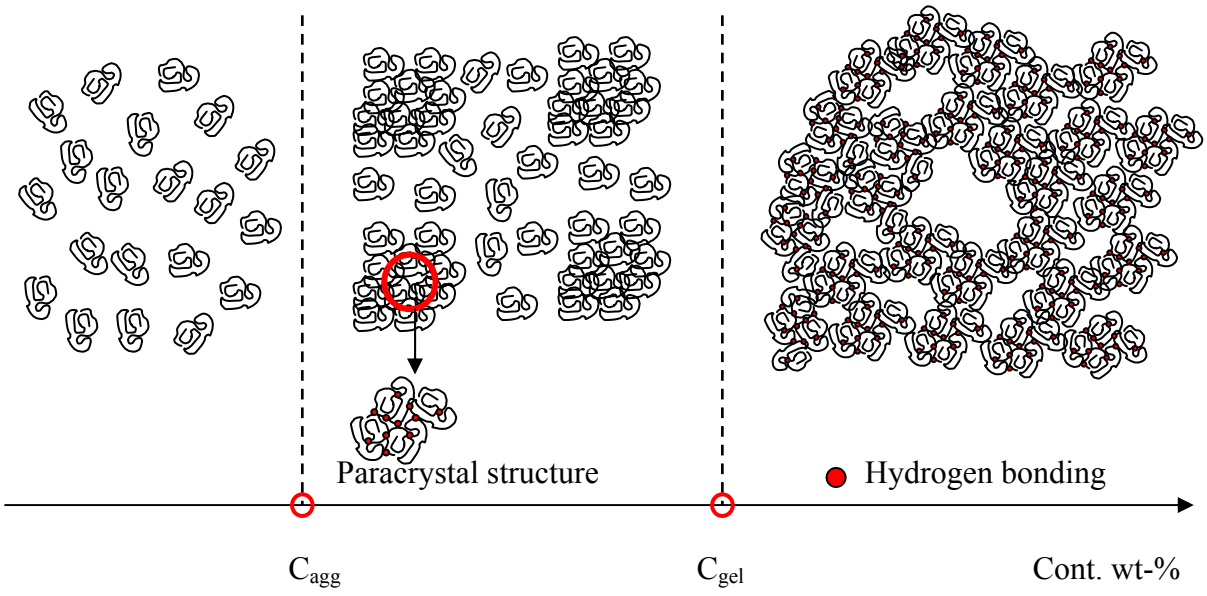


Figure 2.16: Schematic illustration of the aging process of PVA solution based on different concentrations. ($C_{agg}$ - minimum aggregation concentration, $C_{gel}$ - critical concentration of sol-gel transition).

## *2.4 Conclusion*

PVA is prone to aggregate through hydrogen bonding due to its polyhydroxy groups. It is well known that many factors affect the dynamic behavior of polymer solutions, including temperature, molar mass and concentration of the polymer, and the types of the solvent used. Physical aging is a process in which the formation of supermoelcular aggregates is related to the concentration of PVA solution and the molar mass of the polymer. The present study primarily explains the dynamic characteristics and aggregation behavior of PVA aqueous solutions at various concentration ranges. The result indicated that the chain aggregation behaviour is dependent on the polymer concentration and molar mass. PVA polymer chains undergo two main aggregation processes over time, weakly bound supermolecular aggregation and thermostable paracrystal formation. Concentrated PVA solutions exhibit gelation, owing to the formation of thermostable paracrystal structures as junction points with aging. High molar mass PVA exhibits higher $C_{agg}$ and lower $C_{gel}$ than low molar mass PVA. $C_{agg}$ of low molar mass PVA-26k is located in the range of 1 ~ 2 wt-%. $C_{agg}$ of high molar mass PVA-195k is located in the range of 2 ~ 3 wt-%. Below $C_{gel}$, the aging process does not result in obvious effects on the shear viscosity behaviour of PVA solutions. The water crystallization temperature of PVA aqueous solutions are not a function of the concentration and molar mass. The appearance of paracrystal PVAs in aged PVA solution cannot influence the water crystallization.

# Chapter 3

# 3 Poly(vinyl alcohol) cryogel – a potential postoperative anti-adhesion agent

## *3.1 Introduction*

### 3.1.1 General introduction

Postsurgical adhesion is a common complication following surgery, chronic inflammations or accidental trauma.[80] Postsurgical peritoneal adhesions take place in more than 90% of the patients following abdominal surgeries, and 55-100% of women suffer pelvic adhesions after pelvic surgeries.[81] The adhesions are formed by over-expressed wound healing. The wound healing processes involve inflammation, cell proliferation and matrix deposition.[82] Within the first 3 h, the release of various cytokines and prostaglandins increases vascular permeability to coordinate the recruitment of macrophages, granulocytes, fibroblasts, and mesenchymal cells. The repair in following 24 to 48 hours is characterized by cell migration. Fibroblast proliferation and vascularization occur in fibrin clots after 3 days that organize into permanent thick, fibrous "scars" between injured tissues or peritoneum.[83] These fibrous adhesions are the significant sources of chronic pain, bowel obstruction, infertility and impaired organ functioning. The treatment of re-operation also brings the hospitals and patients an extra financial burden.[84, 85] For over 100 years, many efforts have been done to prevent these abnormal fibrous connections. Besides different kinds of pharmacological agents and various surgical techniques,[86] barriers to permanently or transiently separate injured tissue surfaces are widely used in adhesion prevention: HA-CMC (seprafilm),[87] Gore-Tex (PTFE),[88] oxidized-regenerated cellulose (interceed)[89] etc. The ideal anti-adhesion barrier would be expected to be noninflammatory, nonimmunogenic, bioadsorbable and biodegradable, and exhibits simple application to both open surgical and laparoscopic procedures. The effective transient barrier is required to locate at the sites of interest without suture during the first 5 – 8 days of peritoneal wound healing.[90-92] Poly(vinyl alcohol) is good biocompatible, non-toxic, non-carcinogenic and applied extensively as biomaterial and for biotechnological purposes by varying concentration, solvents and special techniques to produce contact lenses, artificial cartilage tissue, and protective coating for wounds and burns *etc*.[93, 94] The present work is to optimize the reproducible manufacture of PVA cryogels, which can be used as a postsurgical anti-adhesion barrier.

### 3.1.2 PVA cryogel near gel point

PVA cryogel is a thermoreversible physical hydrogel, which undergoes a phase transition from polymer aqueous solutions to partial crystallized polymer hydrogel by freeze/thawing treatment.[95, 96] The research on the cryogelation mechanism and microstructure of PVA hydrogel was performed widely by differential scanning calorimetry, nuclear magnetic resonance, scanning electron microscopy, transmission electron microscopy, X-ray scattering and small angle neutron scattering (SANS).[97, 98] The current understanding on the PVA cryogel formation is that the three dimensional PVA physical hydrogel framework is formed by physically cross-linked PVA crystallites which are primarily formed at temperatures below the crystallization of water.[99, 100] During the crystallization of water and the defrosting of icy crystallites, the homogenous PVA solution was transferred into two bi-continuous phases, polymer-rich and polymer-poor regions (Fig. 3.1). PVA cryogels are thermoreversible and form solutions again by heating up to 70-90 °C. The mechanical properties of PVA cryogel depend on the molar mass of PVA, initial polymer concentration, freezing temperature, cooling rate, duration of storage in the frozen state, thawing rate and the number of freeze/thawing cycles.[101] Physically cross-linked PVA hydrogel is more suitable for medical application by avoiding toxic chemical crosslinking agents as e.g. glutaraldehyde, boric acid *etc*.[102]

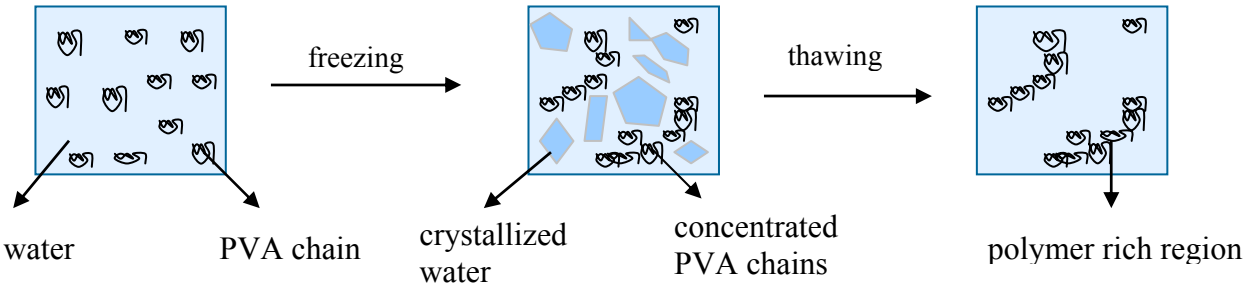


Figure 3.1: Cryotropic gelation process of PVA solutions

Gelation is a process which leads to the formation of a gel with the increase of intermolecular cross-links. The more intermolecular cross-links are formed, the faster the apparent weight average molar mass increase, and eventually it becomes infinite when the whole system is crosslinked completely.[103] The divergence point of molar mass growth up to infinity is known as gel point or sol-gel transition. Polymer solutions pass from the state of viscous liquid to that of crosslinked elastic gel.[104] The gelling system near gel point combining liquid and solid characteristics has advantageous properties for powerful adhesives. The maximum tack

(corresponding to adhesive strength) can be reached at the gel point.[105] The critical gel combines the surface-wetting property of liquids with the cohesive strength of solids. Adhesion and cohesion exhibited an optimum in this transition range. At the critical state the molar mass of the system diverges to infinity and molecular sizes range from the smallest single polymer chains to the infinite cluster, which induced the divergence of rheological properties of the system. Rheology studies the flow and deformation of materials.[106] Elasticity is the ability of a material to store deformation energy, and viscosity is the resistance of a material to flow. Most common are rotational rheometer with concentric disk fixtures, cone and plate fixtures, or Couette geometry. The dynamic oscillatory shear experiment has been commonly used in viscoelastic materials measurement.[107] The dynamic test is performed applying a small sinusoidal strain (or stress) and measuring the resulting stress (or strain). The elastic or storage modulus G′ provides information on the energy stored by the sample, while the viscous or loss modulus G′′ is related to the energy dissipated by the sample (Fig. 3.2). The tests are called microscale experiments compared to macroscale tests like rotational or viscometry tests. Small strain tests are preferable for materials with very broad distributions of relaxation modes, since they avoid rupturing the fragile network structure. Another advantage of the dynamic mechanical experiment is that each of the moduli G′ and G′′ independently contains all the information on the relaxation time distribution. This helps in detecting systematic errors in dynamic mechanical data. In general, complex modulus G* is determined by measuring stress after small angular deformation and it is comprising of storage (real) (G′) and loss (imaginary) (G′′) components and frequency dependent, showing vastly different behavior at low shear rates and high shear rates. The phase angle tan δ (G′′/G′) quantifies the balance between energy loss and energy storage. Tan δ is associated with the degree of viscoelasticity of the sample. Physical gels can be divided into so-called “strong” and “weak” kinds,[108] but both respond as solids at small deformations. As the values of the two moduli are balanced (δ = 45° and tan δ =1), the behavior is sometimes called “the gel point”. A value for tan δ greater than 1 indicates more "liquid" properties, whereas values lower than 1 means more "solid" properties (Fig. 3.3).

$$G' = \text{storage modulus} = \frac{\sigma_0}{\gamma_0} \cos\delta \qquad (3.1)$$

$$G'' = \text{loss modulus} = \frac{\sigma_0}{\gamma_0} \sin\delta \qquad (3.2)$$

$$G^* = \frac{\text{complex stress amplitude}}{\text{complex strain amplitude}} = \frac{\sigma_0}{\gamma_0} \cos\delta + \frac{\sigma_0}{\gamma_0} j \sin\delta \qquad (3.3)$$

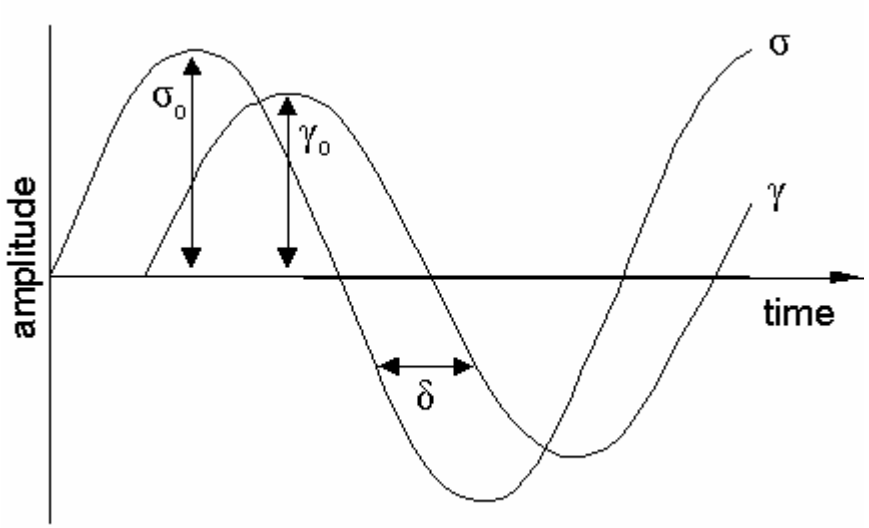


Figure 3.2: Sinusoidal wave forms for stress and strain functions in dynamic oscillatory test ($\sigma_0$ - stress amplitude, $\gamma_0$ - strain amplitude, $\delta$ - phase lag).[109]

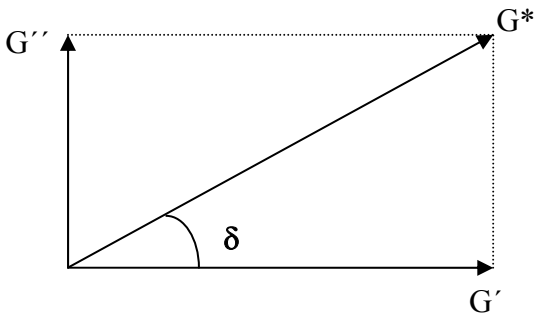


$G^* = G' + iG''$ (3.4)

$\tan(\delta) = G''/G'$ (3.5)

$\eta^* = G^* / \omega$ (3.6)

$\omega = 2\pi f$ (3.7)

$0° < \delta < 90°$ $\Rightarrow$ viscoelastic sample

$\delta = 90° \Rightarrow G^* = G''$ and $G' = 0 \Rightarrow$ viscous sample

$\delta = 0° \Rightarrow G^* = G'$ and $G'' = 0 \Rightarrow$ elastic sample

$\delta > 45° \Rightarrow G'' > G' \Rightarrow$ semi liquid sample

$\delta < 45° \Rightarrow G' > G'' \Rightarrow$ semi solid sample

Figure 3.3: Vector representation of moduli in dynamic oscillatory test (G´ - elastic modulus or storage modulus, G´´ - viscosity modulus or loss modulus, tan $\delta$ - phase angle or loss angle, $\omega$ - the angular frequency).[109]

### 3.1.3 Supercooling and ice nucleation agents

The phenomenon in which aqueous solutions remain in liquid state below the freezing point is known as supercooling. Water supercooling as a significant phenomenon of nature has been intensively studied for many years. In nature the supercooling phenomenon is connected with the formation of snow and hail and freezing of various water reservoirs. One practical influence is that supercooled water instantly frozen on airplane wings may deform the shape of wings and cause plane crashes. In industry it plays an important role in many production processes such as ice making and foodstuffs freezing and their storage. Supercooling is also

very important to our entire ecosystem. Many ectothermic animals and plants can produce themselves some substances such as glycerol and antifreeze proteins to counteract water nucleation in order to survive exposure to subzero temperatures. Certain bacteria such as *Pseudomonas syringae* possess a very potent ice nucleation ability, which can promote water crystallization on the surface of various fruits and plants. The freezing causes frost-damage in the epithelia and makes the nutrients in the underlying plant tissues available to the bacteria.[110] Lacking any nucleus, the liquid phase can be maintained until the temperature at which crystal homogeneous nucleation occurs. Homogeneous ice nucleation takes place stochastic in water or aqueous solutions absent of foreign ice nucleation agents. Solutions may supercool to varying degrees. For pure water, the degree of supercooling may be around -40 °C. In order to form an ice crystal, it needs a nucleation site. The nucleation site can be homogeneous or heterogeneous. When a critically large nucleus is formed by spontaneous aggregation of water molecules themselves, the nucleation is called homogenous crystallization. Homogeneous nucleation requires a greater degree of metastability - supercooling – than heterogeneous nucleation. Due to the electrostatic attraction between their polar parts, water molecules tend to aggregate spontaneous. Once a critical nucleus is formed by spontaneous aggregation of water molecules, additional water molecules rapidly crystallize around this seed crystal and the remaining water will also start to freeze. Water can exist in many different crystalline forms, 13 of which have been identified to date. Ordinary hexagonal ice is stable at atmospheric pressure between 72 and 273 K.[111] The size of critical nucleus at -5 °C is about 45,000 water molecules and at -40 °C only 70 water molecules.[112] If the aggregation of water molecules is catalyzed by a substance on which the initiation of freezing in aqueous solution can take place, the nucleation is referred to as heterogeneous crystallization.[113]

#### 3.1.3.1 Thermodynamic theory of heterogeneous nucleation

If the aggregation of water molecules is attached to some pre-existing structure, most likely a solid surface, then the possibility of the germ to reach stability is increased. Nucleation is a kinetic process by which a free energy barrier must be overcame to form a new interface of embryo and reach a critical radius $r_c$. Thereafter, the new phase grows spontaneously.[114-116] The simplest and most fundamental visualization of heterogeneous nucleation derives from the phenomenon of wettability and its reflection in the contact angle. On an insoluble substrate (S), the germ of the new phase (G) is assumed to have a spherical cap shape with the

contact angle characterizing the relationship between the three interfacial energies involved. This is illustrated in Fig. 3.4:

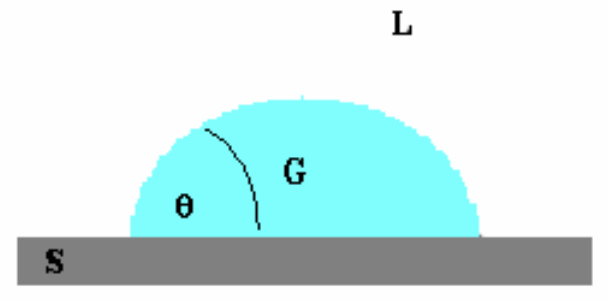


$$m = \cos\theta = \gamma_{SP} - \gamma_{SG} / \gamma_{GP} \qquad (3.8)$$

$$f(m) = ¼ (2\text{-}3m + m^3) \qquad (3.9)$$

$$f(m) = \Delta G^*/\Delta G^*_{homo} \qquad (3.10)$$

Figure 3.4: Schematic heterogeneous nucleation: germ (G) on the substrate (S), liquid phase (L), contact angle (θ).

In Eq. (3.8), $m$ is a function of the interfacial free energy differences between the different phases, and $f(m)$ is a measure for the lowering of the nucleation barrier ($\Delta G^*_{homo}$: homogeneous nucleation barrier). $f(m)$ changes from 0 to 1. When the interaction between the nucleating phase and the substrate is strong, the nucleating energy will be suppressed due to the very low interfacial energy. In this case, one has $f(m) \rightarrow 0$. On the other hand, if the interaction between the germ and the substrate is very poor, one has $f(m) \rightarrow 1$, meaning that the substrate has almost no influence on the nucleation barrier.[117] A number of possibilities of ice germs are shown in Fig. 3.5.

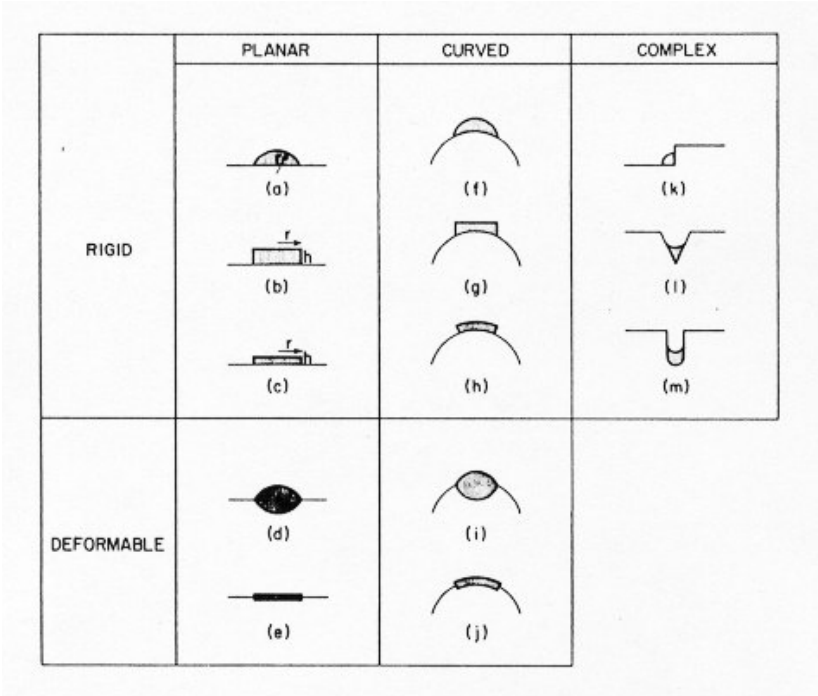


Figure 3.5: Some simple shapes of ice germs on solid or deformable substrates.[118]

### 3.1.3.2 Ice nucleation agents

High levels of water supercooling are not generally required for water nucleation in industrial processes for two related reasons. Firstly, the supercooled state is unstable and spontaneous crystallization can theoretically occur at any time. Secondly, nucleation from a highly supersaturated system is rapid, leading to small crystal sizes. In many industrial processes, where crystallization is used as a separation technique, large crystals rather than small crystals are required.

Heterogeneous nucleation agents can promote the formation of such "embryo crystal" at higher temperature than homogenous nucleation and successfully control the degree of water supercooling in different applications.[119, 120] Ice nucleation agents may be inorganic, organic substances or micororganisms.[121, 122] An effective ice nucleation agent should have the following properties, 1) a small lattice mismatch of ice nucleation agent lattice constant with one of the ice lattice constants, 2) the ice nucleation agent surface should be hydrophilic, 3) ice nucleation agent surface should have defects, and 4) a low net surface charge.[123] The most effective chemical ice nucleation agents, e.g. silver iodine,[124] lead iodine, and cupric sulphide, are all hexagonal crystals with atomic spacing in the basal plane very similar to those in ice. The lattice constant of ice $I_h$ and AgI is 4.52 Å and 4.58 Å, respectively. Threshold nucleation temperatures of chemical ice nucleation agents are between -4 and -16 °C. The threshold nucleation temperature of AgI is -4 °C.[125] *Pseudomonas syringae* possess very potent ice nucleators,[126] the best biological ice nucleation agent may trigger freezing at -1 to -2 °C. The water supercooling temperature of poly(vinyl alcohol) aqueous solutions vary in the range of -18 to -25° which makes it very difficult to reproduce the production of PVA cryogel near the gel point. Long-chain aliphatic alcohols[127] and amino acids[128, 129] have efficient ice nucleation activities, which are chosen to test the water crystallization activity in PVA solutions by DSC (Differential Scanning Calorimetry) measurements.

## *3.2 Experimental section*

### 3.2.1 Materials

Different concentrations of poly(vinyl alcohol) aqueous solutions were prepared by dissolving PVA-195k in distilled water or $D_2O$ for 4 h at 96 °C. Some biocompatible ice nucleation agents were chosen to test the water crystallization ability in 8.3 wt-% PVA-195k aqueous solutions (Tab. 3.1).

Table 3.1: Molecular formula, molar mass, and solubility of tested substances as ice nucleation agents.

| Name | Molecular formula | Molar mass (g/mol) | Solubility (g/dl $H_2O$, 25 °C) |
|---|---|---|---|
| Triacontanol | $C_{30}H_{62}O$ | 438.82 | - |
| Heptacosanol | $C_{27}H_{56}O$ | 396.8 | - |
| L-Leucine | $C_6H_{13}NO_2$ | 131.18 | 2.43 |
| L-Tryptophan | $C_{11}H_{12}N_2O_2$ | 204.23 | 1.136 |
| L-Cystine | $C_6H_{12}N_2O_4S_2$ | 240.3 | 0.011 |
| L-Aspartic acid | $C_4H_7NO_4$ | 133.1 | 0.778 |
| L-Glutamic acid | $C_5H_9NO_4$ | 147.1 | 0.864 |
| L-Isoleucine | $C_6H_{13}NO_2$ | 131.18 | 4.117 |
| L-Tyrosine | $C_9H_{11}NO_3$ | 181.19 | 0.0453 |
| L-Asparagine | $C_4H_8N_2O_3$ | 132.2 | 8.85 |
| Silver Iodine | AgI | 234.77 | - |

### 3.2.2 Preparation of poly(vinyl alcohol) cryogel by using different freezing temperatures and freezing times

PVA aqueous solutions filled in 10 ml syringes or Petri dishes were placed into the climate chamber. Freezing temperature, freezing time, freeze/thawing rate and freeze/thawing cycles are controlled by computer programming. To study the properties of PVA cryogel after repeated freeze/thawing cycles, PVA cryogel samples were prepared by submitting the PVA solution to one to three freeze/thawing cycles (freeze step at -32 °C for 60 min, and thawing step at 20 °C for 60 min). To get PVA cryogel in the critical state of sol-gel transition, two different methods had been tested. One way is to freeze PVA aqueous solutions filled

syringes in dry/ice bath (-78 °C) for 3 to 5 min in interval of 30 s; then thawed at the room temperature (20 °C). L-aspartic acid containing PVA aqueous solutions (0.5 g/dl 8.3 wt-% PVA-195k) were used to prepare PVA cryogel samples in the climate chamber by using different freezing temperatures (-5, -10, -13, -15. -20 and -32 °C) and freeze times (30, 60, 120, 240 min). The thawing temperature is 20 °C.

## *3.3 Experimental methods*

### 3.3.1 $^{1}$H pulse NMR spectroscopy

$^{1}$H pulse NMR measurements were performed on MARAN Ultra NMR instrument operating at 23.5 MHz proton resonance frequency. PVA-195k cryogels were prepared in different solvents ($H_2O$ or $D_2O$) and with different freeze/thawing cycle treatments. PVA-195k cryogels were cut into small pieces and moved immediately into sample tubes of outer diameter of 10 mm. The temperature was kept at 25 °C. The spin–spin relaxation time (T2) was determined by using a CPMG pulse sequence. The time distance between the initial $\pi/2$-pulse and the following $\pi$-pulse was set to $\tau$ = 135 ms. The duration of a $\pi/2$-pulse was determined to be 10 ms. All data were transferred to a PC for post-processing. All data were fitted to a continuous distribution model using a Windows-based toolbox software denoted RIWinDXP, which is a distributed exponential analysis software developed for the MARAN Ultra series.

### 3.3.2 Rheological measurements

Oscillatory viscoelastic measurements of PVA cryogels were performed using a RFSII rheometer. The Two-Plates-Model (cone-plate or parallel plate geometry) was used for oscillatory tests. The bottom plate is stationary. The upper plate is moved back and forth by the shear force. The distance between the plates is the shear gap dimension. The cone diameter, angle and gap were 25 mm, 0.04 rad and 50 μm, respectively. The diameter of parallel plate is 25 mm (Fig. 3.6). The temperature was set at 25 °C for all measurements. The samples were placed between the cone (or parallel plate) and plate, and protected from drying by a plastic cover.

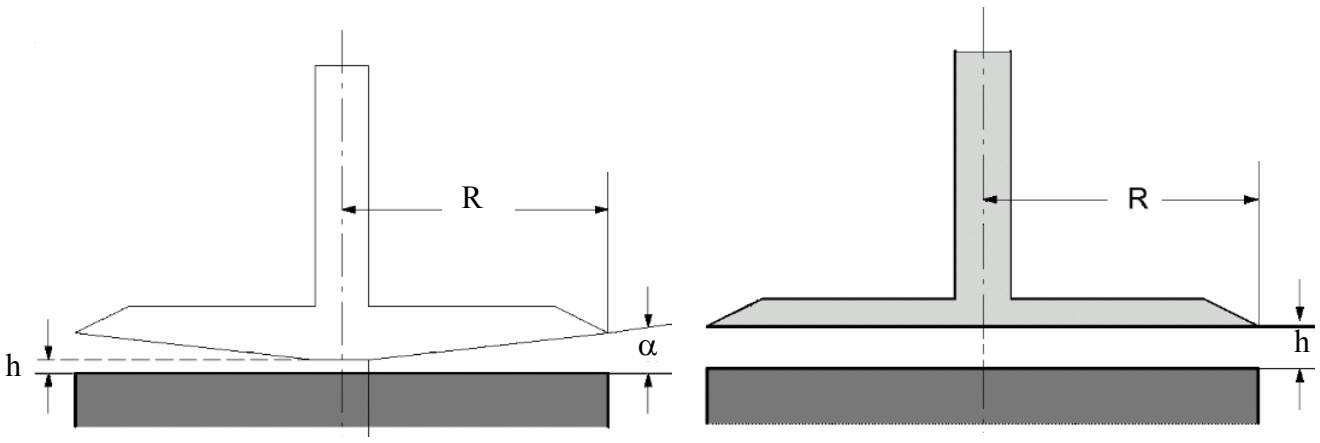


(a) (b)

Figure 3.6: Illustration of (a) cone-plate geometry and (b) parallel plate geometry (R – radius of cone, α - opening angle, h - gap distance).[107]

In frequency sweep experiments, the storage modulus G′ and loss modulus G′′ should be measured in the linear viscoelastic region for frequencies in the range from 0.1 to 100 rad/s The preliminary strain sweep test was performed on samples of PVA cryogel, in which the storage modulus G′ and loss modulus G′′ were measured as a function of strain at a fixed frequency value of 1 Hz to check if the deformation imposed on the gel structure by the rheological experiment was entirely reversible (Fig. 3.7). The strain value of 1% was chosen for all gel samples. Strain controlled rheometers have an electromechanical servomotor controlling the movement of one fixture and a torque transducer measuring the resulting torque attached to the other fixture. Each measurement was repeated at least three times from the same sample.

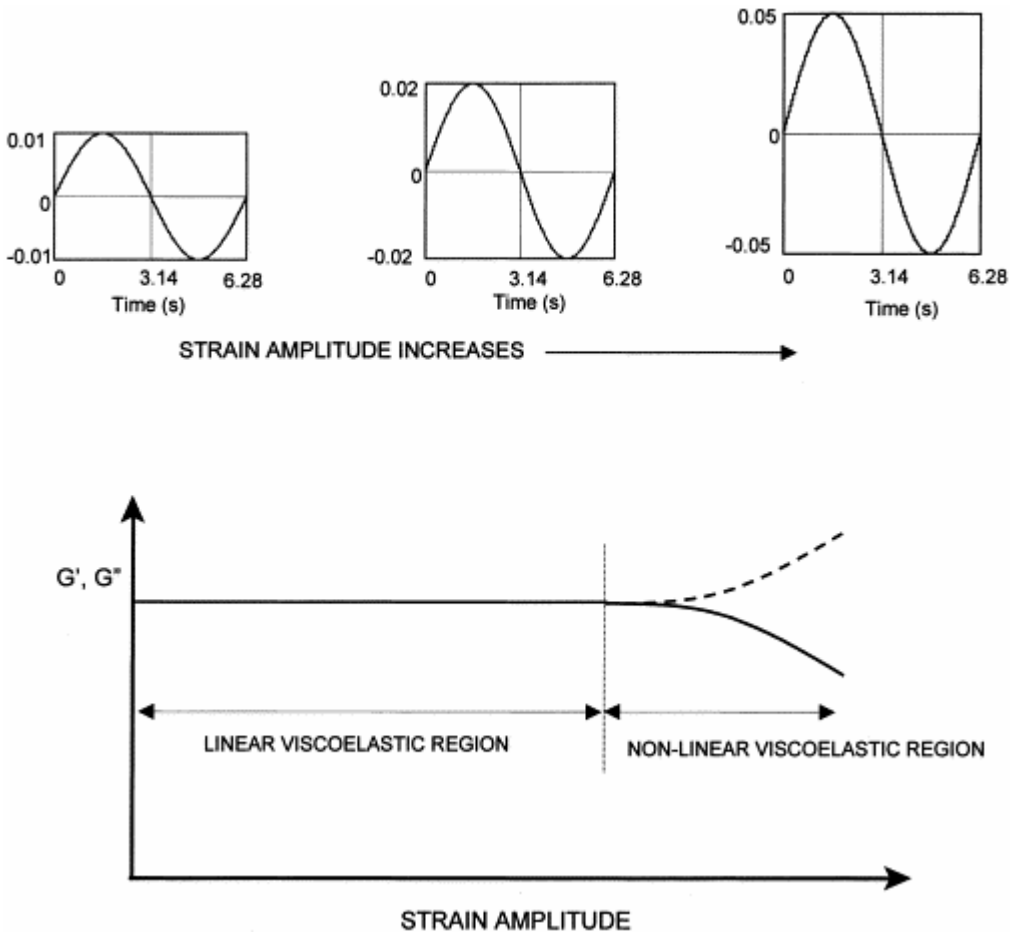


Figure 3.7: Illustration of linear viscoelastic region by strain control test.[107]

### 3.3.3 Differential scanning calorimetry measurements

Differential scanning calorimetry (DSC) experiments were carried out using a DSC 822e (Mettler Toledo, Greifensee, Switzerland) to identify water crystallization of PVA aqueous solutions and estimate water crystallization ability of selected biocompatible ice nucleation agents for 8.3 wt-% PVA-195k solution. 10 ~ 20 mg PVA solutions were inserted into aluminium pans, which were moved into the DSC oven and investigated with cooling rate -1 °C/min and heating rate 2 °C/min in nitrogen atmosphere. The procedure is composed of three successive steps with a cooling, isotherm, and heating process from 22 °C to -25 °C, 5 min isotherm, and from -25 °C to 22 °C. The different heat flow signals obtained in the scanning experiments indicated the ranges of homogenous and heterogeneous water crystallization temperatures of PVA solutions. The peak areas represent the phase transition enthalpies.

### 3.3.4 Scanning electron microscope

The morphology of freeze-dried PVA cryogel was examined using a scanning electron microscope (SEM) (voltage 12kv, 20 °C, pressure 1.6 mbar, Philips XL30 ESEM FEG, Holland).

## *3.4 Results and discussion*

### 3.4.1 PVA cryogel produced by repeated freeze/thawing

Aqueous PVA solutions can be gelled physically by repeated freeze/thawing treatments. Morphology, rheological properties and the state of the water of PVA cryogels which were prepared by repeated freeze/thawing cycles, were studied by SEM, rheology and NMR spectroscopy. Obvious changes of rheological properties can be observed after different numbers of freeze/thawing cycles used for preparation of PVA cryogels (Fig. 3.8). The strain was controlled at 1 % to ensure linear viscoelasticity. 8.3 wt-% PVA-195k samples exhibit Newtonian liquid viscous behavior in which the loss modulus G´´ is larger than the storage modulus G´ over the entire frequency range and the ratios of G´´ and G´ are constant over the frequency range used. PVA solutions that experienced one freeze/thawing cycle displayed viscoelastic behavior. A crossover of G´ and G´´ appeared at high frequencies, which indicated that this gel has weak elastic properties and shows more viscous properties at higher shear rates. With increasing the number of freeze/thawing cycles, the storage modulus G´ increased faster than the loss modulus G´´; and tan δ presenting the ratio of viscous and elastic modulus decreased obviously. Both changes implied that the elasticity of PVA cryogel grew up very quickly with more freeze/thawing cycles. The storage modulus G´ of PVA cryogel prepared with 3 freeze/thawing cycles is almost independent of frequency, which indicated the deformation imposed on the network of PVA cryogel is reversible. PVA cryogels behaved like linear-elastic Hooke materials. After repeated freeze/thawing cycles, much more energy was stored in the PVA cryogels, which became fragile and much more stress is needed for the deformation of samples. The promotion of elasticity was based on more PVA crystals as physical connections formed in PVA cryogel by repeated freeze/thawing processes.

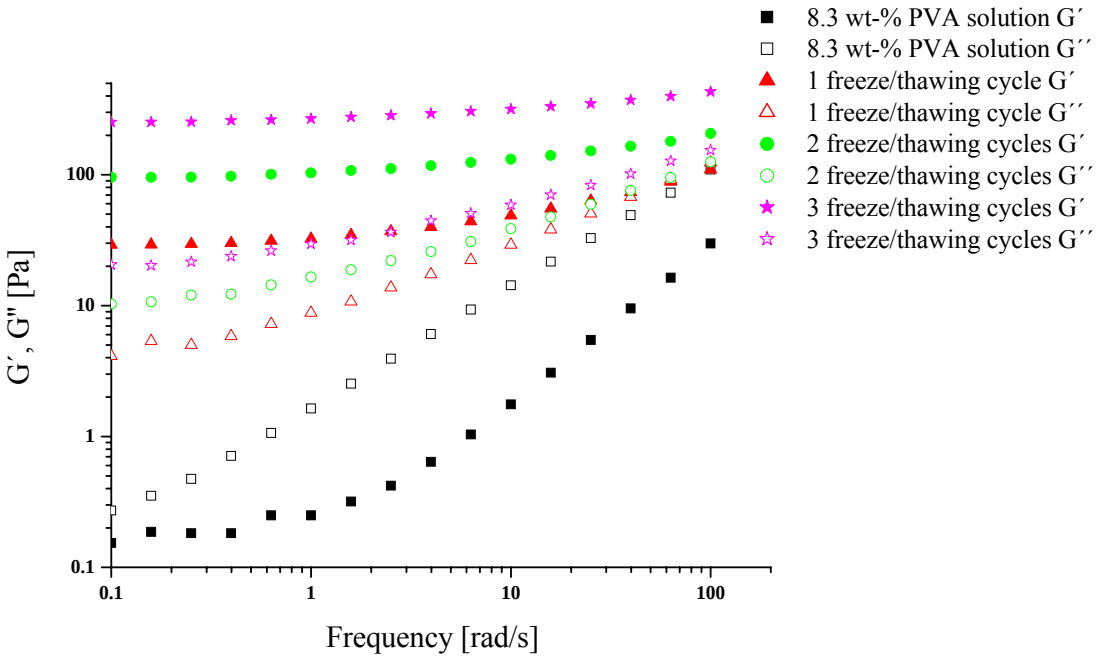


(a)

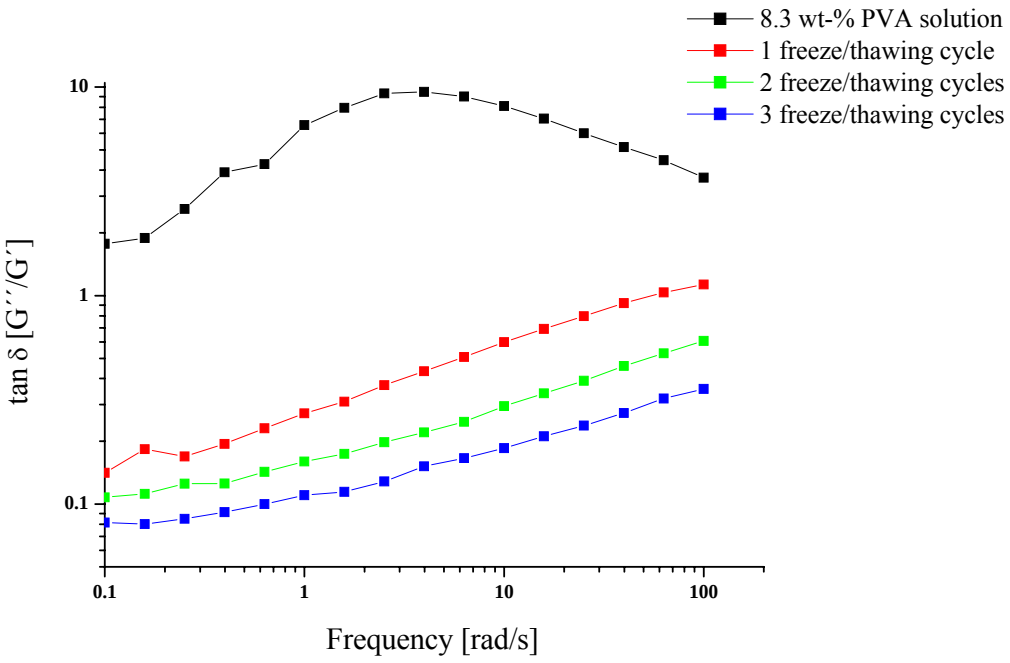


(b)

Figure 3.8: Rheological characterization of 8.3 wt-% PVA-195k cryogel prepared by 1 to 3 freeze/thawing cycles (-32 °C, 60 min/20 °C, 60 min) (a) G´, G´´ as a function of angular frequency (filled symbol – G´, empty symbol – G´´), (b) tan δ as a function of angular frequency.

Measurements of the spin-spin ($T_2$) relaxation time with magnetic resonance are useful for studying specific interactions between macromolecules and water. The polymer molecular mobility and the state of water in PVA cryogels have been revealed by $^1H$ pulse NMR measurements. Only one component can be observed in Fig. 3.9, which was spin–spin relaxation time ($T_2$) distributions of the PVA cryogels prepared by dissolving in $D_2O$ with freeze/thawing cycles. Three discrete components appeared in Fig. 3.10, which were spin–spin relaxation time ($T_2$) distributions of the PVA cryogels prepared by dissolving in $H_2O$ with repeated freeze/thawing cycles. The component in Fig. 3.9 and the first two components in Fig. 3.10 have the similar $T_2$ distribution between 5 ~ 100 ms in lower relaxation mode. They are considered as the spin–spin relaxation times of the PVA cryogel matrix. The component distributed in the range of 400 ~ 1500 ms in Fig. 3.10 is the spin–spin relaxation time ($T_2$) distribution of $H_2O$ in PVA cryogels. All curves shifted to lower relaxation modes with increasing the number of freeze/thawing cycles that indicated the loss of molecular mobility as the increase of elastic properties of PVA cryogels. Water exists in PVA solutions in two states: bound and unbound state. The $T_2$ peaks of $H_2O$ shifted to shorter relaxation time as a result of water bound to the PVA cryogel matrix, which became more rigid with repeated freeze/thawing cycles. The water mobility in PVA cryogels is dependent on the number of freeze/thawing cycles. From spin–spin relaxation times of the PVA cryogel matrix (Fig. 3.11), it was found that there are two different fractions in the polymer part of the PVA cryogels (solvent $H_2O$). The $T_2$ signal in the lower relaxation time range (5 – 20 ms) was from the crystallized PVA rigid part in PVA cryogels. The $T_2$ signal between 50 – 80 ms indicated water bound mobile polymer chains, which behave more mobile than physical crosslinked PVA chains.

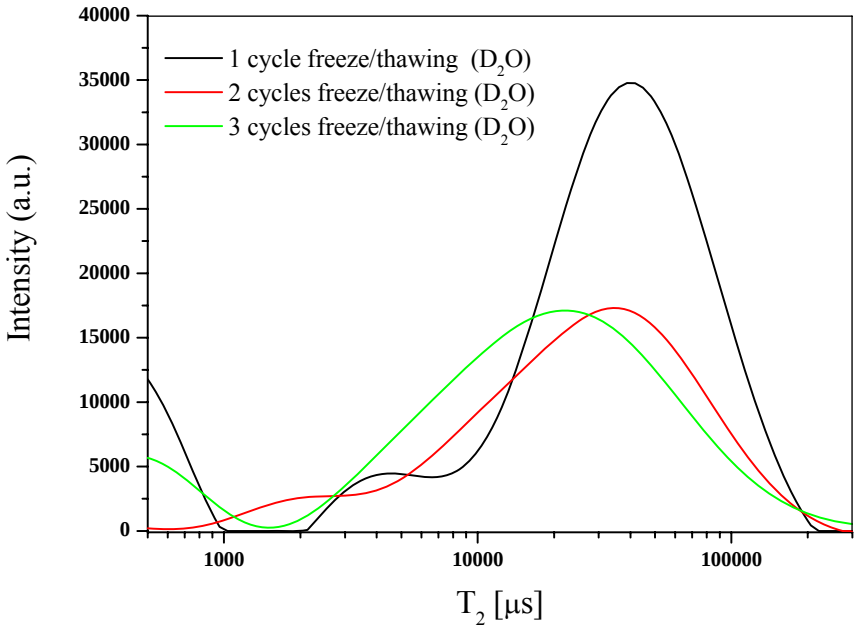


Figure 3.9: Spin–spin relaxation time ($T_2$) signal of PVA-195k cryogels (solvent $D_2O$, 1 to 3 freeze/thawing cycles (-32 °C, 60 min/20 °C, 60 min)) by $^1H$ pulse NMR measurements.

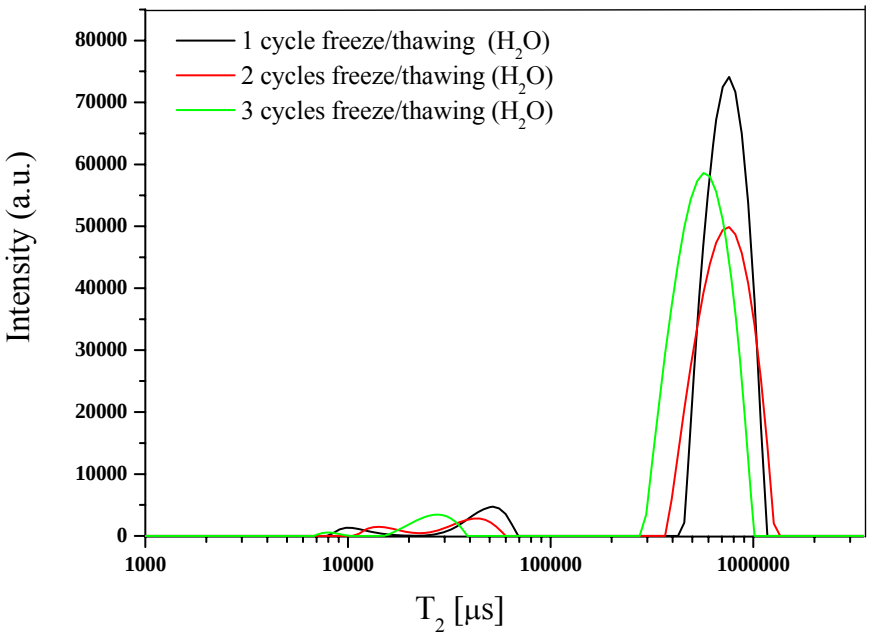


Figure 3.10: Spin–spin relaxation time ($T_2$) signal of PVA polymer chain in PVA cryogels (solvent $D_2O$, 1 to 3 freeze/thawing cycles (-32 °C, 60 min/20 °C, 60 min)) by $^1H$ pulse NMR measurements.

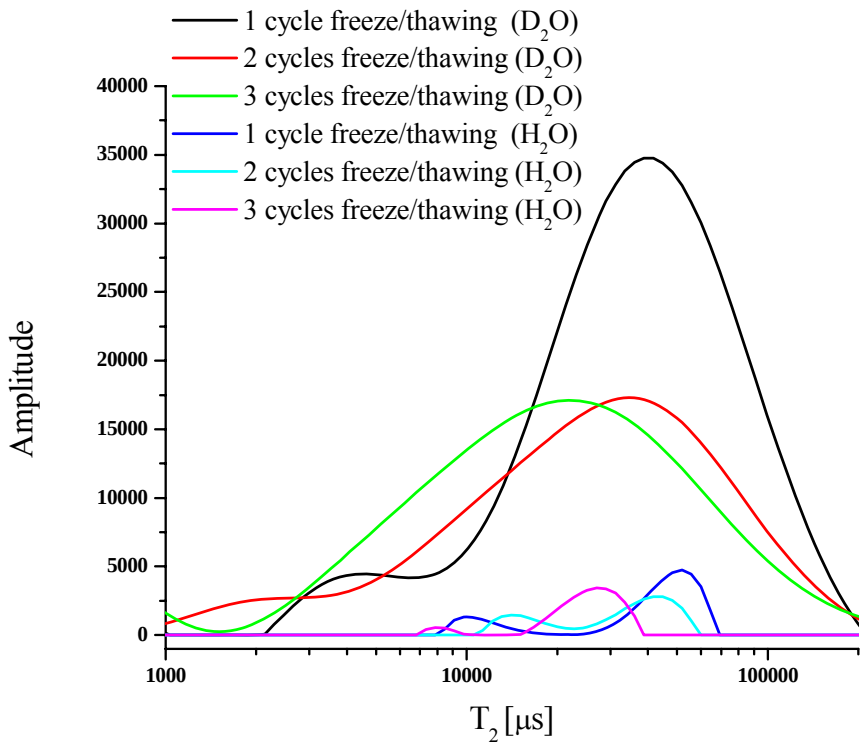


Figure 3.11: Spin–spin relaxation time ($T_2$) signal of polymer part of PVA cryogels (solvent $D_2O$ or $H_2O$, 1 to 3 freeze/thawing cycles (-32 °C, 60 min/20 °C, 60 min)) by $^1H$ pulse NMR measurements.

The formation of the polymeric network in PVA cryogel is determined by conditions of freeze and thawing, storage in the frozen state and the number of freeze/thawing cycles. The final products of PVA cryogenic gelation have a porous polymer matrix (Fig. 3.12). Pores left in freeze-dried PVA cryogels were the traces of crystals of ice. Ice crystals grew up and leave bigger pores in PVA cryogel after repeated freeze/thawing. The growth of ice crystal in PVA cryogel forced polymer-rich regions to connect tightly, that process promoted the formation of PVA crystals in the PVA cryogel matrix and reduced the volume fraction of the polymer-rich region to the polymer-poor region. The PVA cryogel matrix became a sharper border around pores after more freeze/thawing cycles. The shrunken volume fraction of the polymer-rich regions can be observed in Fig. 3.12 (b) of the PVA cryogel prepared by 10 freeze/thawing cycles.

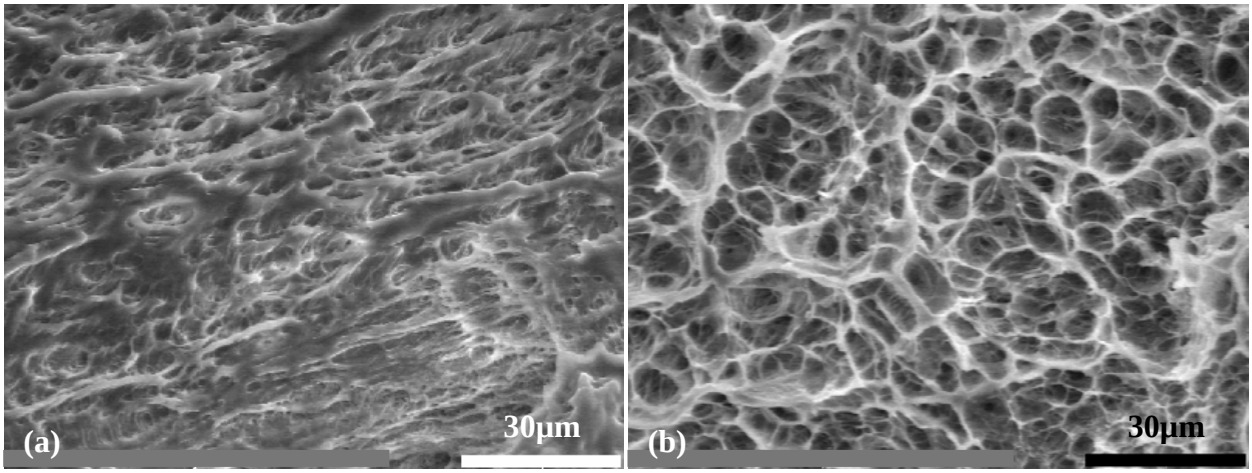


Figure 3.12: SEM images of the broken surface of freeze-dried PVA cryogel (a) 8.3 wt-% PVA-195k underwent 1 freeze-thawing cycle (-32 °C, 60 min/22 °C, 60 min), (b) 8.3 wt-% PVA-195k underwent 10 freeze-thawing cycles (-32 °C, 60 min/22 °C, 60 min).

### 3.4.2 Effective ice nucleation agents applied for production of PVA cryogel

#### 3.4.2.1 Water crystallization temperature of PVA aqueous solutions

The water supercooling phenomenon can be observed when PVA aqueous solution is frozen at subzero temperatures to produce PVA cryogel. Water crystallization temperatures of 1, 2, 3, 4, 5, 6, 7, 8.3 and 10 wt-% PVA-195k aqueous solutions were investigated by DSC measurements (cooling rate -1 K/min). Water crystallization temperatures scatter in the range of -18 to -24 °C (Fig. 3.13) and are independent of concentrations of PVA in aqueous solutions.

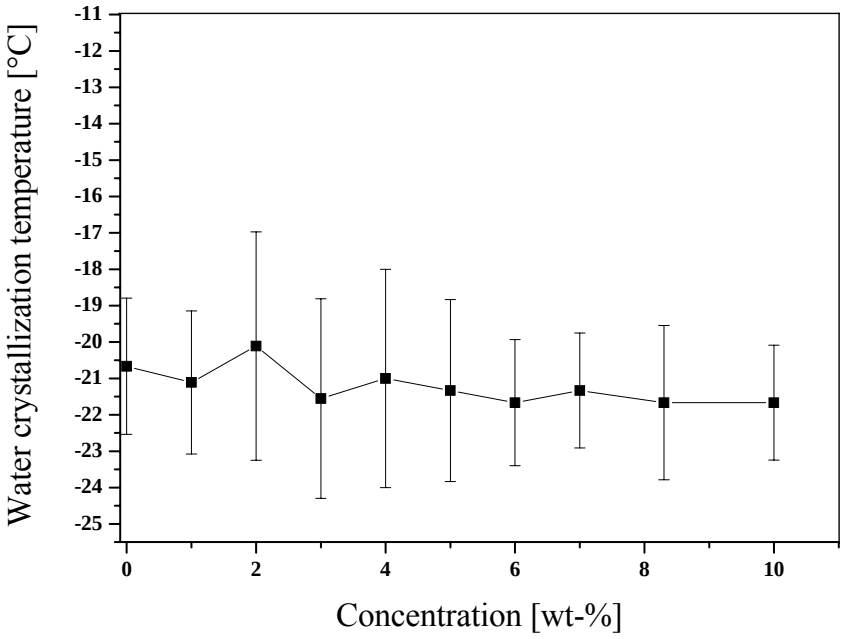


Figure 3.13: Distribution of water crystallization temperatures of different concentrations of PVA in aqueous solutions.

### 3.4.2.2 Water crystallization ability of ice nucleation agents in PVA aqueous solution

Ice nucleation agents are added into PVA aqueous solutions for medical application. Several biocompatible ice nucleation agents were chosen to test the water crystallization ability for the production of PVA cryogel. Silver iodine (AgI) has a similar crystalline structure as ice and has the longest history of use as ice nucleation agent for making rain and snow. But it is poisonous. Here AgI is a reference to estimate the supercooling release capacity of other ice nucleation agents. Water crystallization temperatures of all tested ice nucleation agents in 8.3 wt-% PVA-195k solution were detected by DSC measurements (cooling rate -1 °C/min) and listed in Tab. 3.2 and compared with silver iodine. According to the solubility of amino acids in water, the oversaturated amino acids/PVA solutions were prepared (see Tab. 3.2). Since AgI and long chain aliphatic alcohols are water insoluble, suspensions with PVA solutions (0.1 g/100 ml 8.3 wt-% PVA) were prepared for tests. AgI, triacontanol, heptacosanol and L-aspartic acid which were green marked in Tab. 3.2 can promote water crystallization in PVA solution at subzero temperatures (Tab. 3.2 and Fig. 3.14).

DSC exothermal peaks in cooling traces indicated that AgI and long-chain aliphatic alcohols exhibited similar water crystallization ability in PVA solution, whose onsets of water crystallization are at around -11 °C. The most effective ice nucleation agent in all tested

substances is L-aspartic acid, whose onset of water crystallization is at around - 5.5 °C. Other amino acids show slight or no effect on water crystallization of PVA solution.

Table 3.2: Water crystallization temperatures of 8.3 wt-% PVA-195k aqueous solutions added with silver iodine, different aliphatic long-chain alcohols and amino acids (detected by DSC).

| Name | solubility ($g/dl\ H_2O$, 25 °C) | Concentration (g/dl 8.3 wt-% PVA) | Supercooling point ( °C) |
|---|---|---|---|
| Triacontanol | - | 0.1 | -11 ± 1 |
| Heptacosanol | - | 0.1 | -9.7 ± 0.6 |
| L-Leucine | 2.43 | 3 | -20 ± 4 |
| L-Tryptophan | 1.136 | 2.5 | -22 ± 1.5 |
| L-Cystine | 0.011 | 0.2 | -17.7 ± 0.6 |
| L-Aspartic acid | 0.778 | 0.9 | -6.3 ± 0.6 |
| L-Glutamic acid | 0.864 | 1 | -20 ± 3 |
| L-Isoleucine | 4.117 | 5 | -20.7 ± 3.2 |
| L-Tyrosine | 0.0453 | 0.08 | -20 ± 3.6 |
| L-Asparagine | 3.53 | 4 | -19.6 ± 0.7 |
| Silver Iodine | - | 0.1 | -11.3 ± 0.6 |

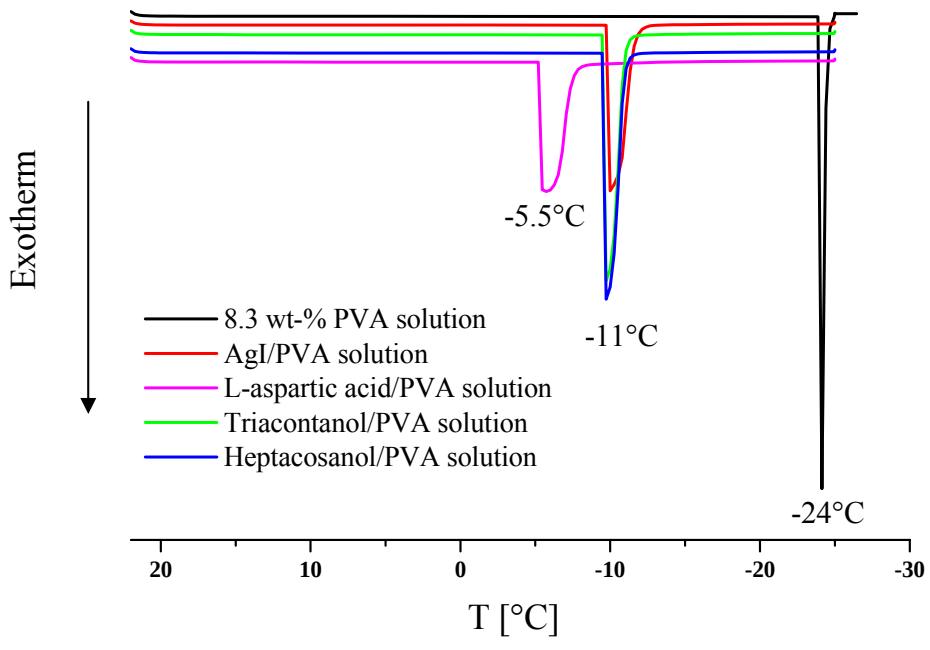


Figure 3.14: DSC cooling traces of water crystallization of 8.3 wt-% PVA-195k aqueous solution added with effective ice nucleation agents (AgI, triactontanol and heptacosanol: 0.1 g/dl, and l-aspartic acid: 0.9 g/dl; cooling to -25 °C, -1 °C/min).

### 3.4.2.3 Critical concentration of L-aspartic acid as ice nucleation agent

The effect of concentration of L-aspartic acid for the promotion of water crystallization of PVA aqueous solution was investigated by DSC measurements (Fig. 3.15). 0.2 to 0.9 g/dl L-aspartic acids in 100 ml 8.3 wt-% PVA-195k were prepared in steps of 0.1 g/100ml. The critical concentration is 0.5 g/100 ml 8.3 wt-% PVA-195 k. The ability of L-aspartic acid on preventing water supercooling of PVA aqueous solution is dependent on the concentration. However, the water crystallization activity becomes independent of L-aspartic acid concentration and remains in a plateau (-5.6 ± 0.65 °C), when the critical concentration is reached.

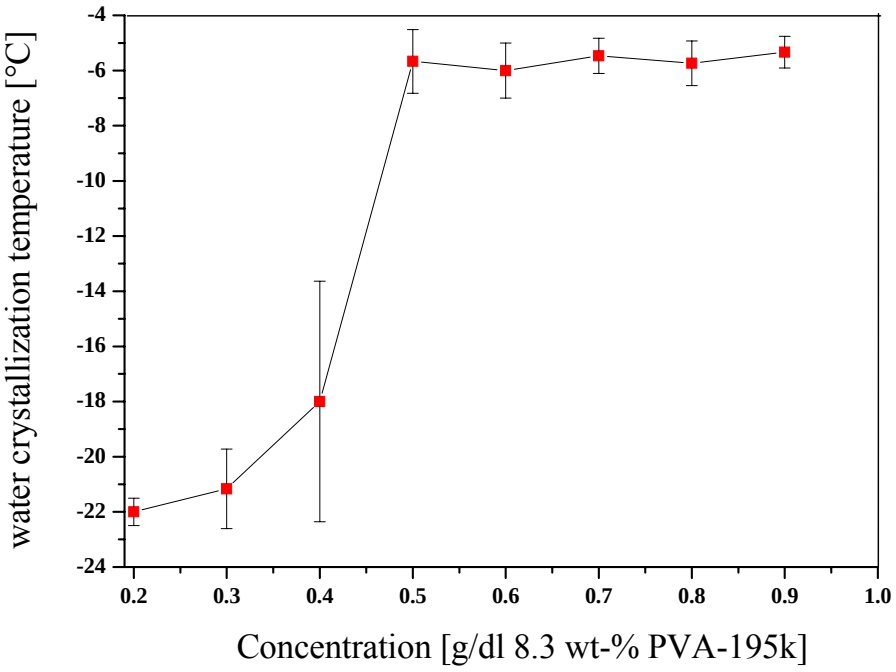


Figure 3.15: Water crystallization activity of L-aspartic acid in 8.3 wt-% PVA-195 k solutions (detected by DSC, cooling to -25 °C, -1 °C/min).

## 3.4.3 PVA cryogel near gel point

The gelation of PVA aqueous solution by freeze/thawing processing is attributed to the crystallization of PVA chains as network.[96] PVA cryogel is a physically crosslinked gel, whose properties are mainly determined by the amount of PVA crystallites formed during freezing.[98] The crystallinity of PVA cryogel is related to many factors, i.e. freeze/thawing temperature, storage time, cooling/heating rate and the number of freeze/thawing cycles.[99, 100]

It is difficult to quantify the formation of PVA crystallites to control the properties of PVA cryogel. Rheological tests can characterize the mechanical properties of the hydrogel and provide indirect information about crystallinity of PVA cryogel. The sol/gel phase transition of PVA solutions was obtained by freezing at -32 °C for 30 min. But water supercooling of PVA aqueous solution results in difficulties with reproducing PVA cryogel properties near the critical gel point. Water crystallization is the most important step to affect the formation of PVA crystallites. PVA solutions cannot be crosslinked without ice formation when even kept under subzero temperature for a very long time. Homogeneous ice nucleation is stochastic, that induced different starting times of water crystallization for separately stored PVA aqueous solutions. After the same short-storing time, the properties of PVA cryogels showed very big scattering. Aiming to reproduce PVA cryogel properties near the gel point, two different methods were used to try to diminish the influence of the water supercooling phenomenon. One way is to use dry ice/ethanol bath (-78 °C) as the cooling media, which was expected to minimize the deviation of starting time of water crystallization. Another way is to use L-aspartic acid as ice nucleation agent to reduce the effect of water supercooling. L-aspartic acid has been proved to be a very effective ice nucleation agent for PVA aqueous solutions, which can promote supercooling from -20 °C to -5 °C. The dynamic oscillatory shear experiment has been used here to evaluate the mechanical properties of PVA cryogels.

#### 3.4.3.1 PVA cryogel produced in dry ice/ethanol bath

10 ml 8.3 wt-% PVA aqueous solution filled syringes were dipped into dry ice/ethanol bath (at – 78 °C) for 3 to 5 min of freezing time, then thawed at the room temperature (~ 20 °C). All PVA samples looked white after freeze treatment. After thawing, these PVA cryogels displayed different turbidity. The sample which was frozen for 5 min was opaque that is attributed to increase in size and amount of PVA crystallites after longer freezing time (Fig. 3.16, sample 4).


Figure 3.16: PVA cryogels (prepared by freezing 8.3 wt-% PVA-195k in dry ice/ethanol bath at -78 °C, thawing at 22 °C; sample 1 - frozen for 3 min 30 s, sample 2 - frozen for 4 min, sample 3 - frozen for 4 min 30 s, sample 4 - frozen for 5 min).

The shear storage moduli G´ and loss moduli G´´ of PVA cryogel are illustrated in Figure 3.17 as a function of angular frequency. Storage and loss moduli increased with extending freeze times. Initially, G′ and G″ increase in a nearly parallel manner but after some time the storage modulus starts to grow faster than the loss modulus. Eventually, G′ exceeds G″ and, at the end, G′ dominates. The sample which was frozen for 3 min, still displayed the viscous property (G´´> G´). The samples which were frozen for 3 min 30 s, 4 min and 4 min 30 s, showed viscoelastic properties; the crossover of G´ and G´´ shifted to the high-frequency range with increase in freeze times. The sample which was frozen for 5 min, showed a sharp increase in complex viscosity (Fig. 3.18); and the storage modulus G´ dominated over the loss modulus G´´ in the entire frequency range (Fig. 3.17), which indicated that the PVA cryogel lost its viscous property progressively and behaved as an elastic gel. Comparing with rheological properties of the sample which was frozen for 4 min 30 s, obvious changes in viscosity and elasticity can be observed in Fig. 3.17 and 3.18. It can be concluded from these differences that the sol/gel phase transition occurred during this short time period (freeze time between 4 min 30 s and 5 min). From the results, we can say that the problem of water supercooling can be solved by using dry ice/ethanol bath (freeze temperature -78 °C). The liquid ethanol surrounding the syringes can produce higher heat transfer efficiency than the cold air in the refrigerator and the high cooling rate reduced the influence of supercooling on the production of PVA cryogels. But the disadvantage of this method is that the sol/gel phase transition occurred in very short time scales under deep freeze temperatures and the produced PVA cryogel displayed non-homogeneous rheological properties, which can be observed by

the big scattering of the measurements of complex viscosity at 5 min samples (Fig. 3.18). The PVA solution in the center of syringes experienced shorter freeze time than PVA solution close to the wall of syringes. However, rheological properties of PVA cryogels varied with differences of only several second freezing under deep freeze temperature, which makes it difficult to control the production of PVA cryogel near the gel point accurately.

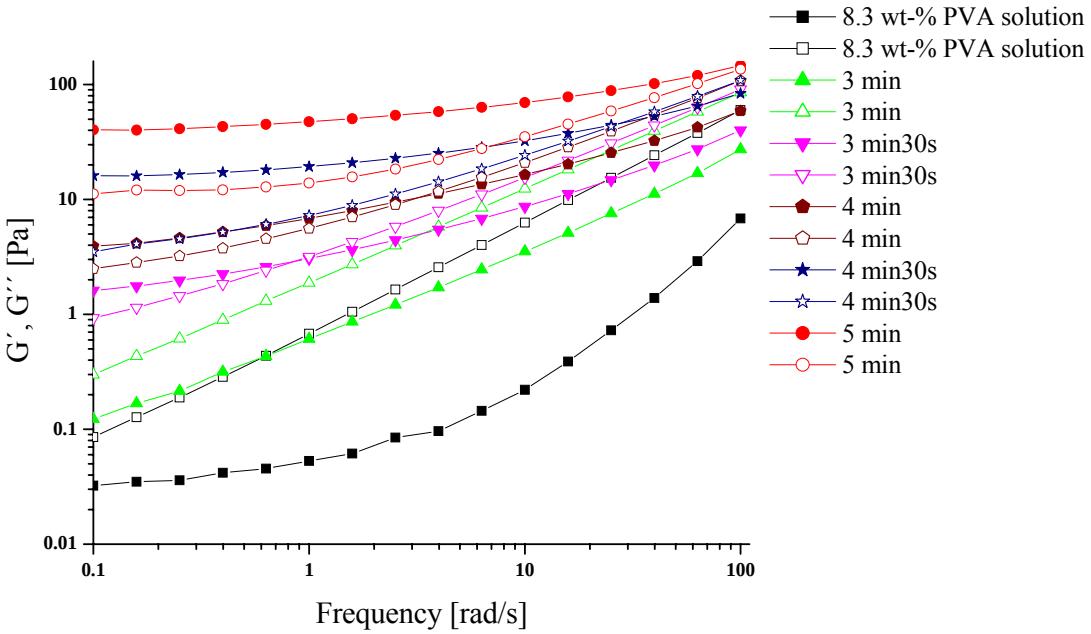


Figure 3.17: Storage and loss moduli of PVA cryogels as a function of frequency (8.3 wt-% PVA-195k produced by freezing in dry ice/ethanol bath at -78 °C for 3 to 5 min, thawing at 20 °C; G´ - solid symbol and G´´ - open symbol).

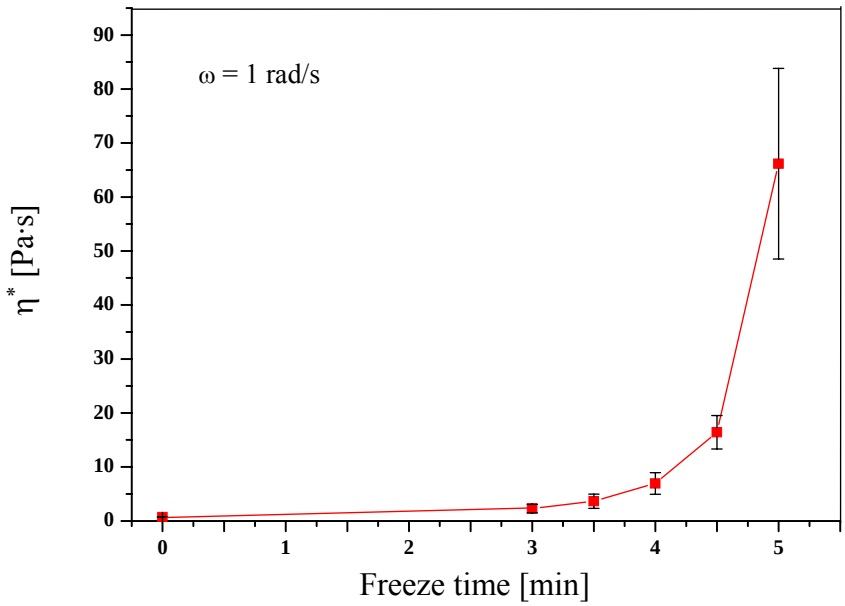


Figure 3.18: Complex viscosity of PVA cryogels (angular frequency: ω =1 rad/s) versus freeze time (8.3 wt-% PVA-195k produced by freezing in dry ice/ethanol bath at -78 °C for 3 to 5 min).

### 3.4.3.2 PVA cryogel produced by adding ice nucleation agent

It has been examined that L-aspartic acid crystals have water crystallization activity in PVA aqueous solution in previous work (Fig. 3.15). L-aspartic acid is one of the nonessential amino acids and plays an important role as general acid in enzyme active centers with a pKa of 4.0. Chemical structure and crystal morphology can been seen in Figure 3.19. Toxicity data of L-aspartic acid are ORL-RAT $LD_{50}$ 5000 mg/kg and SKN-RBT $LD_{50}$ 5000mg/kg (ORL-oral, RAT- rat, SKN- administration onto skin, RBT- rabbit, and LD 50- lethal dose 50 percent kill).[130]

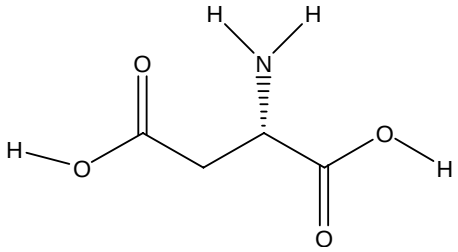


(a)

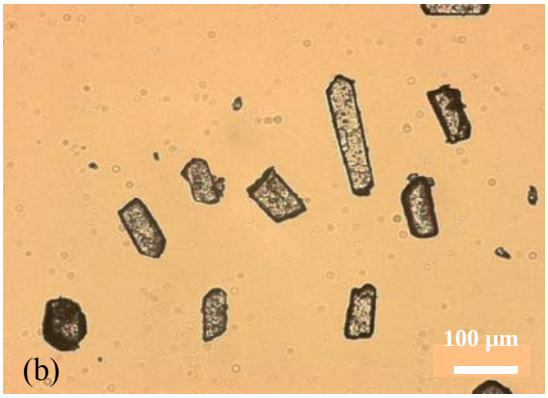


(b)

Figure 3.19: L-Aspartic acid (a) chemical structure (b) morphology under light microscope.

PVA solutions with homogenously dispersed L-aspartic acid (0.5 g/dl 8.3 wt-% PVA-195k) were filled into 10 ml syringes. PVA cryogel samples were prepared by using different freeze temperatures (-5 ~ -32 °C) and freeze times (15 min to 5 h). The water crystallization of 8.3 wt-% PVA-195k aqueous solution occurs usually at around -20 °C. Water supercooling phenomena of 8.3 wt-% PVA aqueous solutions can be released from -20 °C to -5 °C by adding L-aspartic acid (Fig. 3.20). The morphology of L-aspartic acid in PVA cryogels was detected by SEM. Small L-aspartic acid crystals are dispersed in the pores of freeze-dried PVA cryogel (Fig. 3.21).

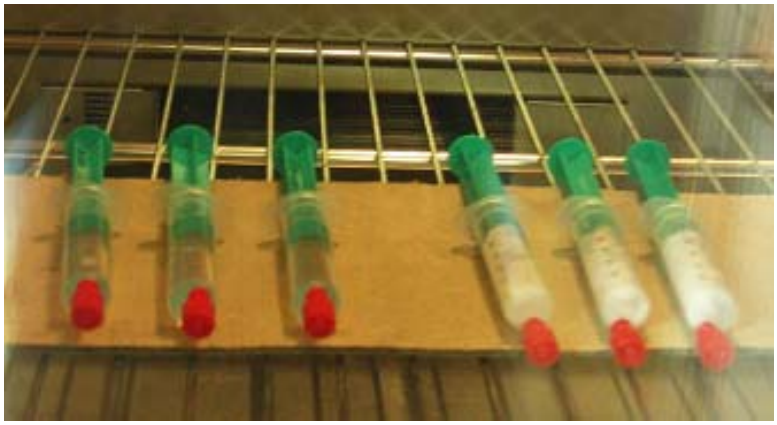

Figure 3.20: Supercooled PVA aqueous solution (left 3 syringes) and water crystallized PVA aqueous solution added with water nucleator (right 3 syringes) (0.5 g L-aspartic acid/dl 8.3 wt-% PVA-195k , in the climate chamber at -13 °C).

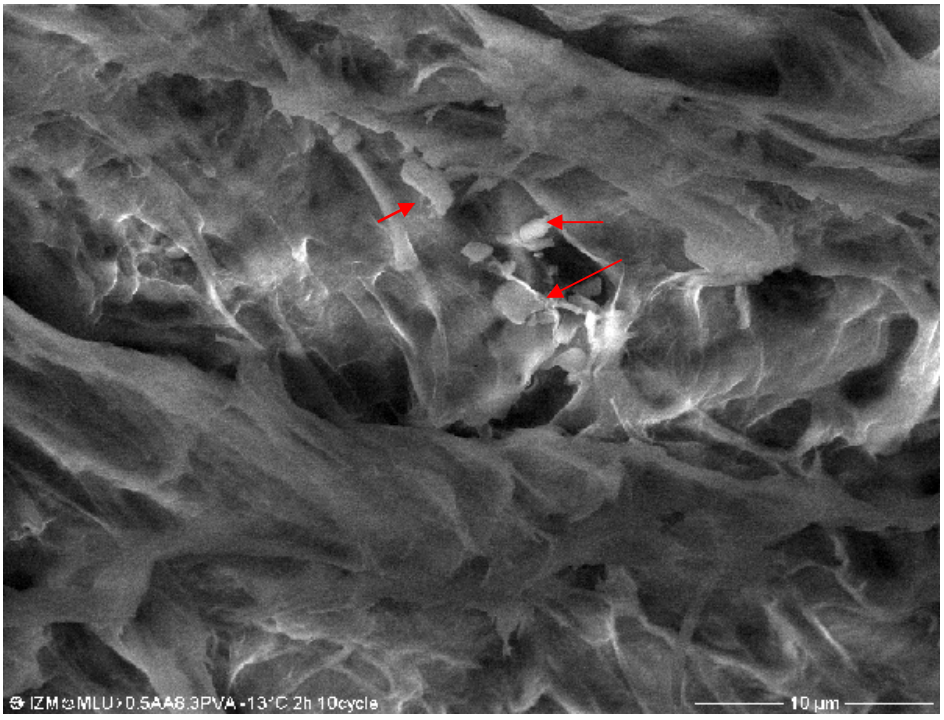


Figure 3.21: Scanning electron micrographs (SEM) of the broken face of freeze-dried PVA cryogel – the arrows indicate crystals of L-aspartic acid (0.5 g L-aspartic acid/dl 8.3 wt-% PVA-195k after 10 freeze/thaw cycles (-13 °C, 2 h/20 °C, 2 h)).

PVA cryogels near the gel point are expected to be reproduced by adding L-aspartic acid after applying an identical freeze/thawing process. Oscillatory dynamic mechanical measurements were performed on PVA cryogels. The results of the total resistance of the samples to oscillatory shear (complex moduli G*) are shown in Fig. 3.22. The plot shows the evolution of complex moduli G* data at different freeze temperatures. As the freeze temperature decreased and freeze time prolonged, the complex moduli G* increased and reached a plateau

value after respective freeze time at different freeze temperatures. Before reaching the relative stable state, complex moduli G* increased obviously with extending freeze time. After some critical freeze time, the complex modulus G* of PVA cryogels was still in a stable state even extending the freeze time. It can be concluded that crystallization of PVA is mainly affected by freeze temperature (or cooling rate), lower freeze temperatures (or high cooling rates) promote the formation of PVA crystallites and produce more elastic PVA cryogels.

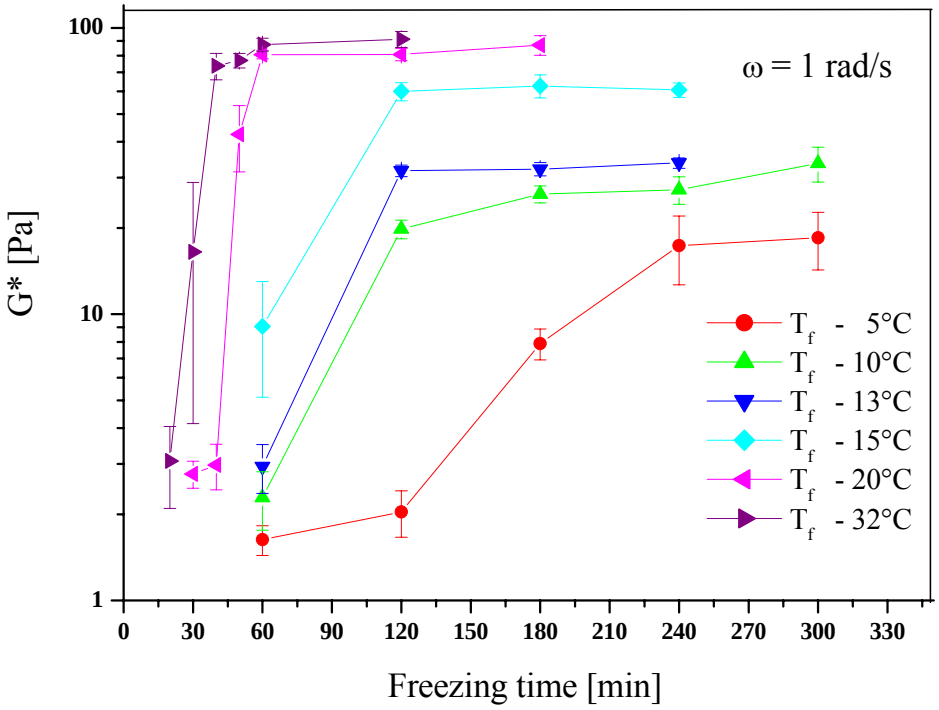


Figure 3.22: Complex modulus G* of PVA cryogels produced by using different freeze temperatures vs. freeze time (0.5 g L-aspartic acid/100ml 8.3 wt-% PVA-195k, angular frequency: ω = 1 rad/s).

The properties of PVA samples can reach the stable state after 2 h freezing by one freeze/thawing cycle. PVA cryogels prepared at different freeze temperature for 2 h freezing were used to study the sol-gel transition (critical gel point) (Fig. 3.23). The way of defining the gel point was experimentally examined for PVA solutions that underwent a sol-gel transition upon freezing. The rheological behavior before, near, and beyond the sol-gel transition as a function of the freeze temperature was observed. The crossover of G´(ω) and G´´(ω) was once used as an indicator of the gel point. Actually, it is not an accurate way, while the crossover only indicates that the tested material has both viscous and elastic

properties over the entire frequency range. The crossover can shift from low frequency to high frequency with increase in elasticity. The frequency-independence of tan δ is known as a useful method to determine the gel point.[131-133]

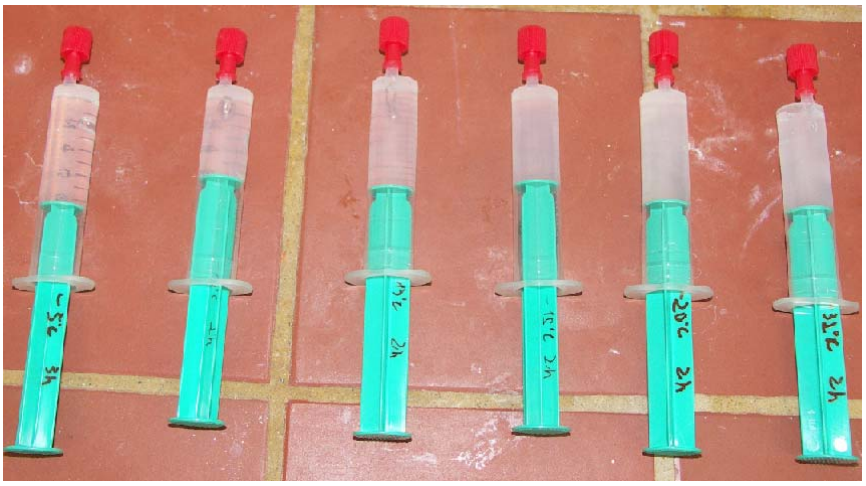

Figure 3.23: PVA cryogels prepared by using different freeze temperature in the climate chamber (0.5 g L-aspartic acid/100ml 8.3 wt-% PVA-195k, freeze temperature from left to right -5, -10, -13, -15, -20 and -32 °C, freeze time 2 h).

From the oscillatory shear experiments, the logarithmic plots of G′ and G′′ against frequency are shown in Figure 3.24. The gel point of PVA cryogel can be determined by observing a frequency-independent tan δ obtained from a multifrequency plot of tan δ as a function of freeze temperature (Fig. 3.25). The loss factor (tan δ) reveals the ratio of the viscous and the elastic parts of the viscoelastic deformation behavior. Tan δ decreased with decrease in freeze temperature, which indicated that the elasticity of PVA cryogel grew up after cryogenic treatment at lower temperatures. 8.3 wt-% PVA-195k solution (with L-aspartic acid) displayed three states during one freeze/thawing cycle treatment at different freeze temperature: i) a sol state where tan δ >1, the PVA system is dominated by the loss modulus G′′ over the entire frequency range (Fig. 3.25, sample -5 °C), which indicated that the systems were still fluid solution; ii) a viscoelastic state where tan δ < 1 in the low-frequency range, the crossovers of G′ and G′′ can be observed (Fig. 3.25, sample -10 °C, -13 °C, -15 °C), the system is dominated by elasticity in the low-frequency range and the viscous property in the high-frequency range after the point of crossover, the shift of crossovers of G′ and G′′ to the high-frequency range indicated that the elasticity of the PVA system grew up with increase in crystallization of PVA at lower freeze temperatures; iii) a gel state where tan δ < 1 over the entire frequency range, G′ increased and dominated over G′′ (Fig. 3.25, sample -20 °C, -32 °C), the PVA system exhibited elastic properties. Polymers during their liquid-solid

transitions develop a rheological behavior which is distinct from that of liquids or solids. As the system goes through the gelation process, tan δ fell off obviously from -13 °C to -15 °C. Complex viscosity $\eta^*$ showed a consistent divergence in the temperature range from -13 °C to -15 °C (Fig. 3.26). A high value for the complex viscosity means the greater resistance to flow in the crosslinked state, which indicated the divergence of the apparent molar mass to infinite. At the same time mobile PVA chains were constrained in the crystallized PVA matrix and lost fluidity. More PVA crystallites reinforced the elasticity of the PVA cryogel. It was also found that the sol/gel transition of 8.3 wt-% PVA-195k solution occurred in the range of freeze temperatures from -13 °C to -15 °C. Tack properties of PVA cryogels were tested on smooth glass slides, which also provide the evidence of the sol/gel transition. As the crosslink density is increased beyond the gel point, the strength of the network increases (stronger cohesion) while the adhesive strength decreases. PVA cryogel prepared at -13 °C showed good tack on the slide, but PVA cryogel prepared at -15 °C could not stick on the slide under slight push force (Fig. 3.27). Beyond sol/gel transition, PVA cryogel gained more elasticity and lost the polymer chains mobility with more crosslinks of PVA crystallites. PVA cryogel that possesses the maximum tack (corresponding to adhesive strength) can be obtained by freeze 0.5 g aspartic acid/100ml 8.3 wt-% PVA-195k at – 13 °C for 2 h.

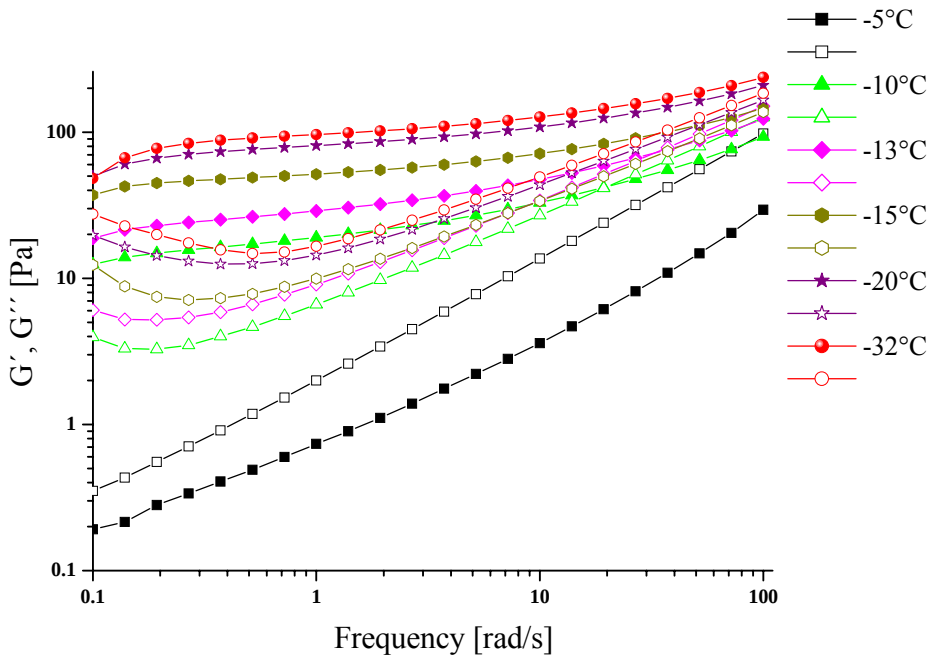


Figure 3.24: Storage modulus G′ (solid symbol) and loss modulus G′′ (open symbol) of PVA cryogels as a function of angular frequency for different freeze temperatures (0.5 g l-aspartic acid/100ml 8.3 wt-% PVA-195k, freeze time 2 h).

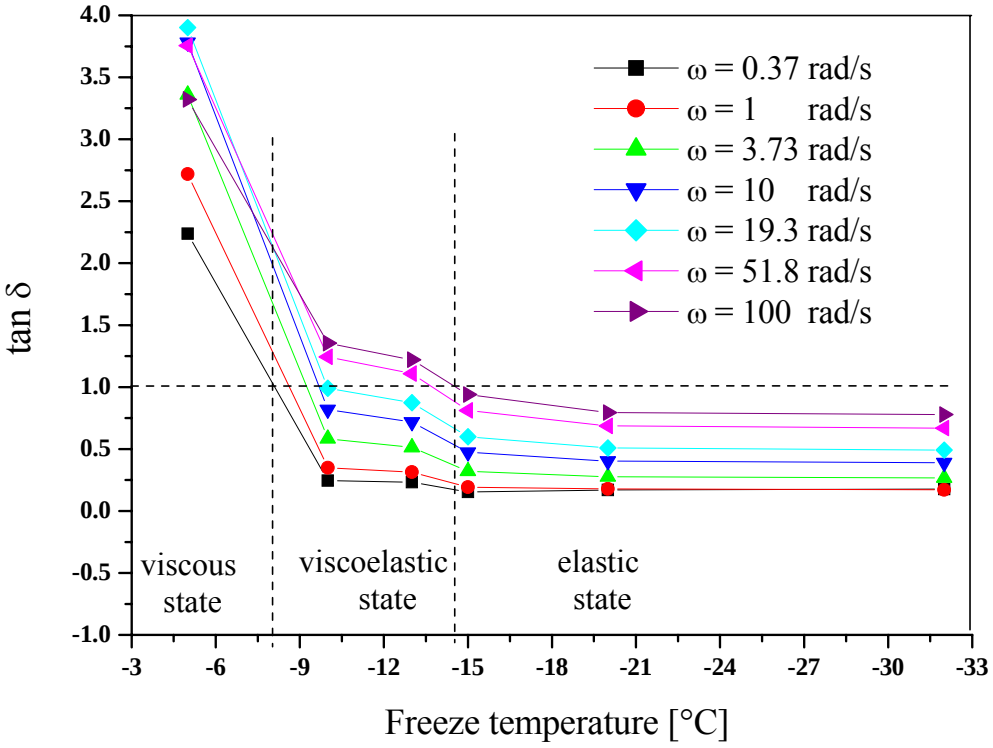


Figure 3.25: Loss tangent (tan δ) as a function of freeze temperature (0.5 g L-aspartic acid/100ml 8.3 wt-% PVA-195k, freeze time 2 h).

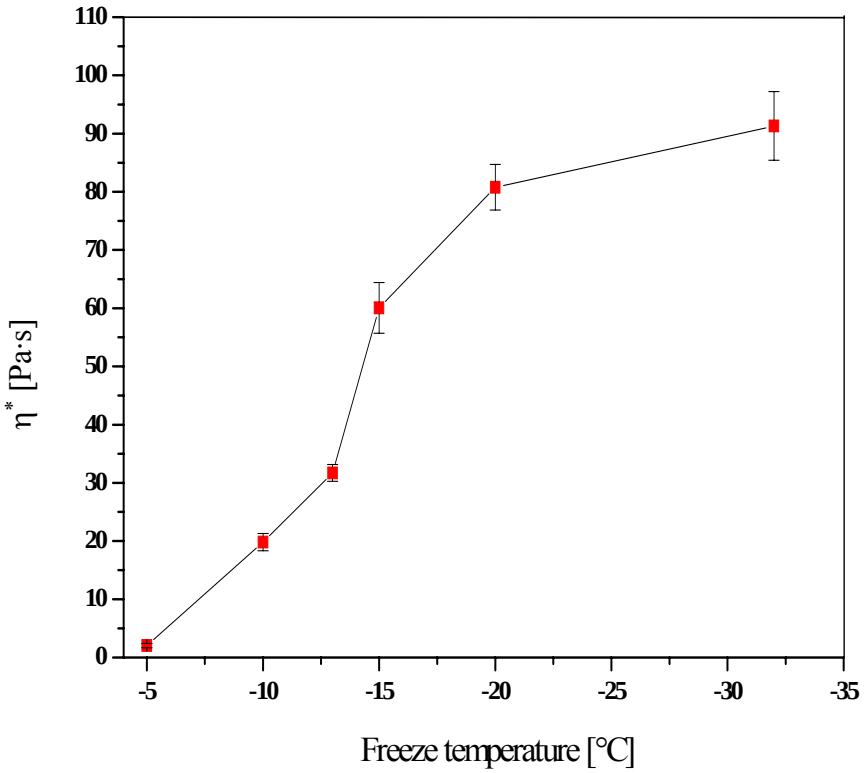


Figure 3.26: Complex viscosity $\eta^*$ as a function of freeze temperature (0.5 g L-aspartic acid/100ml 8.3 wt-% PVA-195k, freeze time 2 h, angular frequency: ω = 1 rad/s).

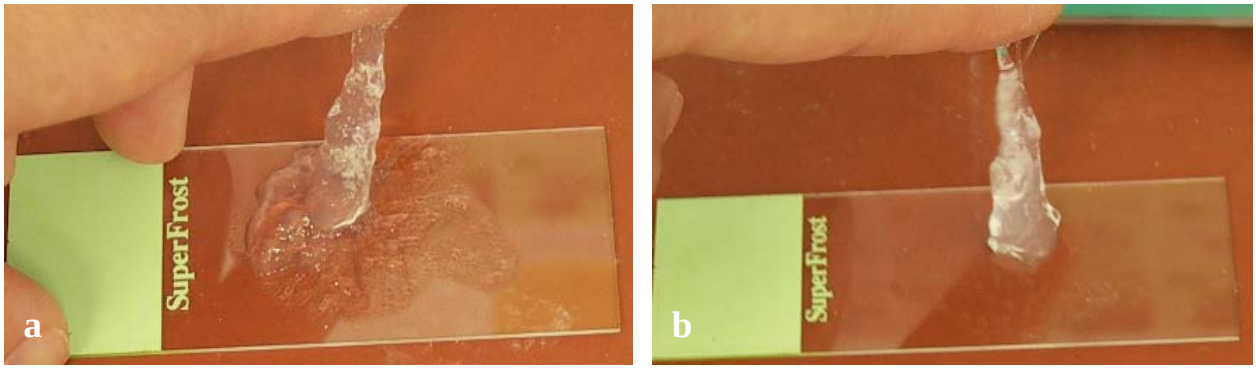


Figure 3.27: Tack tests of PVA cryogel near gel point on glass slide (a) high tack PVA cryogel (0.5 g L-aspartic acid/100ml 8.3 wt-% PVA-195k , freeze temperature -13 °C, 2 h) (b) low tack PVA cryogel (0.5 g L-aspartic acid/100ml 8.3 wt-% PVA-195k, freeze temperature -15 °C, 2 h).

## *3.5 Conclusion*

Polymer gels have both solid and liquid-like properties. Once the polymer system is cross-linked, either chemically or physically, the polymer chains lose their individual identity and become a large three-dimensional interconnected network spreading through the entire volume of the sample. The physical gel, crosslinked by crystallized polymer, comprises polymer melts and solvents in which network junctions are formed by small crystalline regions. The PVA physical gelation process goes from Newtonian liquids to viscoelastic PVA cryogel by freeze/thawing treatment. The behaviour of freeze/thawing PVA cryogel was studied by using rheometer, $^{1}H$ pulse NMR spectroscopy and SEM. The different data obtained are consistent. The mechanical properties of PVA cryogel improve with increasing fraction of crystallized PVA. An increase of the storage modulus G´ and a decrease of the loss angle tan δ (< 1) indicated that PVA cryogels became more elastic with increasing numbers of freeze/thawing cycles. The repeated cryogenic treatment induces an increase in the degree of crystallinity in the polymer-rich phase together with an increase in the storage modulus. The analysis of the $T_2$ relaxation times showed that the PVA polymer chains and the water behaves differently in different PVA cryogels which are formed in $H_2O$ or $D_2O$ and by different numbers of freeze/thawing cycles. The NMR spin-diffusion data show three main fractions in the PVA cryogel system: two low intensity factions ($T_2$ 5 – 80 ms) are from polymer rich regions of PVA cryogel indicating two different states of polymer in PVA

cryogel – crystallized PVA and mobile PVA chains; the fraction at high $T_2$ relaxation time (400 – 1500 ms) is from the polymer poor region – the water rich phase. The mobility of all molecules decreases with increasing numbers of freeze/thawing cycles, since the crystalline regions act as crosslinks which connect the molecules into a spanning network. The porosity of PVA cryogels is determined by crystals of the frozen solvent. The repeated freeze/thawing is regarded as a kind of refinement process for ice crystals, polymer chains as impurity were rejected from the growing ice crystals when the PVA-water system is frozen. Thus, with increasing freezing cycle numbers, more PVA crystallites are formed in the PVA-rich solution phases inducing the release of bound water that also promoted the growth of ice crystals. The SEM observations reveal that the structure of the pore walls goes from thick to fine with repeated freeze/thawing treatment due to increase of crystallinity of PVA. The pore size increases with repeated freeze/thawing cycles. Crystallinity of PVA cryogels increased with increasing freeze/thawing cycles, inducing the increase of elastic properties.

All results mentioned above indicated the importance of water crystallization for the formation of PVA cryogel. Water supercooling phenomenon can cause practical difficulties in obtaining reproducible PVA cryogels. Water crystallization temperatures scatter in the range of -18 to -24 °C and are independent of increasing concentrations of PVA aqueous solution when no nucleation agents were added to the system. To control the reproducible processing of PVA cryogels near gel point accurately, some potential biocompatible ice nucleation agents are studied in this work. Long-chain aliphatic alcohols (triacontanol and heptaconsanol) and one kind of amino acid, L-aspartic acid, have been identified to promote water crystallization of 8.3 wt-% PVA aqueous solutions. Heptaconsanol nucleates water at -10 °C and triacontanol nucleates water at -11 °C. Both aliphatic long-chain alcohols have similar water crystallization activities as silver iodine. L-aspartic acid can nucleate water at around -5 °C, and exhibits better water crystallization activity than silver iodine and long-chain aliphatic alcohols. The critical concentration of water crystallization activity of L-aspartic acid for 8.3 wt-% PVA-195k aqueous solution is 0.5 g/100 ml. L-aspartic acid saturates at this concentration. The existence of L-aspartic acid crystals is essential to water crystallization.

The kinetic features of PVA cryogenic gelation are related to the freeze temperature, freeze storage time and number of freeze/thawing cycles. Thawing regimes have been demonstrated to be another key parameter controlling the properties of PVA cryogel. The slower the thawing rate, the stronger is the cryogel sample formed. To simplify the production of PVA cryogels, all samples were thawed under identical conditions at room temperature. The defrosting time is around 1.5 h. PVA solutions exposed to lower freeze temperature showed

more elastic PVA cryogel properties. The rheological properties of PVA cryogel tend to reach a stable state after applying the respective critical freeze time for different freeze temperatures. If the freeze temperature is lower, it reaches more quickly a stable state. As water crystallization occurred, the homogeneous PVA solution was separated into polymer-rich region and polymer-poor region; polymer chains as impurities were expelled to aggregate in high density regions, in which PVA crystallites were formed more easily and quickly. The amount of PVA crystallites increased with increase in freeze time, until the equilibrium was reached. Lower freeze temperatures provide higher cooling rates which can reduce the size of ice crystals. The ice crystals are smaller, the total numbers of ice crystals is larger; which can promote the separation of polymer chains from the solvent and the formation of more crosslinked PVA.

The gel point of PVA cryogel was detected by studying the properties of the PVA cryogels in the stable state, which are produced by freezing 8.3 wt-% PVA-195k aqueous solution (added with 0.5 wt-% L-aspartic acid) at different freeze temperatures (-5, -10, -13, -15, -20, and -32 °C) for 2 h and thawing at 20 °C. The gel point of PVA physical cryogel can be characterized by a dramatic change in the rheological properties. The divergence of frequency-independence of tan δ and complex viscosity indicated the sol/gel phase transition area of 8.3 wt-% PVA-195k between freeze temperatures of -13 to -15 °C after 2 h freezing. The samples close to the gel point combine the surface wetting property of liquids with the cohesive strength property of solids and possess the maximum tack. PVA cryogels produced at -13 °C exhibit good adhesive ability on glass slides. PVA cryogels, produced at -15 °C beyond the gel point where all polymer chains were connected into the network, exhibited the properties of an elastic gel and a loss of the surface wetting properties of liquids. The properties of PVA cryogel near gel point can be reproduced by freeze 0.5 g L-aspartic acid/100 ml 8.3 wt-% PVA 195-k at -13 °C for 2 h.

# Chapter 4

# 4 Preparation of micro-size and nano-size poly(vinyl alcohol) particulate powder using the emulsion-diffusion method

## *4.1 Introduction*

### 4.1.1 General introduction

Poly(vinyl alcohol) is the largest volume, synthetic, water-soluble and biodegradable resin produced in the world. Due to its very low toxicity, PVA has been widely used for biomedical applications. PVA cryogel as a potential postoperative anti-adhesion agent has been studied in previous work. The present work is to try to produce micron-size or submicron-size particulate PVA powders. Polymeric microspheres have a variety of applications in medical and industrial areas since they provide a large surface area and can be handled easily. The PVA powders are expected to have a better solubility in water than original PVA flakes, which could be applied directly on the surfaces of injured tissues by spray to form a barrier separating them. Microparticles or nanoparticles of synthetic and natural polymers have been extensively investigated for arterial embolic agents or drug delivery systems for several decades.[134-136] Synthetic polymers are now most commonly used for medical applications as they are more versatile (in terms of the ease with which their physical and chemical properties can be altered), generally cheaper and have a higher purity than natural polymers.[137, 138] Several methods for the preparation of particulate drug delivery systems were developed, such as single and double emulsification-solvent evaporation method,[139] emulsion – diffusion technique,[140] spray drying,[141, 142] interfacial polymerization[143] and membrane emulsification[144] *etc.*. PVA particles have been prepared successfully for protein/peptide drug delivery by using a water-in-oil emulsion technology plus cyclic freeze-thawing process without cross-linking agents.[145] In the present work, the simple w/o emulsion-diffusion method avoiding freeze-thawing treatment on the emulsion is attempted to produce PVA particles. The biocompatible medium-chain triglyceride (MCT oil) is used instead of the silicone oil as oil phase. The prepared PVA/oil emulsion can be converted into deposits of PVA particles by diffusing directly into acetone. The size and size distribution of PVA particles depends on the formation of aqueous PVA/oil emulsion. The emulsion formation is non-spontaneous and external energy is required to expand the interfacial areas to produce smaller droplets. A number of different types of homogenization devices have been developed

to produce emulsions: high-speed blenders (mechanical stirrer) - the most commonly used method, high-pressure homogenizers,[146] ultrasonic homogenizers,[147] microfluidization,[148] colloid mills,[149] and membrane homogenizers.[150] The choice of a homogenizer depends on the nature of the starting materials, the desired droplet size distribution, the volume of material to be homogenized, and the required physicochemical properties of the final product. A stable, homogenous emulsion is needed for the production of PVA particles. The size of the droplets in emulsion depends on a balance between two opposing physical processes: droplets disruption and droplets coalescence. The stability of emulsions is controlled by a number of different types of physical and chemical processes. Creaming, flocculation, coalescence, phase inversion, and Ostwald ripening are examples of physical instability in the spatial distribution, and oxidation and hydrolysis are examples of chemical instability.[151-154] The aim of the present study is to investigate the possibility of developing a simple way to obtain submicron PVA particulate powders. The emulsion-diffusion method was evaluated for the production of PVA powder, and the morphology, size distribution and water solubility of PVA particulate powders were studied in this work.

### 4.1.2 The formation of PVA particulate powder by emulsion-diffusion method

The whole preparation process involves water-in-oil emulsification and deposition of PVA particles. The change from a droplet to a particle was due to the removal of solvent from the internal to the external phase. This mass transfer could be induced by different ways: extraction by dilution (concentration gradient) or evaporation (temperature and pressure gradients). The extraction by acetone dilution was used to deposit the PVA particles in the present study. In general, the PVA solution is emulsified in the MCT oil phase containing surfactants. The high energy source for emulsification is a mechanical stirrer – Ultraturrax T25 (IKA-Werke, Staufen, Germany). Acetone is applied to dilute the emulsion. The emulsion undergoes a process converting the dispersed droplets into solid particles in acetone. The oil phase and surfactants are dissolved into acetone, and water molecules of PVA aqueous droplets diffuse into acetone phase thus inducing the dehydration of PVA aqueous droplets and deposit of PVA (Fig. 4.1). The solid particles are collected and washed by filtration or centrifugation. The collected PVA particles are lyophilized under reduced pressure in a freeze dryer.

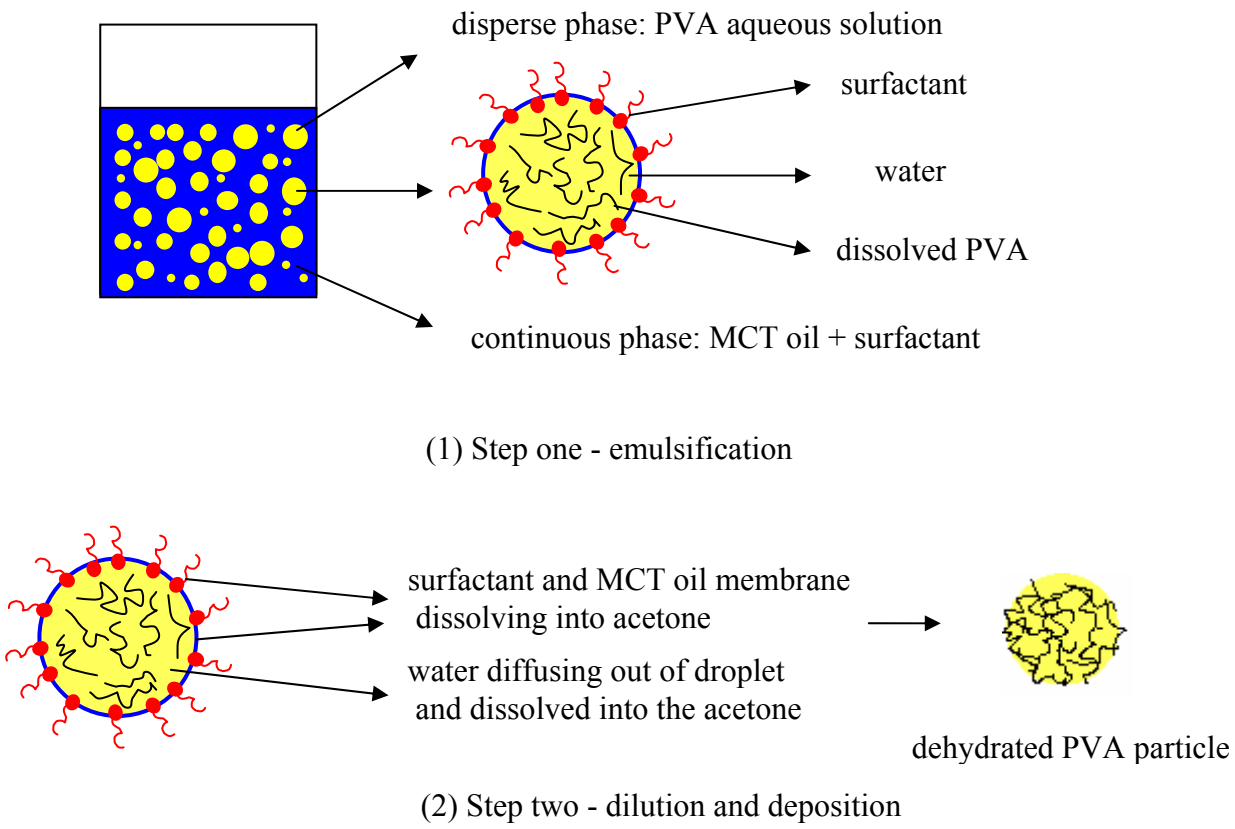


Figure 4.1: Formation of PVA particles by the emulsion-diffusion method.

## *4.2 Experimental section*

### 4.2.1 Materials

Different concentrations of poly(vinyl alcohol) aqueous solutions were prepared by dissolving PVA-26k (Mowiol 4-98 $M_w$ 26,000 g/mol) and PVA-195k (Mowiol 56-98 $M_w$ 195,000 g/mol) in bi-distilled water for 4 h at 96 °C. Two different medium-chain triglycerides (MCT oil, Sasol Germany GmbH) were used as oil phase: Miglyol 812 (viscosity 27- 33 mPas at 20 °C), Miglyol 829 (viscosity 230 - 270 mPas at 20 °C) and Miglyol 840 (viscosity 9 - 12 mPas at 20 °C). Several surfactants are chosen for the preparation of w/o emulsions (Span 80, Span 60, Span 85, Tween 60, Tween 40, Pluronic 8100, Pluronic 6100, Imwitor 780K and Imwitor 600).

### 4.2.2 Preparation of PVA particulate powder

The emulsion-diffusion method is a two-step process, based on the production of an emulsion, followed by a dilution leading to the deposition of the polymer. PVA/MCT oil emulsions were produced by high speed stirring using Ultraturrax T25 (stir speed: from 9,500 to 24,000

rpm). The volume ratio of PVA disperse phase to MCT oil continuous phase was 1 to 2 or 1 to 6. The MCT oil phase with different lipophilic surfactants was tested to produce a stable emulsion. The prepared PVA/MCT emulsions were poured slowly into acetone. MCT oil and surfactant can quickly dissolve in acetone. PVA aqueous droplets are dehydrated by acetone. Through filtration or centrifugation, the solidified PVA particles are collected and cleaned by acetone to remove the residue of MCT oil and surfactant. PVA particles with smaller inner water volumes tend to collapse and coalesce after vacuum drying. To avoid these problems, the cleaned PVA particles are finally dispersed in small amount of ethanol and dehydrated completely by freeze-drying to get the final freely flowing PVA powder. Ethanol is instead of acetone to prevent damages on freeze-drying machine.

### 4.2.3 Experimental techniques

Determination of emulsion stability

Each 35 ml w/o emulsion sample (5 ml PVA/30 ml MCT oil) was prepared in a 50 ml beaker by mechanical stirring. After 24 h storage at room temperature, the height of the total system and the height of the lower opaque sediment of water phase were measured to determine the volume fraction of phase separation. Phase separation was visually apparent in the emulsion samples containing non-efficient surfactants. The appearance of the emulsions was recorded by photographs.

Environmental scanning electron microscope (ESEM)

The size and surface morphology of the freeze dried PVA particles was investigated by using SEM (voltage 12kV, pressure 1.6 mbar, Philips XL30 ESEM FEG, Netherlands). Micrographs were taken at different magnifications in order to determine the morphology as well as the particle size range and mean diameter. 100 individual particle sizes were determined by SEM with analySIS 5 (Image Analysis Software, Olympus) that can perform multiple measurements and statistical processing tasks simultaneously. ESEM (environmental scanning electron microscopy) can perform dynamic experiments in wet mode, the combination of low temperature (e.g., 4 °C) and high water vapor pressure (e.g., 4.9 Torr) permits to achieve 100% relative humidity (RH) in the chamber. The water solubility of PVA

particles was investigated in the wet mode. The particle size and morphology were examined by semi-automatic image analyzer.

Differential scanning calorimetry (DSC)

The dissolution temperatures of PVA samples in water were measured by using a DSC under nitrogen (Perkin-Elmer, Germany). The original PVA flakes or freeze-dried PVA powders (PVA-26k and PVA-195k) (10–20 mg) plus water were placed in sealed aluminium pans and were scanned from 25 °C to 96 °C using heating rates of 1°C/min.

Mastersizer

The mean particle size and size distribution of PVA nanoparticles were determined by Malvern Mastersizer-2000 laser light scattering particle analyzer (Malvern Instruments Ltd., Malvern, UK), which measures particle sizes over an extremely broad range from 0.02 to 2000 μm. Mastersizer 2000 was operated at a beam length of 2.4 mm, range lens of 300 mm, and at 15.5% turbidity.

Viscosity determination

Viscosities of aqueous and oil phases, used for PVA particles preparation by the emulsion-diffusion method, were determined by fluids spectrometer RFSII equipped with the Couette geometry by steady rate sweep tests at 25 °C.

## *4.3 Results and discussion*

PVA nanoparticles have been prepared using emulsion plus cyclic freeze-thawing treatment. The low volume ratio of PVA solution to oil phase (1/20) and very high viscous oil phase are necessary to prevent the creaming of emulsion during the freeze-thawing treatment. The aim of the present investigation was to prepare PVA particles by high volume ratio (1/2 or 1/6) emulsion-diffusion method and the influences of surfactant, volume ratio, viscosity and homogenization speed on the formation of PVA particles were studied.

### 4.3.1 Selection of an efficient surfactant for PVA/MCT oil emulsions

Emulsions with 0.1– 50 μm droplets are thermodynamically unstable and have to be protected against coalescence by surfactant molecules adsorbing at the interface to lower the interfacial tension and increase the surface elasticity and viscosity. The presence of an efficient surfactant is very important to stabilize the emulsions avoiding coalescence and the formation of agglomerates. The size of PVA/water droplets in the emulsions determines the size of the resulting colloid particles obtained by the emulsion-diffusion method. The selection of surfactants depends on their ability to form stable emulsions. The hydrophile-lipophile balance (HLB) value is commonly used for an empirical approach. This dimensionless scale ranges from 0 to 20 for non-ionic surfactants; a low HLB (<9) refers to a lipophilic surfactant (oil soluble) and a high HLB (>11) to a hydrophilic (water soluble) surfactant. Most ionic surfactants have HLB values greater than 20. In general, water–in-oil (w/o) emulsifiers exhibit HLB values in the range of 3 to 8. The ability of several surfactants or surfactant blends (2<HLB<5) for the stabilization of PVA/MCT oil emulsions was studied. One widely used test to study the stability of emulsion is to observe the amount of creaming and water/oil phase separation. A stable, homogenous emulsion shows little or no visible separation of the oil and water phases over time. The greater the degree of creaming and phase separation is, the greater is the instability of an emulsion and the less efficient is the surfactant. The effectiveness of several surfactants and surfactant blends on stabilizing PVA/MCT oil emulsions was valued by observing the rate and amount of phase separation (Tab. 4.1). Commonly used surfactants such as Span and Tween are not efficient for PVA/MCT oil emulsions. The rates of phase separation of PVA/MCT oil emulsion with Imwitor 780K and Pluronic 8100 and 6100 were slower than PVA/MCT oil emulsion with other surfactants or surfactant blends. The most efficient surfactant for PVA/MCT oil emulsion was Imwitor 600

(Fig. 4.2 and Tab. 4.3). The blend of Imwitor 600 and Pluronic 8100 was also studied. It could not stabilize PVA/MCT oil emulsion better than the individual compounds.

Table 4.1: Effectiveness of surfactants on PVA/MCT oil emulsion stability determined by the observation of the volume fraction of phase separation. (PVA-195k/MCT 812: 1/6, 5 wt-% surfactant, homogenization speed 9500 rpm).

| Surfactant | HLB | stability of PVA/ MCT oil emulsion (after staying 24 h) |
|---|---|---|
| Span 80 | 4.3 | (-) |
| Span 65 | 2.1 | (-) |
| Span 60 | 4.7 | (-) |
| 94 wt-%Span 80 + 6 wt-%Tween 40 | 4.98 | (-) |
| 93 wt-%Span 80+ 7 wt-%Tween 80 | 5.05 | (-) |
| 79 wt-%Span 65 + 21 wt-%Tween60 | 4.94 | (-) |
| 78wt-%Span 65 + 22 wt-%Tween60 | 4.94 | (-) |
| 80 wt-%Span 65 + 20 wt-%Tween 20 | 5.02 | (-) |
| 85 wt-%Pluronic 8100 + 15 wt-%Tween 20 | 5.06 | (-)(+)(+) |
| 80 wt-%Pluronic 6100 + 20 wt-%Tween 20 | 4.94 | (-)(+) |
| Imwitor 780 K | 3.7 | (-) (+) |
| Imwitor 600 | 4 | (+) |

(-) 80 % volume of emulsion separated, (-)(+) 60 % volume of emulsion separated, (-)(+)(+) 50 % volume of emulsion separated, (+) 20 % volume of emulsion separated.

The influence of the viscosities of two liquid phases on the emulsion stability has been studied by using different concentrations of PVA solutions and different MCT oils. The viscosities of these Newtonian liquids were measured by Couette geometry by steady rate sweep test at 25 °C (Tab. 4.2). The volume of the dispersed phase was 1/6 and homogenization speed was 9500 rpm. The effectiveness of Imwitor 600 can be seen in Tab. 4.3 and Fig. 4.2. Imwitor 600 is more effective than Imwitor 780k in all emulsions. The relationship of stability of the emulsion and the viscosity can be concluded from Tab. 7. The sample 3, 4, 5, 6 prepared using a low viscous oil phase - Miglyol 840 showed higher degree of phase separations than sample 1, 2, 7, 8 prepared using a high viscous oil phase - Miglyol 812. 15 wt-% PVA-26k emulsions (sample 1, 7) exhibited a higher stability compared with 10 wt-% PVA-195k (sample 2, 8) emulsions prepared under the same conditions. The stability of emulsions increases with the increase of the viscosity of the continuous oil phase and the stability of emulsion decreases with the increase of viscosity of the disperse phase.

Table 4.2: Viscosities of PVA aqueous solutions and Miglyol oils (Couette, T = 25 °C, 0.1 < shear rate < 100 $s^{-1}$).

| Conc. wt-% | PVA-26k (mPa·s) | PVA-195k (mPa·s) |
|---|---|---|
| 5 | 6 | 93 |
| 10 | 31 | 2000 |
| 15 | 88 | - |

| MCT oil (Miglyol) | Viscosity (mPa·s) |
|---|---|
| 840 | 8.5 |
| 812 | 25 |
| 829 | 190 |

Table 4.3: Stability of different PVA solutions/MCT oil phases emulsions with two different surfactants determined by observing the volume fraction of phase separation. (Imwitor 780K and Imwitor 600, homogenization speed 9500 rpm).

| Sample Nr. | PVA solution 5 ml (wt-%) | MCT oil 30 ml | Surfactant (5 wt-%) | Phase separation of emulsion (h) |
|---|---|---|---|---|
| 1 | 15 PVA-26k | 812 | Imwitor 780K | ~ 2 |
| 2 | 10 PVA-195k | 812 | Imwitor 780K | ~ 1 |
| 3 | 15 PVA-26k | 840 | Imwitor 780K | ~ 0.5 |
| 4 | 10 PVA-195k | 840 | Imwitor 780K | ~ 0.5 |
| 5 | 15 PVA-26k | 840 | Imwitor 600 | ~ 1 |
| 6 | 10 PVA-195k | 840 | Imwitor 600 | ~ 1 |
| 7 | 15 PVA-26k | 812 | Imwitor 600 | ~ 5 |
| 8 | 10 PVA-195k | 812 | Imwitor 600 | ~ 2 |

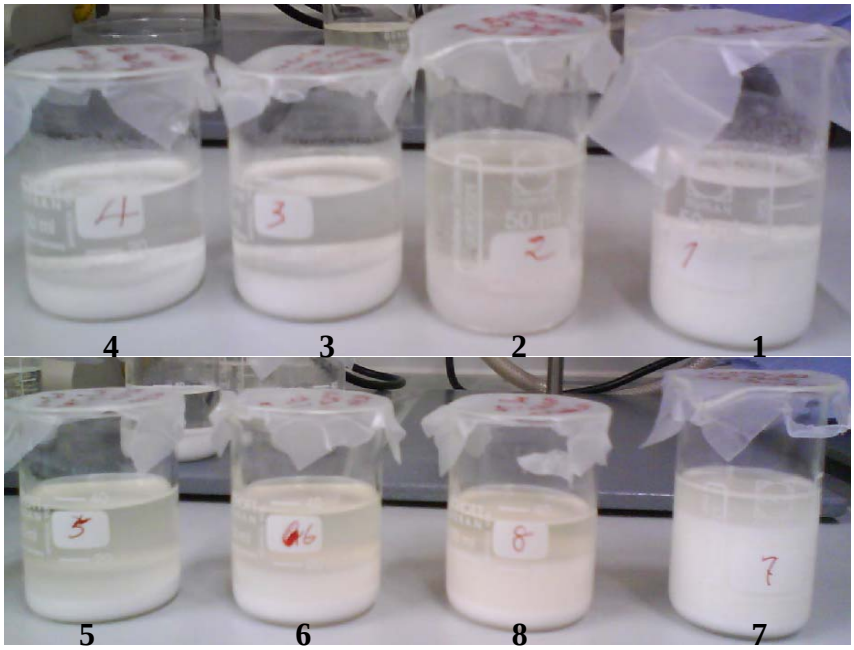


Figure 4.2: Phase separation of PVA/MCT oil emulsions after 24 h storage (the sample details are listed in Tab.4.3).

### 4.3.2 Morphology and size distribution of PVA powder

It has been proved that Imwitor 600 is the most efficient surfactant to form stable PVA/MCT oil emulsions. Imwitor 600 (polyglyceryl-3 polyricinoleate) can be used as w/o surfactant in cosmetics, food industry and pharmacy. 5 wt-% Imwitor 600 was used in the following investigations for preparation of PVA particle powders by the emulsion-diffusion method. The factors that can influence the formation of emulsion have the same effects on the final properties of PVA particles such as morphology and particles size distribution. The volume ratios of dispersed and continuous phase, viscosity of PVA solutions and oil phases and speed of homogenizer have been studied on the influence on the formation of PVA particles.

#### 4.3.2.1 Surface morphology of PVA particles

PVA particles were characterized by using electron microscopy. The freeze-dried PVA powder is white and formed by spherical particles. The surface of PVA microparticles is wrinkled and nonporous (Fig. 4.3). Some coalesced particles can be observed in the SEM image.


Figure 4.3: PVA powder prepared by emulsion-diffusion method with lyophilization
(a) Commercial PVA-195k flakes (b) Optical appearance of PVA-195k powder(c) SEM image – surface morphology of PVA-195k microparticles.

#### 4.3.2.2 Size distribution of PVA particles

The PVA particles prepared by the emulsion-diffusion method showed spherical shapes as well as a broad size distribution range from nanometers to micrometers (Fig. 4.4). The diameter and morphology of PVA microparticles are observed by scanning electron microscopy and particle size analysis. All individual particles on SEM photographs were measured to estimate the particle size distribution by analySIS 5 (Image Analysis Software). The histograms show the scattering of diameters of PVA particles prepared under different conditions. It is difficult to determine the accurate size of PVA particles smaller than 0.1 µm based on SEM photographs. The PVA particles were dispersed in acetone and studied by laser light scattering particle analyzer – Mastersizer 2000 to analyze the particle size distribution

(Fig. 4.5 and 4.6). Factors that can influence the particle size have been investigated by comparing all histograms and particle size distribution curves. The minimum and maximum homogenization speed 9500 rpm and 24000 rpm have been applied to produce PVA/MCT oil emulsions. By increasing the homogenization speed to the maximum 24000 rpm, it was possible to produce nanoparticles as small as 30 nm in diameter. A bimodal particle size distribution was observed in the range of 30 to 800 nm and 1 to 200 μm by laser light scattering particle analyzer (Fig. 4.5). Since the PVA particles larger than 10 μm were rarely observed in SEM photographs, it can be concluded that the detected particles in this range are agglomerated particles that can stick together due to cohesive forces and they are formed during the collection process or storage (Fig. 4.4, 4.5, and 4.6). The percentage of nanoparticles increased with the increasing of homogenization speed and decreasing viscosity of PVA aqueous disperse phase (Fig. 4.4 (c), (e); Fig. 4.5 (c), (d); Fig. 4.6, and Fig. 4.7 (a)). The viscosity of disperse and continuous phases have a great effect on the droplet size of the emulsion and consequently on the particle size. Lower viscous dispersed-PVA phase (low concentration or low molar mass of the PVA used) resulted in smaller particles, while all other experimental variables are kept constant (e.g. dispersed volume fraction, oil phase, and homogenization speed) (Fig. 4.4 (c), (e) and Fig. 4.7 (a), (c)). The higher viscosity of the dispersed-phase results in more difficulties to break the large droplets into the small droplets by having a similar energy input. Low viscous continuous phase can make it easier to produce nanosize emulsions, but the stability of them is worse compared to the high viscosity continuous phase, which induces a more broadly scattering of diameters due to the high rate of coalescence (Fig. 4.5 (a), (c) and Fig. 4.6 (a), (c)). A high interfacial viscosity can provide a good mechanical barrier, which may reduce the rates of aggregation and coalescence of dispersed-phase, and promotes kinetic emulsion stability. In the present experiments, changes of the volume ratio of disperse to continuous phases between 1/2 and 1/6 resulted in the fact that the particles prepared by the high volume ratio (1/2) have a narrower size distribution by comparing with the particles prepared by low volume ratio (1/6) (Fig. 4.4 (a), (b) and Fig. 4.5 (a), (b)). The stability of an emulsion increases with dispersed-phase volume fraction. With high dispersed-phase volume fraction, the droplets are packed closely together so that they cannot easily flow past each other and reduce the frequency of collisions and aggregation.[154] The morphology of PVA microparticles is mostly spherical and independent of the concentration and molar mass of PVA used in the aqueous solutions (Fig. 4.4 (a), (e) and Fig. 4.8 (a), (c)). The morphology of PVA nanoparticles is irregular as indicated in the SEM

images (Fig. 4.6), which have large surface area and tend to stick together to form large particles in the manufacturing process.

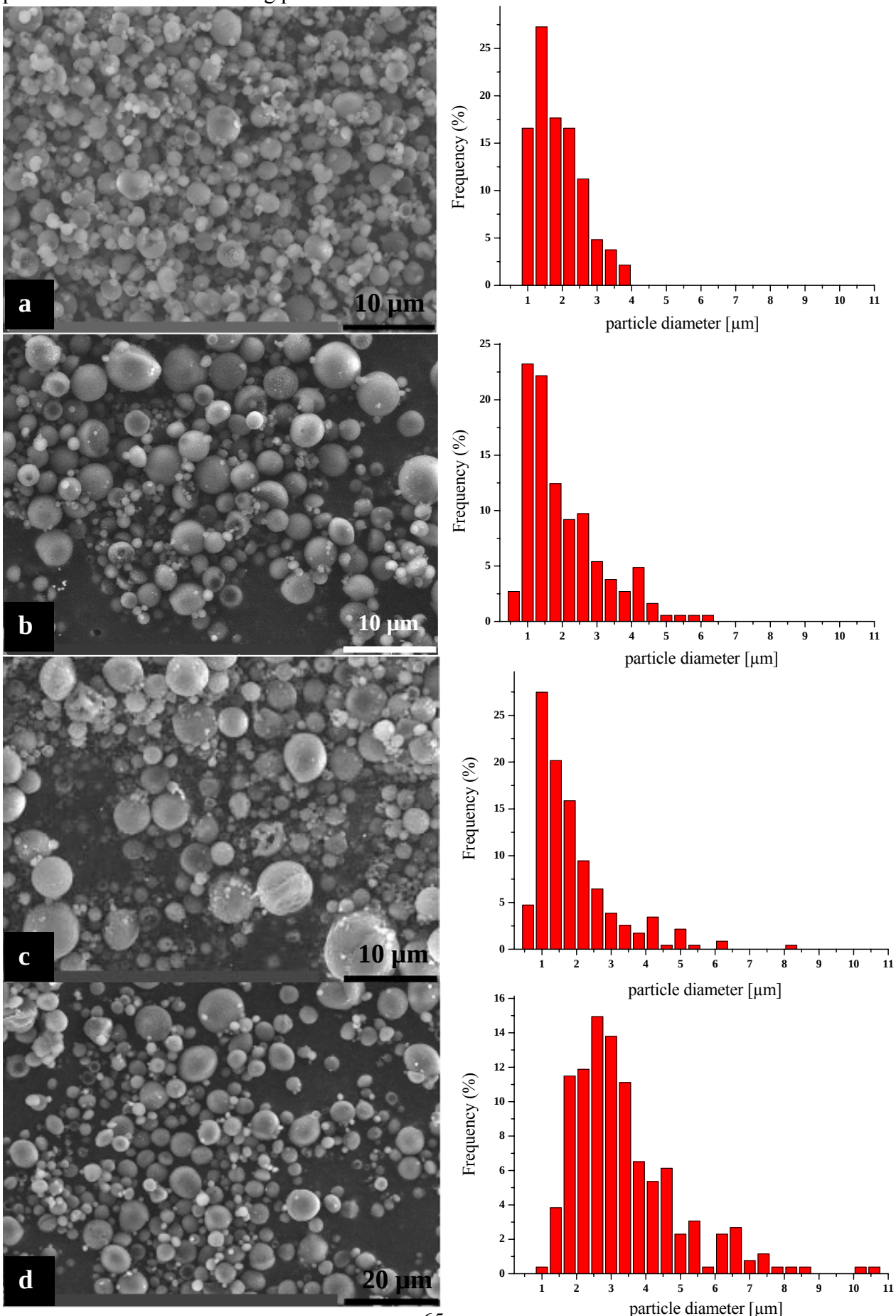

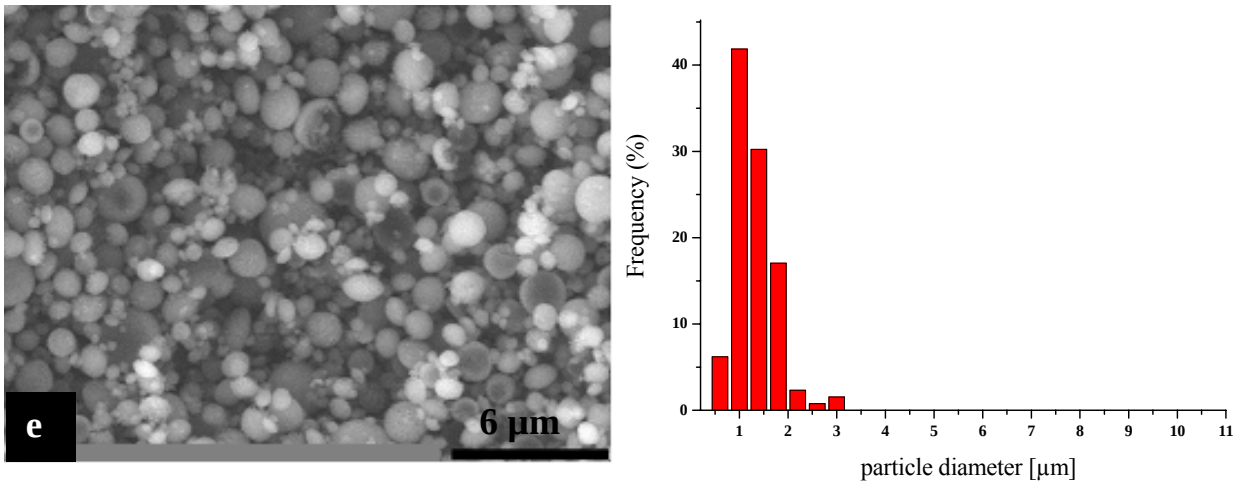


Figure 4.4: Scanning electron micrographs and histograms of size distribution of PVA particles obtained by emulsion-diffusion method under different conditions (a) 10 wt-% PVA-195k/Miglyol 829, homogenization speed: 9500 rpm, volume ratio: 1/2; (b) 10 wt-% PVA-195k/Miglyol 829, homogenization speed: 9500 rpm, volume ratio: 1/6; (c) 10 wt-% PVA-195k/Miglyol 812, homogenization speed: 24000 rpm, volume ratio: 1/6; (d) 15 wt-% PVA-26k/Miglyol 812, homogenization speed: 9500 rpm, volume ratio: 1/6; (e) 15 wt-% PVA-26k/Miglyol 812, homogenization speed: 24000 rpm, volume ratio: 1/6.

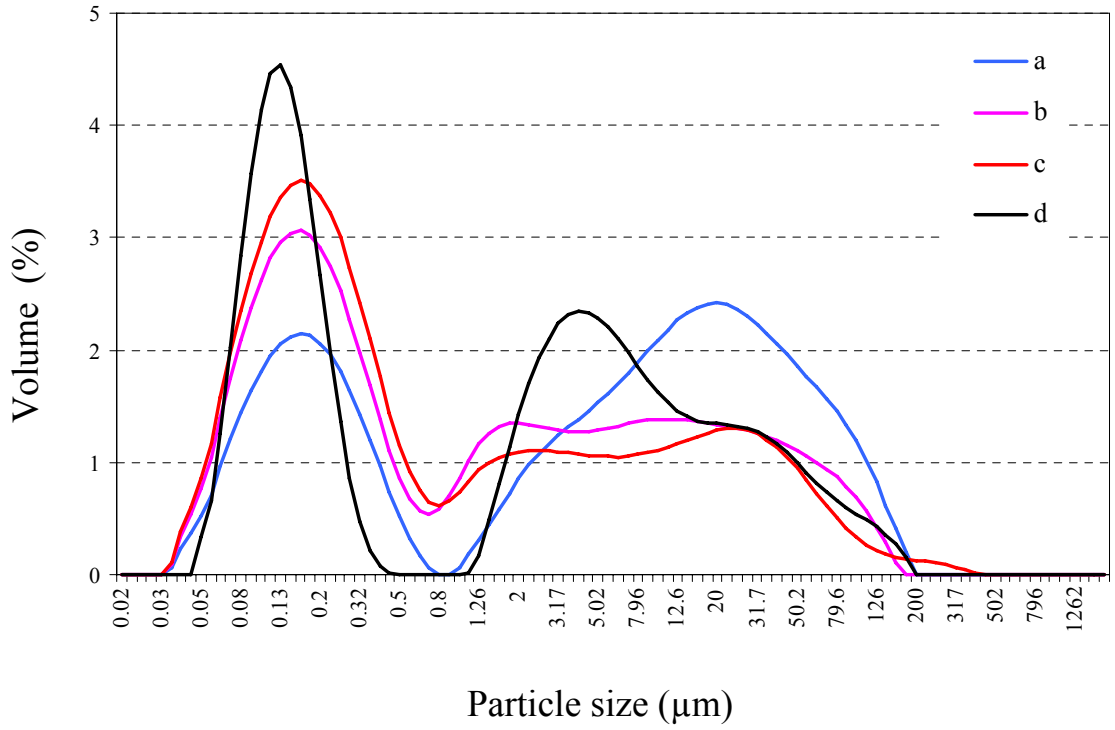


Figure 4.5: Size distribution of PVA particles obtained by emulsion-diffusion method with homogenization speed 24,000 rpm (Ultrarrax Max. speed). (a) 5 wt-% PVA-195k/Miglyol 812, volume ratio: 1/6; (b) 5 wt-% PVA-195k/Miglyol 812, volume ratio: 1/2; (c) 5 wt-% PVA-195k/Miglyol 829, volume ratio: 1/6; (d) 5 wt-% PVA-26k/Miglyol 829, volume ratio: 1/6.

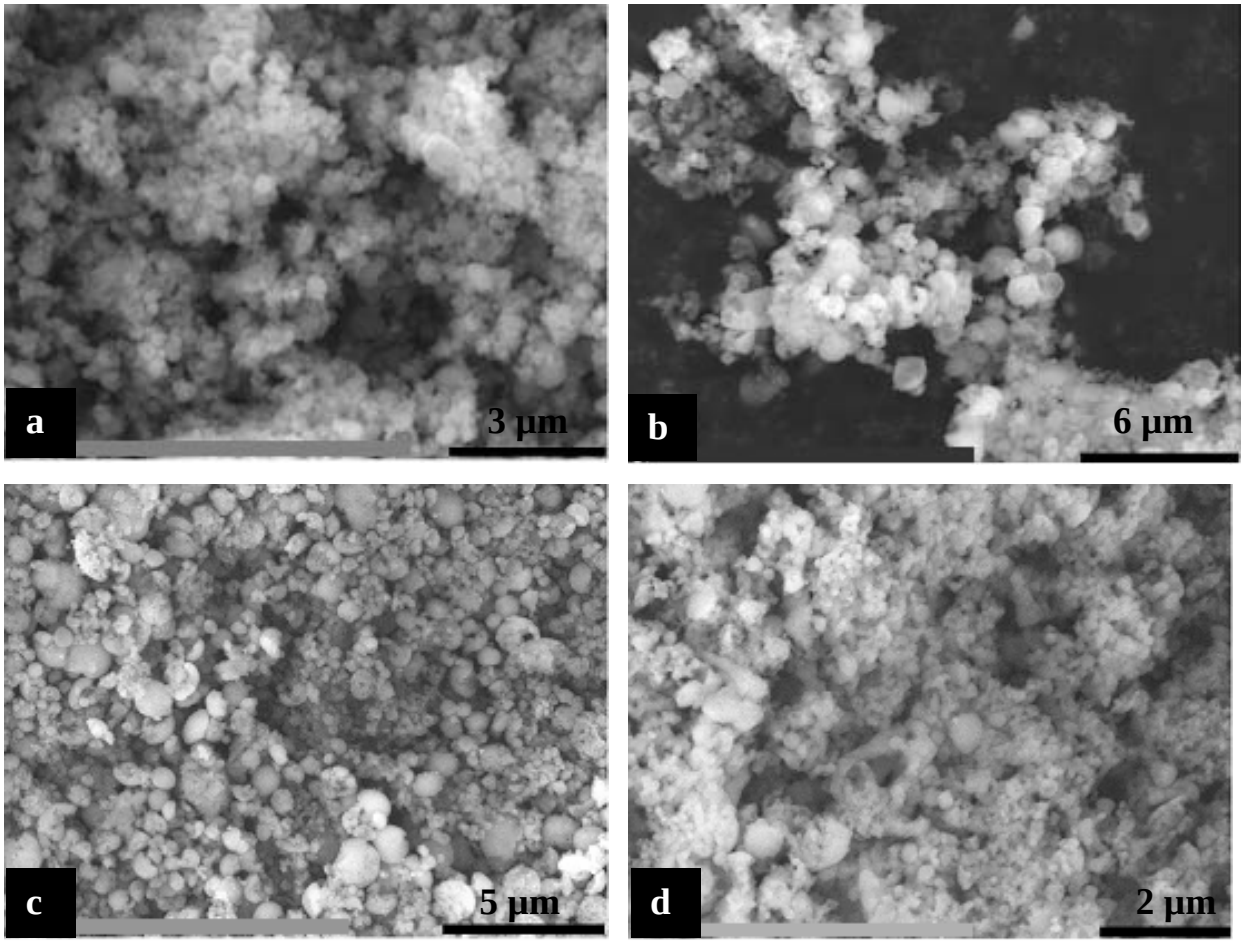


Figure 4.6: Scanning electron micrographs of PVA nanoparticles and microparticles obtained by emulsion-diffusion method with homogenization speed 24,000 rpm (Ultrarrax Max. speed). (details of all samples are explained in the caption of Figure 4.5).

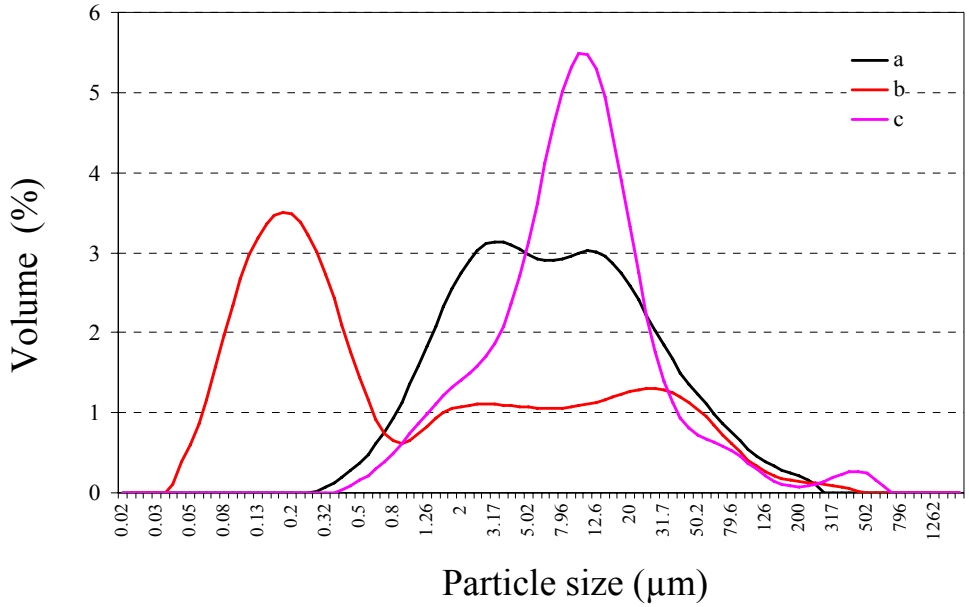


Figure 4.7: Size distribution of PVA particles obtained by emulsion-diffusion method with different homogenization speed (Ultraturrax minimum speed 9500 rpm and maximum speed 24000 rpm) and different viscosities of disperse phase (a) 5 wt-% PVA-195k/Miglyol 829, homogenization speed: 9500 rpm, volume ratio: 1/6; (b) 5 wt-% PVA-195k/Miglyol 829, homogenization speed: 24000 rpm, volume ratio: 1/6; (c) 10 wt-% PVA-195k/Miglyol 829, homogenization speed: 9500 rpm, volume ratio: 1/6.

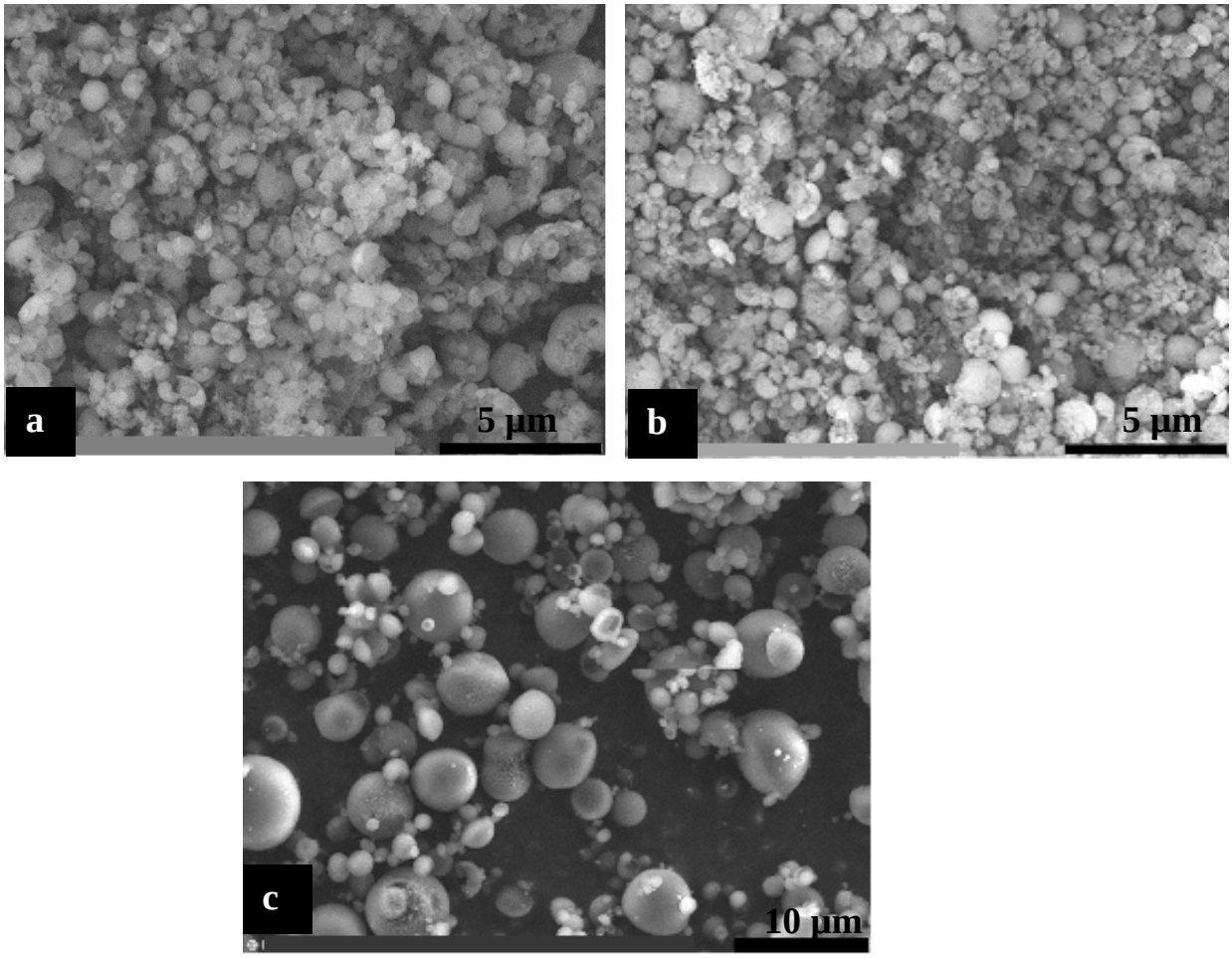


Figure 4.8: Scanning electron micrographs of PVA nanoparticles and microparticles obtained by the emulsion-diffusion method under different homogenization speed and different viscosities of the disperse phases (details of samples written in Figure 4.7).

#### 4.3.2.3 Investigation of PVA powder in water

Micro- and nano-size PVA powders have much larger surface area than original PVA flakes so that they are expected to have a better solubility in water. The PVA samples used in present work are fully hydrolyzed transparent flakes (98 mol-%), which dissolve in water only after several hours heating at high temperature (96 °C). The white PVA powder prepared by emulsion-diffusion method can swell in water to form transparent hydrogel on the moisture uptake to the surface at room temperature. The dissolution behavior of PVA powders (PVA-195k) and PVA flakes (PVA-195k) in water was investigated by DSC measurements. The DSC traces are shown in Figure 4.9. The onsets of the endothermal peak characteristic for PVA powders dissolving in water shifted from 88 °C to 78 °C by comparing with reference PVA-195k flakes, which indicated that PVA powder is easier to dissolve into water. The morphology of PVA particles was investigated with high water vapor pressure (100% relative humidity on the sample surface) by ESEM in wet mode. A bit of PVA powder was mounted

on a metal plate with Scotch tape. All PVA particles on the sample holder dipped into condensed water, when the humidity arrived 100% in the chamber. The sample holder can be dried by through increasing the temperature and decreasing the pressure of the chamber. Spherical PVA particles lost the clear boundaries when water diffused into the surface of particles. SEM photographs of PVA particles before and after humidity treatment are compared in Fig. 4.10. The humidity treated PVA particles collapsed and the dissolved PVA connected together and formed a membrane on the Scotch tape after drying.

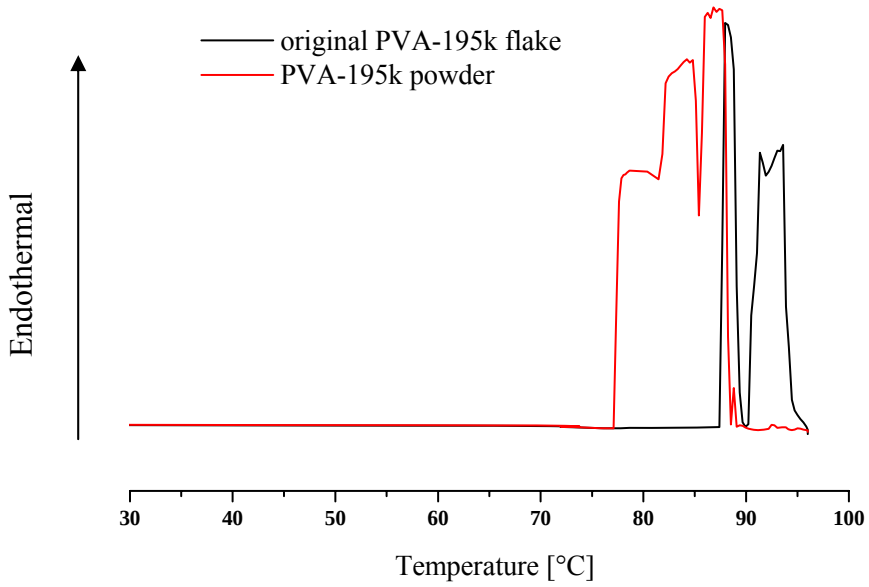


Figure 4.9: DSC thermograms of PVA dissolving in water recorded (heating rate 1 °C/min)

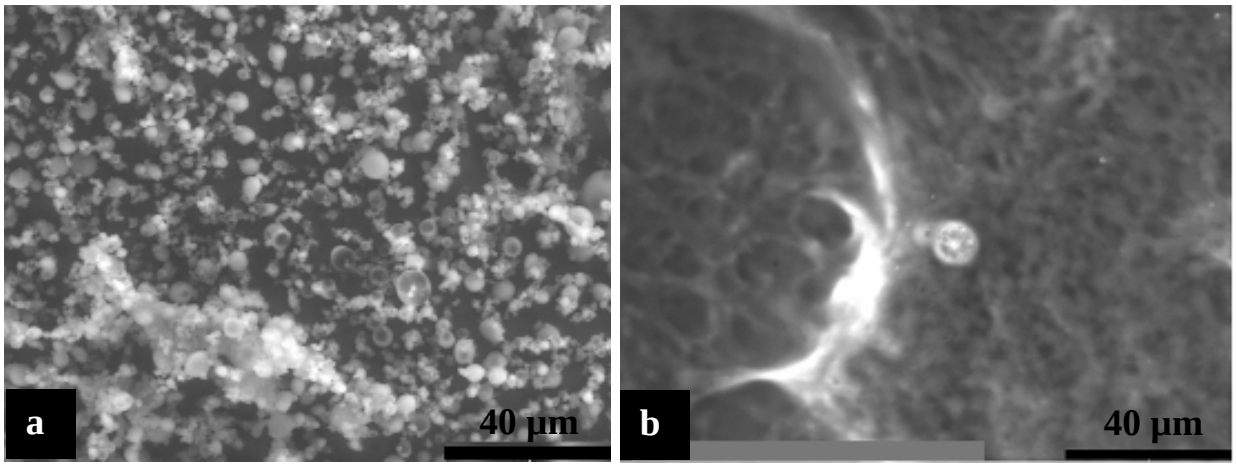


Figure 4.10: Scanning electron micrographs of PVA powder and 100 % humidity treatment on PVA powder (a) dry PVA-195k particles mounted on carbon scotch (mean diameter = 1.84 µm) (b) morphology of sample (a) after humidity treatment (100% relative humidity achieved at 4 °C and 4.9 Torr)

## *4.4 Conclusion*

The aim of the present investigation was to prepare good water soluble PVA dry powders as a potential postoperative anti-adhesion spray formulation. PVA particles ranging from nanometers to micrometers (0.03 – 200 μm) can be obtained by using the emulsion-diffusion method. The mechanism of formation of PVA particles is based on the diffusion of solvent from the emulsified PVA aqueous droplets towards acetone phase. PVA chains are converted from the dissolved state into the un-dissolved state and finally it forms the PVA solid particles. The solvent elimination in the PVA particles was complete after lyophilization. This method is a simple, economic and efficient way to produce PVA particles. SEM pictures revealed spherical and nonporous surface morphologies of PVA particles. The size of PVA particles is determined by the production of PVA/MCT oil emulsions. Proper molar masses and concentrations of PVA in aqueous solutions, speed of homogenizer and surfactants are the main factors in controlling the droplet size of PVA emulsions. The emulsions were prepared using a high-speed mechanical stirrer (Ultraturrax T25). From the present results it can be concluded, that Imwitor 600 is the most efficient surfactant to stabilize PVA/MCT oil emulsions. An increase in homogenization speed and the decreases in viscosities of disperse and continuous phases allow the reduction of particle size. Low viscosity MCT oil phase and low dispersed-phase volume fraction resulted in broader size distributions. The PVA dry powders provide a large surface area and show better water solubility than original PVA flakes. SEM photographs of PVA particles before and after humidity treatment show that PVA particles can absorb water at room temperature resulting in a membrane formation on the surface after drying. The wetted PVA powders behave like hydrogels and form a high viscous liquid under stirring at room temperature. PVA-195k powders exhibit better water solubility than the original PVA flakes. The onset temperature of PVA-195k powders dissolving into water was determined by DSC measurement. The dissolution temperature of PVA-195k powder is at 79 °C, and is shifted to lower temperatures when compared to the dissolution temperature of original PVA flakes 88 °C. The good water soluble PVA powders are expected to be useful as a potential postoperative anti-adhesion agent used directly on moist injured tissues. Haemostatic therapeutics entrapped into PVA particles could be a more effective application in postoperative anti-adhesion.

# Chapter 5

# 5 *In vivo* studies on intraperitoneally administered poly(vinyl alcohol)

## *5.1 Introduction*

Poly(vinyl alcohol) (PVA) is widely used in the area of industrial, medical and pharmaceutical application, cosmetics and food packaging since the 1930.[155] PVA - non-ionic water-soluble polymer with the simplest chemical structure, as a potential synthetic biomedical material has been studied for several decades.[156, 157] PVA is included in the *Handbook of Pharmaceutical Excipients*. Specifications for pharmaceutical use are provided in *Japanese Pharmaceutical Excipients*, *United States Pharmacopeial/National Formulary and the European Pharmacopeia.* Physiological responses of the administrated PVA are dependent on the molar mass and the route of administration. Orally administrated PVA is relatively harmless.[158] Subcutaneously administered PVA showed that low and large molar mass PVA had no severe adverse effects in rat, but medium molar mass PVA induced severe tissues damages of the whole body.[159] Pharmacokinetics and biodistribution of PVA were studied after intraperitoneal (i.p.), subcutaneous (s.c.), and intramuscular (i.m.) administration, which indicated that the translocation rate from the injection sites into the blood circulation were i.p. > i.m. > s.c.[160] The absorption of intraperitoneal administrated PVA solution contains two main pathways through large area peritoneum to distribute in the whole body. One way is that the PVA molecules were absorbed into peritoneal blood microcirculation and drained into the portal vein by passing through the liver to arrive blood circulation;[161] another way is PVA molecules were transported through the peritoneal lymphatic system directly into blood circulation. Lymphatic absorption plays a more important role in draining of macromolecules.[162, 163] The blood concentration increased with time for all PVA after i.p injection, reached a maximum, and decreased quickly with decreasing molar mass of PVA. PVA maximum blood concentration became higher as the molar mass of PVA increased. The absorption rate of i.p administered PVA showed no molar mass dependence. PVA with $M_w$ 196,000 g/mol was retained in the blood in the highest concentration, and almost half of the total dose was detected in the blood circulation 10 h after i.p injection. Comparing with i.p administrated PVA with $M_w$ 68,000 g/mol and 14,000 g/mol, PVA with $M_w$ 14,000 g/mol can be almost completely excreted from blood after 10 h. PVA with $M_w$ 68,000 g/mol has less blood concentration than PVA with $M_w$ 196,000 g/mol after 20

h.[164] The body fate of PVA is mainly governed by hydrodynamic size (single polymer chain or microgel) and the route of injection.[165] Less amount PVA can be deposited in the body, high molar mass PVA took several weeks or months to be finally excreted through urine and feces.[166, 167] There are several main routes of excretion from the body: renal excretion, hepatic excretion, pulmonary excretion and salivary excretion. Since the main routes for elimination of PVA from the blood circulation seems to be the excretion via the renal glomeruli and hepatic bile ducts, PVA of smaller size will be more rapidly excreted from the kidney into the urine.[168-170] The critical cut-off molar mass of PVAs for the glomerular permeability was reported to be 30,000 g/mol.[171] Significant accumulation of high molar mass PVA was observed in the liver and spleen. Fluorescence microscopic examination revealed that PVA was endocytosed by the liver parenchyma cells. PVA agglomerated in liver was slowly transported via the bile canaliculi and gall bladder to the intestine and excreted into the feces.[172]

Biodegradation in the environment is one of the most important features of PVA, which is the only purely C-C backbone macromolecule that can be biodegraded.[173] Irrespective of different metabolic pathways, PVA is in general degraded by two repeated processes: oxidation of two pendant hydroxyl groups either by oxidase or dehydrogenase, following hydrolysis, cleavage of the carbon–carbon chain at a carbonyl group and the adjacent methine group, yielding a carboxylic acid and a methyl ketone as terminal groups on the PVA-cleaved chains (Fig. 5.1).[174-176] Until now, PVA is usually regarded as a non-biodegradable polymer in the body. Limited information is available on PVA biodegradation mediated by cells other than microorganisms and bacteria. The urinary excretion of high molar mass PVA i.p administered in rabbits can last over 3 weeks, which cannot be explained simply by low permeability of high molar mass PVA in the kidney. While the i.p administered PVA distributed much less in kidney than in the liver and spleen, one assumption for the delay of the urinary excretion of PVA could be the degradation of high molar mass PVA in the body, and results in the release of the smaller fragments, which can be eventually excreted through the renal clearance route. The chemical structure of excreted polymer different from original PVA has been mentioned in recent studies.[167] To gain a better understanding of urinary excreted PVA, we used GPC, FTIR, TGA and $^{1}$H NMR spectroscopy to characterize the urinary extracted polymer, which was collected from rabbit's urine for successive 28 days. 20 ml 10 wt-% PVA ($M_w$ 195,000 g/mol) aqueous solution was intraperitoneally administered using the Rabbit sidewall model.

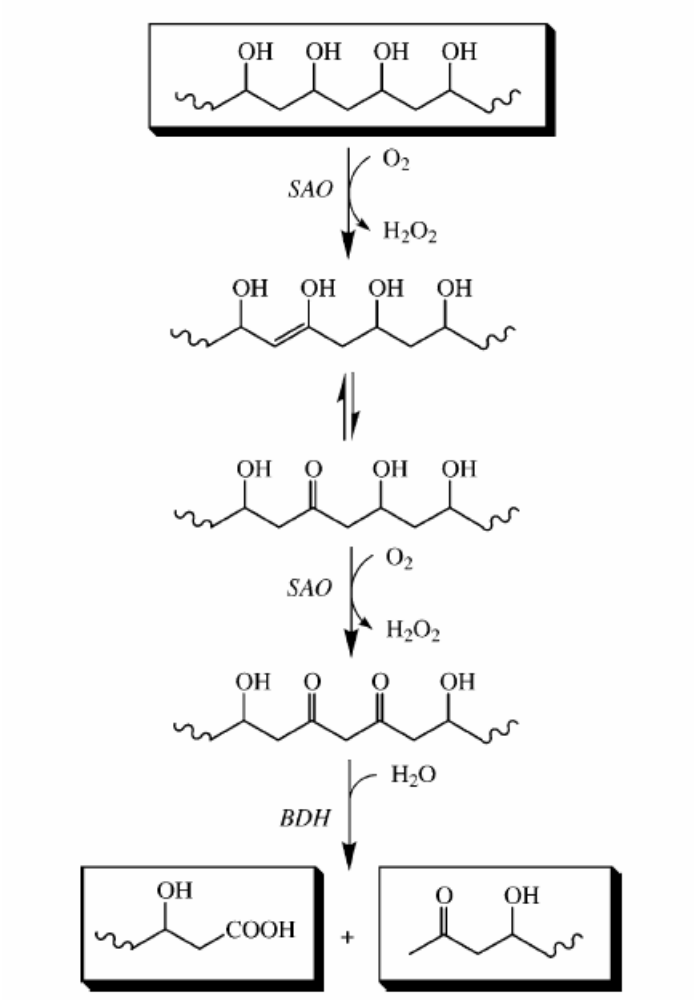


Figure 5.1: Reported bacterial degradation mechanism of PVA. SAO: secondary alcohol oxidase, BDH: β-diketone hydrolase.[175]

## *5.2 Experimental section*

### 5.2.1 Materials

Poly(vinyl alcohol) (PVA) (Mowiol 56-98) with $M_w$ of 195,000 g/mol, $M_w/M_n$ of 1.53, and degree of hydrolysis of 98.4 mol-% was purchased from Kuraray, Japan. Spectra/Pro3 Dialysis membrane (MWCO 3,500 g/mol) was purchased from Roth GmbH, Germany. All other chemicals and solvents were used as received.

### 5.2.2 Dialysis and precipitation of urinary excreted polymer

Sterilized 20 ml 10 wt-% PVA-195k ($M_w$ = 195,000 g/mol) solution was injected into the abdomen of 3 female albino rabbits (namely No. 3196, No.3242 and No.3965) by laparotomy. Urine was collected for consecutive 28 days and deep frozen immediately preventing from the influence of bacteria. After 28 days urine collection, all urine samples were filtered to remove any solid material (e.g. hay particles from the animal cage). The urine of 28 consecutive days (generally 1,100-1,500 ml, deep brown colour) was placed into a dialysis tube (MWCO 3,500 g/mol, Spectra/Por3, Spectrum Laboratories, CA) and dialyzed against distilled water for 4 days with changing distilled water three times per day. Then the dialyzed urine (light brown colour) was distilled under vacuum to remove most of the water. The concentrated urine (generally 30-50 ml, deep brown colour) was dialyzed against distilled water for 2 days with changing distilled water three times per day. Some kinds of precipitates can be extracted by pouring the concentrated urine into acetone (see Fig. 5.2). Then the precipitated polymer was filtered and dried at 80 °C. The precipitated polymers of three urine samples Nr.3196, Nr.3242 and Nr.3965 filtered by glass filters MN615 (retention 4-12 μm) was about 200 mg, 500 mg and 140 mg respectively. The control sample was dialyzed-precipitated by mixing original PVA aqueous solution with rabbit urine at room temperature. 1 ml 10 wt-% PVA (100 mg) aqueous solution was added into 200 ml rabbit urine. The same procedure was applied to these samples such as filtered, dialyzed for 4 days, distilled to 30 ml, concentrated PVA urine mixture dialyzed again for 2 days, at the end, the concentrated PVA urine mixture was poured into an excess of acetone to get precipitates.

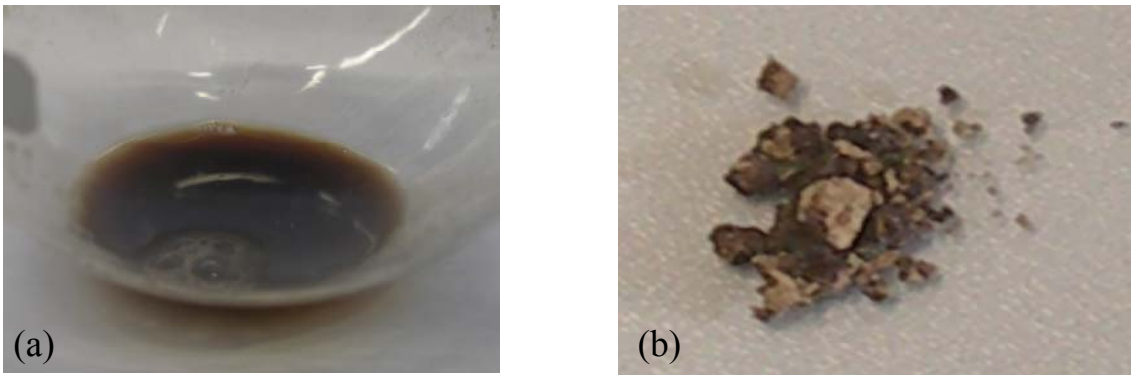


Figure 5.2: Collection of urinary excreted polymer (i.p administered PVA rabbits)
(a) Concentrated urine (ca. 30ml) obtained by distillation of dialyzed 28 days rabbit urine; (b) precipitated polymer from concentrated urine by adding acetone.

### 5.2.3 Experimental methods

The original PVA-195k, control sample PVA-195k mixed with usual rabbit urine and 3 urinary dialyzed-precipitated samples (No. 3196, No.3242 and No.3965) were used for all the following tests.

#### 5.2.3.1 Gel Permeation Chromatography

Molar masses of polymers were measured by gel permeation chromatography (GPC) at ambient temperature using a Waters GPC equipped with a Knauer pump**.** Poly(ethylene oxide) calibration curve was used to calculate the molar masses. Samples were measured in an aqueous environment. The GPC traces were normalized so that the highest peak represents 100 % of detector response.

#### 5.2.3.2 $^{1}$H-NMR spectroscopy

The molecular structures and composition of polymers were determined by $^{1}$H-NMR spectroscopy. $^{1}$H-NMR spectra were recorded using Varian Magnetic Resonance equipment with "Gemini 2000" spectrometer at 400 MHz and 20 °C in DMSO-$d_6$. The internal standard was TMS.

#### 5.2.3.3 Thermal gravimetric analysis and FT-IR spectroscopy

Thermogravimetric measurements of the polymers were performed with Mettler Toledo TGA/SDTA851. Samples (5-10 mg) were placed in 30 µl alumina pans. The TGA curves were obtained on a thermoanalytical complex from TA instruments in nitrogen at heating rate of 10 °C/min within the limits of 25 to 700 °C. The flow rate of nitrogen was 20 $cm^3$/min. Infrared spectra of samples were recorded on pressed KBr tablets using the transmission mode of Bruker Tensor 37 MIR spectrometer with a resolution of 2 $cm^{-1}$. Interferogram scans were averaged to give spectra from 400 to 5000 $cm^{-1}$.

#### 5.2.3.4 Histological test

To observe if the high molar mass PVA can produce toxicities in the liver and kidney, the histopathologic changes of the liver and kidney tissues of control and PVA treated rabbits were examined by hematoxylin and eosin (H&E) stained slides. After 28 days of urine collection 3

PVA i.p administrated rabbits and one control rabbit (without PVA administration) were killed and autopsied and the liver and kidneys were removed and deep frozen (at -32 °C) immediately. The section (4 x 10 x 10 mm) of tissues were sampled from deep frozen organs and fixed in 4 wt-% neutral-buffered formaldehyde-solution, processed through graded alcohols and xylene and embedded in paraffin blocks. Tissue sections were cut for 2-8 μm at multiple levels and routinely stained with haematoxylin-eosin. Mounted slides were examined and photographed under a light microscope.

## *5.3 Results and discussion*

### 5.3.1 Characterization of dialyzed-precipitated polymer

The polymers extracted from the dialyzed urine of PVA i.p administered rabbits have a brown look that is supposed to be the mixture of excreted PVA and urine pigments. In order to characterize the precipitated polymer clearly, original PVA-195k, control sample (PVA-195k mixed with rabbit urine, brown colour), 3 urinary extracted samples and urine pigments were investigated by using GPC, TGA, FTIR and NMR. This brown color is mainly from urobilin, which is tetrapyrrole dicarboxylic acid – the final degradation product of hemoglobin (Fig. 5.3).[177] The urine pigment sample as a reference is used to identify the influence on the precipitated polymers, which were achieved through acid hydrolysis of urinary extracted sample.

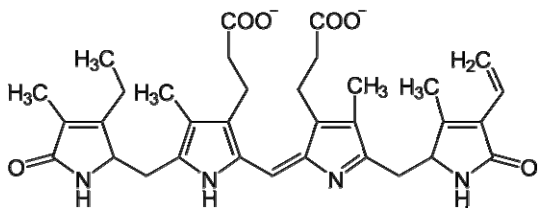


Figure 5.3: Chemical structure of urobilin.[178] (Bilirubin reduction in the gut leads to urobilinogen which is oxidized to urobilin by intestinal bacteria. Urobilin is absorbed into the blood stream and is finally excreted in urine.)

Figure 5.4 shows the infrared spectra of urinary extracted samples, PVA-195k, the control sample and the urine pigment. The IR spectra exhibit several bands characteristic of stretching and bending vibration of O-H, C-H, C-O and C=O groups. The significant observed IR band positions and respective functional groups are listed in Table 5.1. The characteristic bands of pure PVA are located at 3332, 2942, 1440, 1325, 1094, 916 and 850 $cm^{-1}$. The broad and strong band observed at about 3300 $cm^{-1}$ corresponds to the O-H stretching vibration. A weak band at 1325 $cm^{-1}$ has been assigned to the combination frequency of (C-H and O-H) groups. The strong band at 1094 $cm^{-1}$ is attributed to the stretching mode of C-O of PVA. The band at 916 $cm^{-1}$ is assigned as the stretching mode of syndiotactic C-O, which is sensitive to the tacticity of PVA and practically undetectable in IR spectrum of isotactic PVA. Other bands appear at 2942, 1440 and 850 $cm^{-1}$ which are related to the stretching and bending modes of the $CH_2$ group, respectively. The broad band at 2942 $cm^{-1}$ (3000 to 2800 $cm^{-1}$) was assigned to the overlapping of asymmetric and symmetric C-H stretching of $CH_3$ groups and $CH_2$ groups. Most

of all characteristic bands of PVA can also be observed in the IR spectra of urinary extracted polymers. The extra bands at 1649, 1542, 1406 and 1237 $cm^{-1}$ can be observed in the IR spectra of urinary extracted samples. These intense bands can be identified that are from the urine compounds by comparing the IR spectra of the control sample and the urine pigment.[179, 180] The medium band at 1373 $cm^{-1}$ overlapped with band of $CH_2$ bending mode and represents the methyl symmetric bending vibration "umbrella mode", which can be observed only in IR spectra of urinary extracted samples and indicated the presence of a methyl groups in urinary extracted samples. The strong band at 1094 $cm^{-1}$ and the weak band at 916 $cm^{-1}$ are attributed to the stretching mode of the C-O group in PVA. The intensity of the band at 916 $cm^{-1}$ is used as a measure of the syndiotacticity of PVA. The broad band at 1094 $cm^{-1}$ of the urinary extracted sample displays the slight deformation of the absorption peak and a shift to lower frequency compared to pure PVA and the control sample. The disappearance of the band at 916 $cm^{-1}$ can be detected in the IR spectra of urinary extracted samples. These changes on the IR spectra can be assumed that the chemical reaction could take place between PVA and urine pigment. Some O-H groups of PVA are substituted by ester groups which induces the variations of these characteristic bands. The $CH_2$ stretching modes at 850 $cm^{-1}$ of urinary extracted samples is remarkable different from the pure PVA, which could be indicates the decreasing amount of $CH_2$ groups in urinary extracted polymer comparing to original PVA.

Table 5.1: IR absorption frequency region and vibrational modes related to poly(vinyl alcohol) and dialyzed-precipitated polymer of the rabbit urine samples.

| IR band position ($cm^{-1}$) | Functional group |
|---|---|
| 3332 | O-H stretching |
| 2940 | C-H stretching |
| 1649 | C=O (carboxylate) |
| 1542 | C=C stretching in pyrrole ring (urobilin) |
| 1440 | C-H bending in $CH_2$ group |
| 1373 | Umbrella motion in $CH_3$ group |
| 1325 | O-H bending and C-H stretching (PVA) |
| 1237 | C-C stretching in propionic side chain (urobilin) |
| 1094 | C-O stretching (PVA) |
| 916 | C-O syndiotactic (PVA) |
| 850 | $CH_2$ out of plane bending (PVA) |

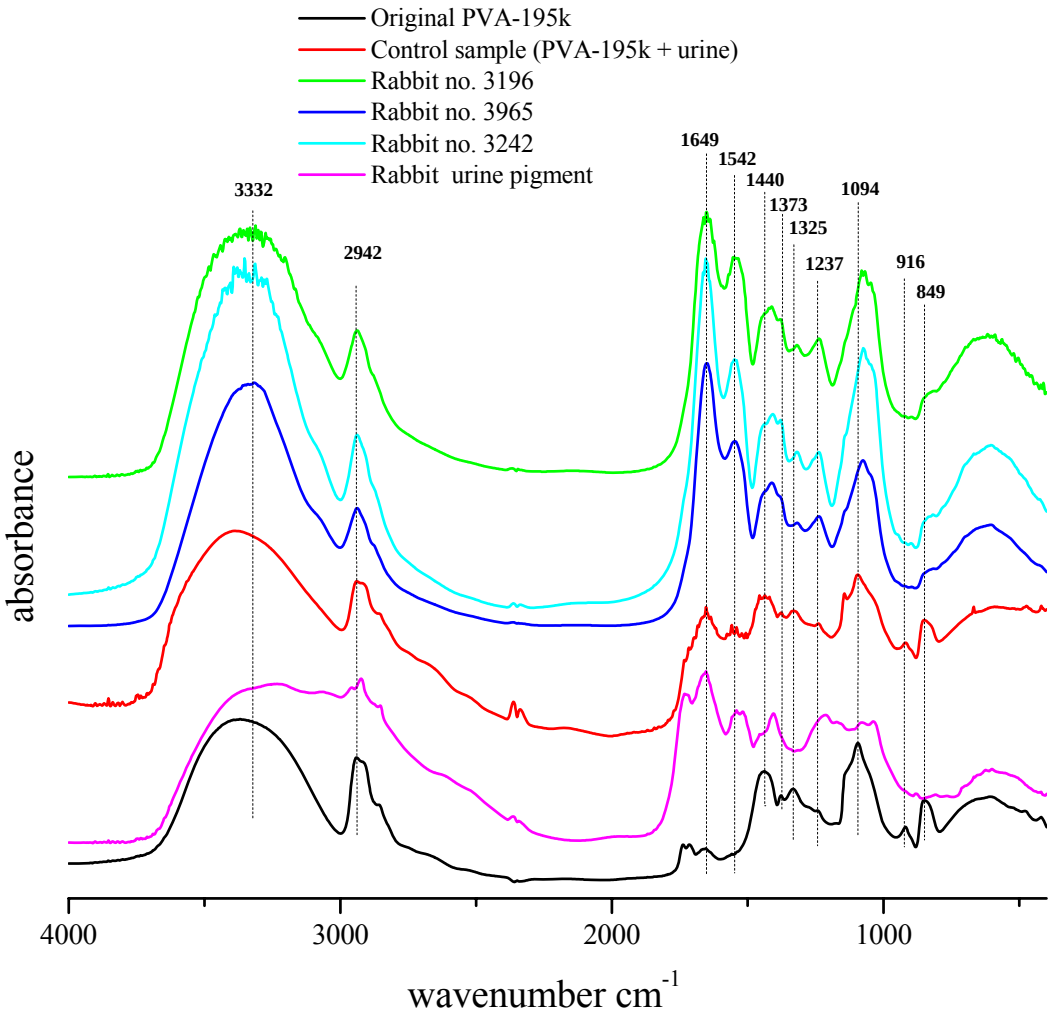


Figure 5.4: FTIR spectra of original PVA-195k, control sample PVA-195k mixed with rabbit urine and dialyzed-precipitated polymer of the rabbit urine samples (PVA i.p. administered rabbits No. 3196, No. 3965 and No. 3242) and rabbit urine pigment.

In general, the characteristic bands observed in IR spectra at 1649, 1542 and 1237 $cm^{-1}$ are attributed to the combined brownish urine pigment. The variations in the intensity of several characteristic bands of PVA and several other bands do not show in the IR spectra of the control sample and the urine pigment that are supposed to be attributed to urinary extracted polymer. $CH_3$ groups as an extra functional group is detected in the urinary extracted samples. The loss of the syndiotactic structure of urinary extracted polymer indicated changes of chemical structure of the excreted PVA.

$^1H$ NMR spectroscopy was applied to reveal more structural information of the urinary extracted polymer. The $^1H$ NMR spectra were recorded in DMSO-$d_6$ (Figure 5.5). Peaks at chemical shift of 2.5 and 3.3 ppm are the proton resonance of the solvent DMSO and the

residual water, respectively. The peak a and the peak b at the chemical shifts of 1.29-1.46 and 3.75-3.84 ppm are the proton resonance of $CH_2$ and CH group of PVA. The peak c at chemical shift of 4.11 – 4.62 ppm is the proton resonance of the OH group of PVA. The small peak at chemical shift of 1.95 ppm is from the protons of the $CH_3$ group of residual acetate units.[181, 182] All characteristic proton resonances of PVA can be detected in spectra of the urinary extracted samples. Some extra peaks are also observed at chemical shift of 1.8, 1.2 and 0.8 ppm in these spectra. In comparison to the control sample and the urine pigment, the proton resonance at 1.2 and 0.8 ppm can be detected in the $^1$H NMR spectra. The resonance at 1.8 ppm could be attributed to the protons of the excreted PVA.

Furthermore, the comparison of the ratios of the integral values is listed in Table 5.2. The ratio of a/b/c integral values of PVA is approximately 2: 1: 1. That is consistent with the repeat unit of fully hydrolyzed PVA. Peaks a, b, and c are the characteristic proton resonances of PVA. The ratio of a/b/c integral values of the urinary extracted sample is about 1.5: 1: 1.6. In general, the decrease in the ratio of $CH_2$/CH integral values and the increase in the ratio of OH/CH integral values may indicate that the samples collected from the rabbit urine do not represent pure PVA.

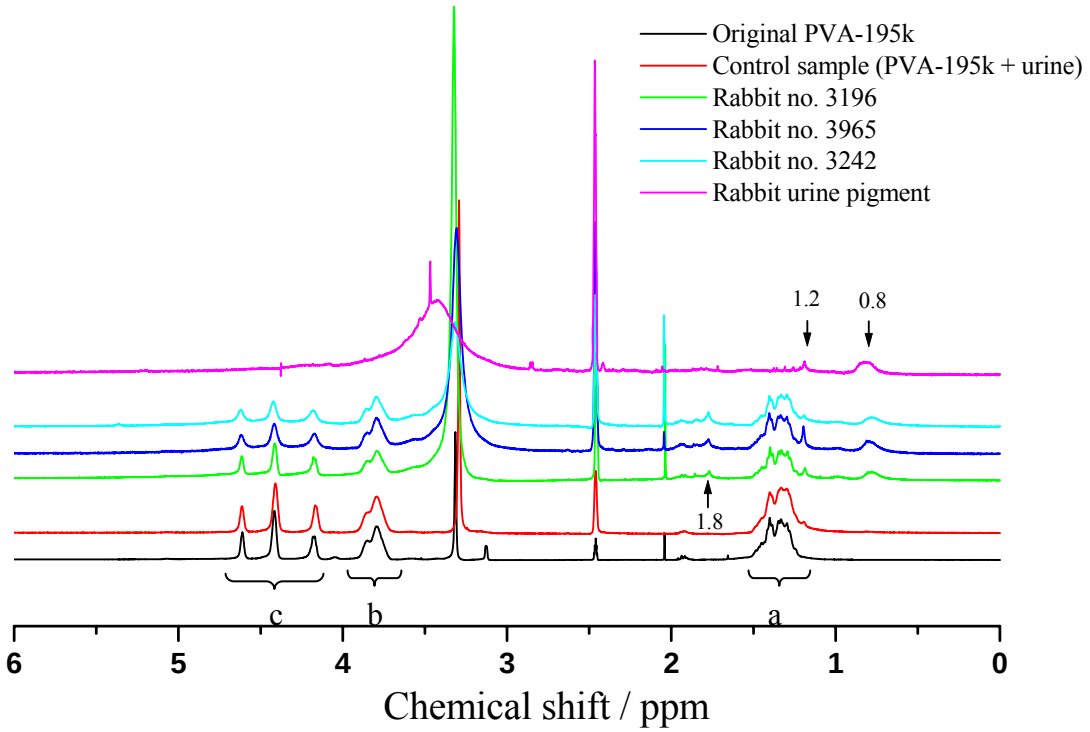


Figure 5.5: $^1$H-NMR spectra (DMSO as solvent): original PVA-195k, control sample (PVA-195k mixed with rabbit urine), dialyzed-precipitated polymer of the rabbit urine samples (PVA i.p. administered rabbits No. 3196, No. 3965 and No. 3242).

Table 5.2: Integral ratio of $^{1}$H-NMR spectra from original PVA-195k, control of PVA-195k mixed with rabbit urine and dialyzed-precipitated polymer of the rabbit urine samples (No. 3196, No. 3965 and No. 3242).

| Sample | Peak a (-$CH_2$) | Peak b (-CH) | Peak c (-OH) |
|---|---|---|---|
| Original PVA-195k | 2.1 | 1 | 1.1 |
| Control sample (PVA+urine) | 2.1 | 1 | 1.1 |
| Rabbit no. 3196 | 1.3 | 1 | 1.5 |
| Rabbit no. 3965 | 1.5 | 1 | 1.6 |
| Rabbit no. 3242 | 1.5 | 1 | 1.7 |

The thermal stability and thermal degradability of urinary extracted samples and original PVA-195k were investigated using TGA. The pyrolysis characteristics - both the thermogravimetry curves (TG, in units of wt-%) and differential thermogravimetry curves (DTG, in units of %/°C) - of the urinary extracted polymers and i.p administered PVA are shown in Figure 5.6. The weight loss in mg/°C is given for 10 mg of all samples. The shape of the mass loss curves for the 3 urinary extracted samples under the inert atmosphere were identical. They were different from the mass loss curves of the original PVA and the control sample. The first mass loss steps below 100 °C result from the elimination of water, which could be from the hygroscopic urine compounds. In the inert atmosphere, pyrolization occurs producing some organic volatiles resulting in the second mass loss step (Fig. 5.6 rabbit no. 3196, 3965, 3242). In all thermograms, the major weight losses were observed in the range from 200 to 500 °C.

The changes of urinary extracted samples were manifested by the maximum rate of decomposition and extension of the temperature region of decomposition of the polymer compared with pure PVA. The observed important shift in the maximum rate of decomposition in the temperature range from 300 to 370 °C indicated that the excreted samples collect from the rabbit urine are not pure PVA.

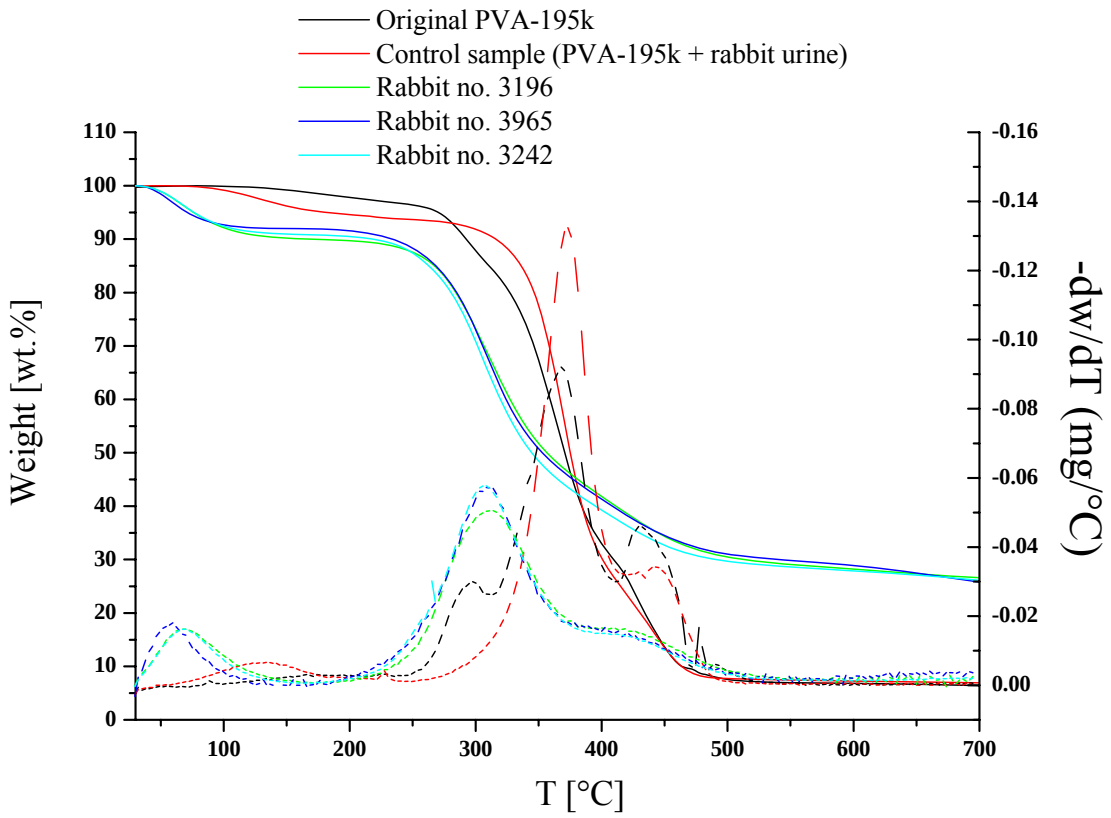


Figure 5.6: TGA and DTG curves of original PVA-195k control of PVA-195k mixed with rabbit urine and dialyzed-precipitated polymer of the rabbit urine samples (No. 3196, No. 3965 and No. 3242).

The GPC traces show the distinct variations of molar mass and molar mass distribution of the samples under investigation (Fig. 5.7). The elution volumes ($V_E$) of 3 urinary extracted samples and the control sample compared to original PVA shifted to smaller values. The GPC trace of the control sample showed a similar shift to smaller $V_E$ indicating the strong interactions between PVA and urine pigments to form apparently higher molar mass aggregates. For this reason, the present GPC results of urinary extracted samples cannot reveal the exact molar mass of excreted PVA. The bimodal GPC traces of urinary excreted samples indicate that the excreted polymers are more complex than the i.p administered original PVA.

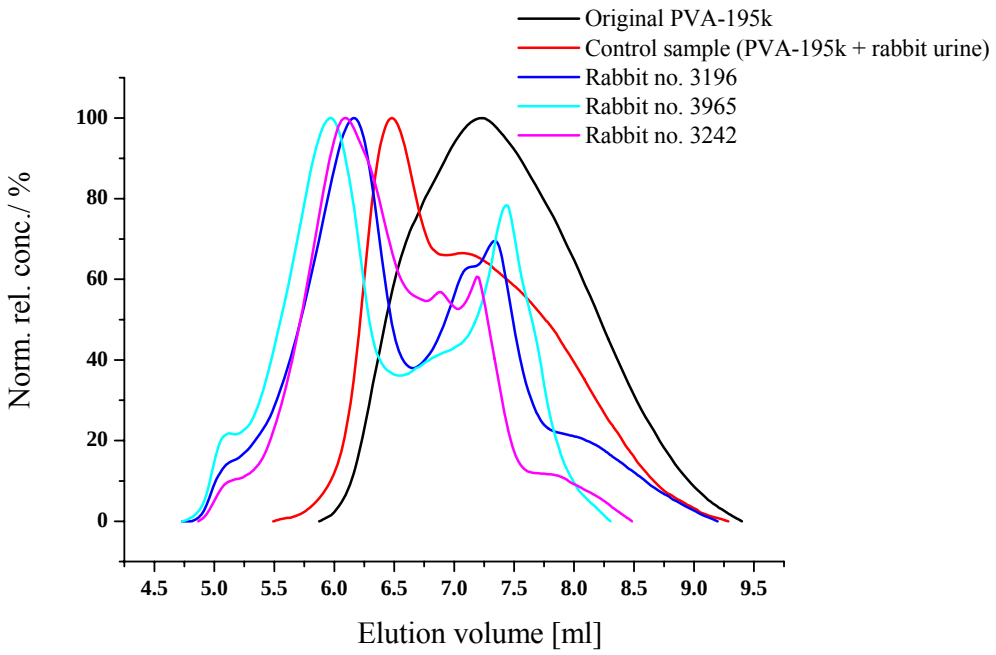


Figure 5.7: GPC traces from original PVA-195k, control of PVA-195k mixed with rabbit urine and dialyzed-precipitated polymer of the rabbit urine samples (No. 3196, No. 3965 and No. 3242).

To identify the molar mass of urinary excreted polymer, the breaking of interactions between polymer and urine pigments was tried by adding base or acid. 1 mol/l NaOH or HCl were added to the sample solutions prepared for GPC measurements and heated at 80 °C for one day. After the hydrolysis in basic or acidic environment, urine pigment interacting with PVA molecules is released from the polymer chains. Some changes were observed in the Figure 5.8: the GPC peaks of the urinary extracted sample shifted to higher $V_E$ comparing to the non-treated sample of No. 3242; the sharp peaks appeared around at $V_E$ of 12 ml indicating the released urine pigment (e.g. urobilin $M_w$ 590 g/mol).

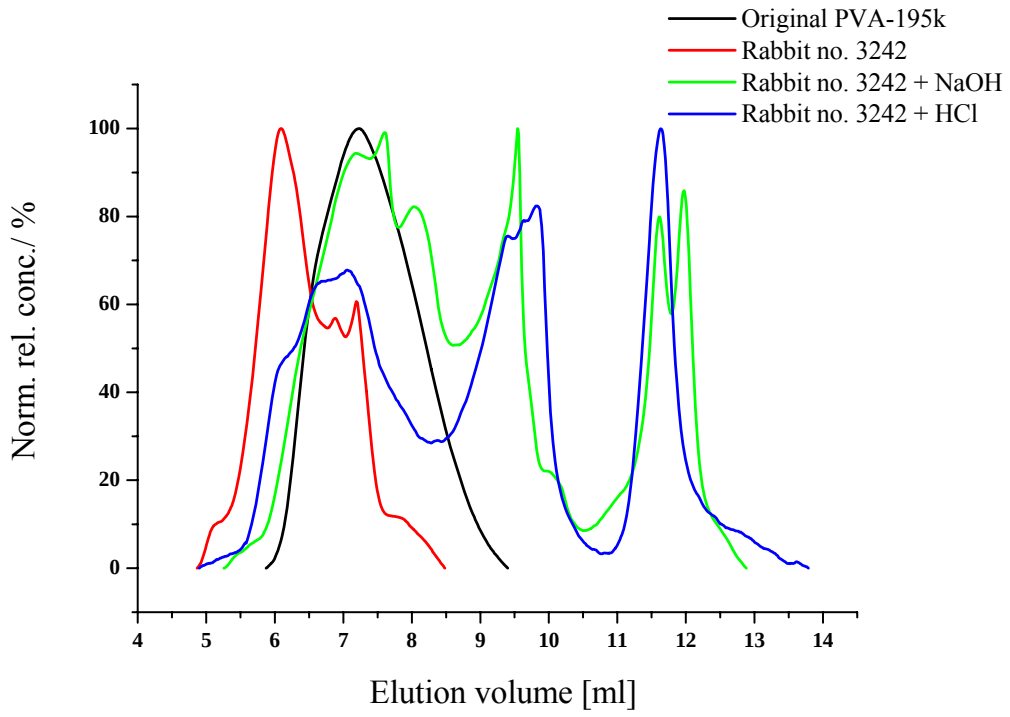


Figure 5.8: GPC traces of the urinary extracted sample (No. 3242) treated by base or acid (1 mol/l NaOH or HCl).

Base and acid treatments show a similar influence on the breaking of the aggregates of excreted polymer and urine pigments. 1 mol/l NaOH was chosen to hydrolyze all 3 urinary extracted samples. GPC traces exhibit 3 obvious peaks in base treated urinary extracted samples that indicated 3 main compounds contained in the urinary extracted sample (Fig. 5.9). The peaks at $V_E$ of 12 ml represent the released urine pigment after basic treatment. The other two peaks distribute broadly at $V_E$ of 6 and 10 ml. The nonuniform distribution of these two peaks points out the existence of different polymer – urine pigment aggregates in the urinary excreted samples. The shape and the different shifts of $V_E$ of these peaks make it difficult to characterize the excreted PVA exactly. The peaks that appeared in the range of 9-11 ml can also be observed in GPC trace of the control sample, which indicates that some high molar mass compounds of urine might aggregate with the extracted polymer.

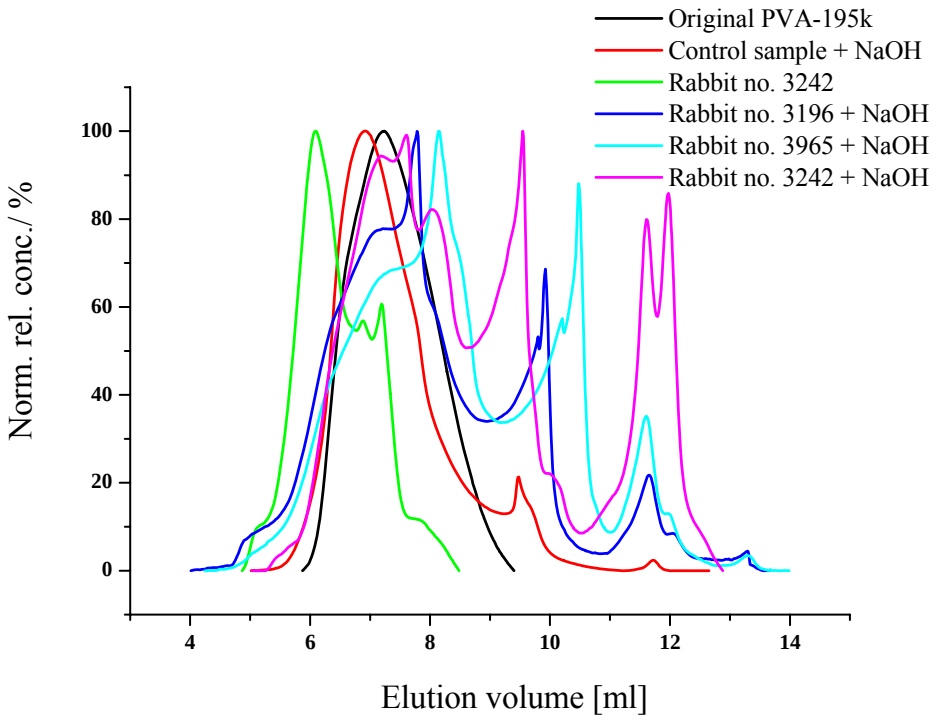


Figure 5.9: GPC traces of dialyzed-precipitated polymer of the rabbit urine sample with NaOH treatment.

### 5.3.2 Histological tests

The biocompatibility of PVA was investigated by histopathological tests of the liver and the kidney which were excised from the PVA i.p administered rabbits. H&E (hematoxylin and eosin) stain is a popular staining method in histology. The staining method involves application of the basic dye hematoxylin, which colors basophilic structures with blue-purple hue, and alcohol-based acidic eosin, which colors eosinophilic structures bright pink. The basophilic structures are usually the ones containing nucleic acids, such as the ribosomes and the chromatin-rich cell nucleus, and the cytoplasmatic regions rich in RNA. The eosinophilic structures are generally composed of intracellular or extracellular protein. Most of the cytoplasm is eosinophilic. Red blood cells are stained intensely red.

Liver and kidney are the most important metabolic organs, and the urinary excretion and biliary excretion are also the main routes of excretion for the administered material from the body. One important method to value the biocompatibility of biomaterials is to do histological testing. In the present study, the appearance of nephrotoxicity, PVA accumulation or depositions were not observed in the histological sections of PVA-treated rabbits (No. 3196, No.3242 and No.3965) by comparing with the control rabbits (non-PVA-treated). Morphological changes of nephrons, vasculitic lesions and inflammation infiltration cannot be

seen in renal cortex of PVA-treated rabbits. The elimination of high molar mass PVA through the kidneys did not bring any damage in the renal glomeruli (Fig. 5.10, 5.11, 5.12). Renal tubule epithelial cells did not show any degeneration, necrosis, inflammatory infiltration or fibrous proliferation which could be induced by PVA accumulation and deposition in kidney (Fig. 5.13).

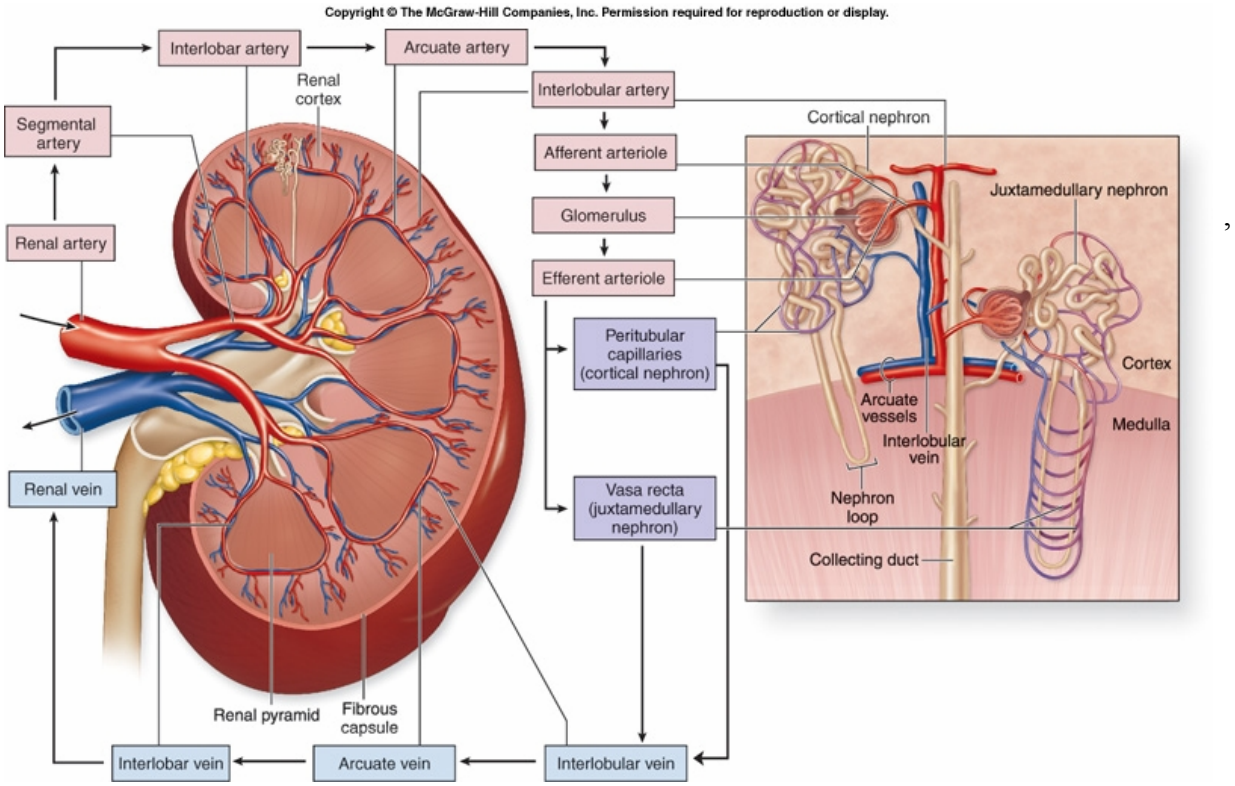


Figure 5.10: The kidney: cross section and nephron.[183] Each kidney has 1-2 million functional units – nephrons. Each nephron contains a glomerulus. The glomerulus, Bowman's capsule and the proximal and distal tubules lie in the cortex, while the long tubule portions are in the medulla.[184]

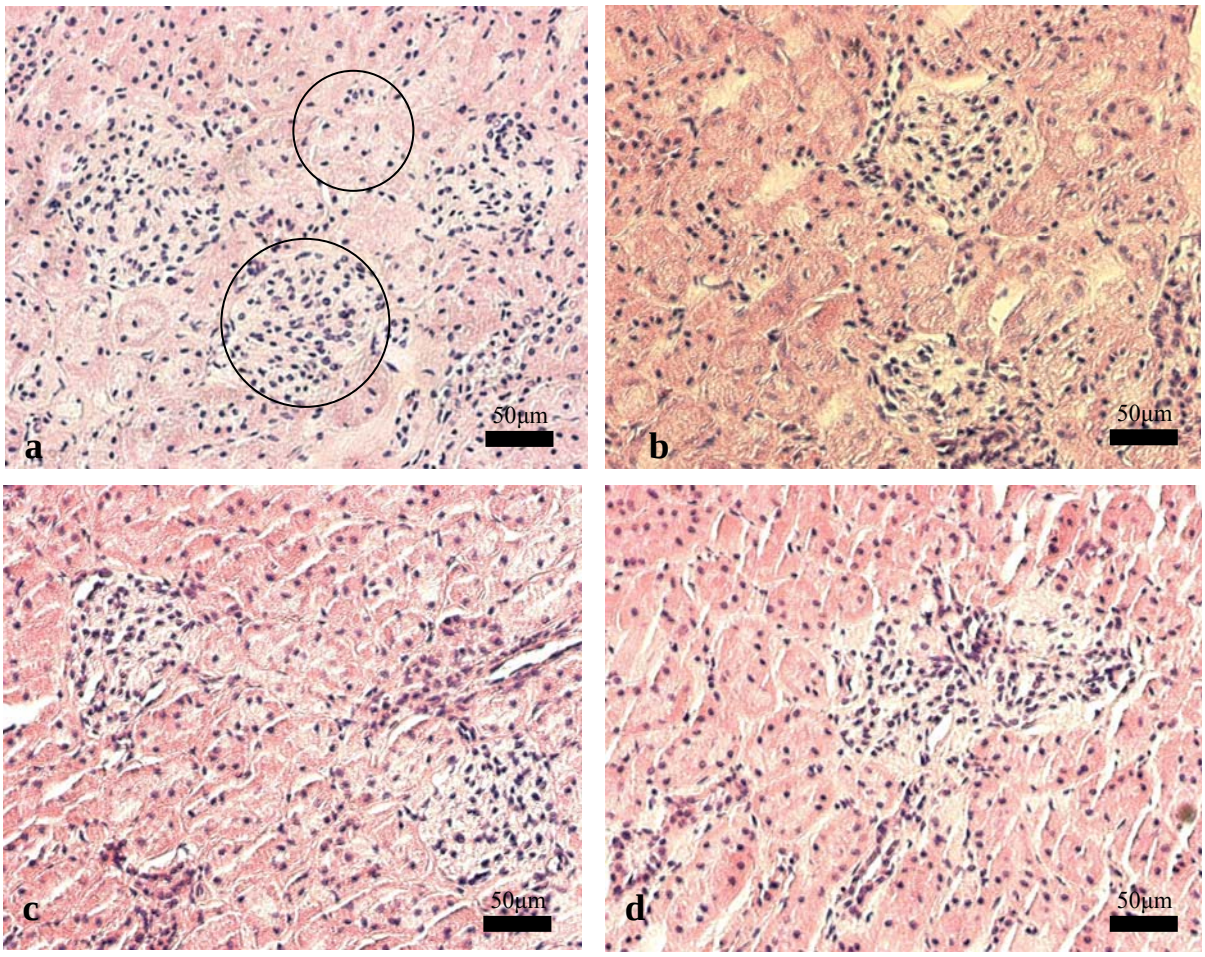


Figure 5.11: Glomerular structures and tubular structures of nephrons are seen in the renal cortex of rabbits (H&E, x 20) (a) control (large circle area - glomerulus, and small circle area – tubule's system of nephron), (b) No.3196, (c) No.3242 and (d) No.3965.

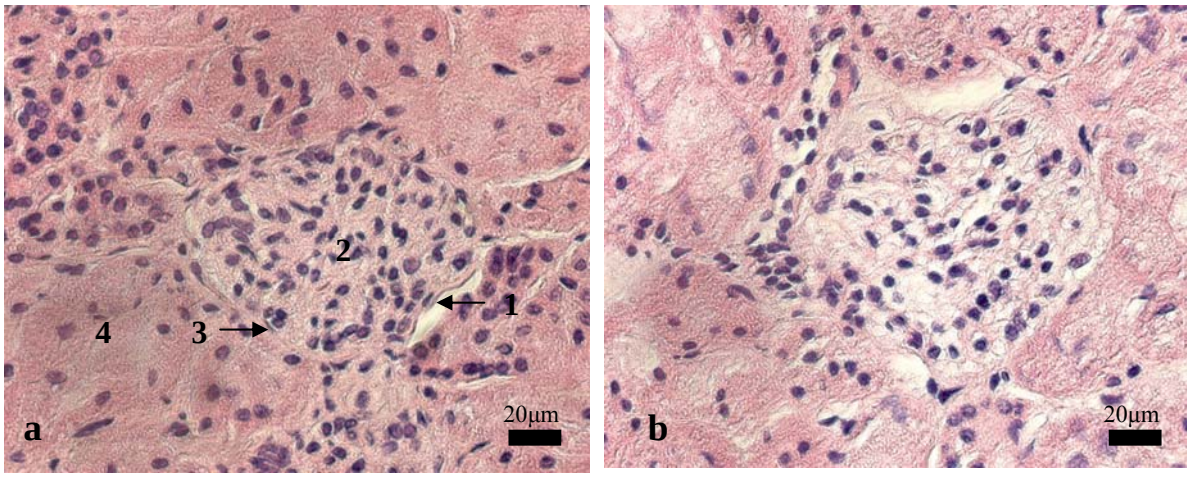

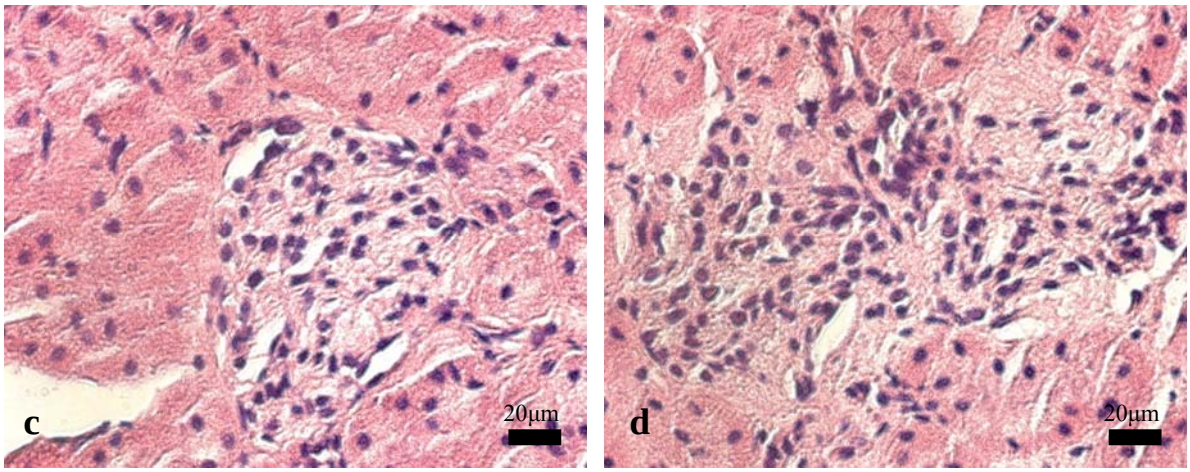


Figure 5.12: Glomerular structures in the renal cortex of rabbits (H&E, x 40) (a) control (1. lumen of Bowman's capsule; 2. glomerulus (blood capillary); 3. squamous epithelial cell; 4. cross-section tubule), (b) No.3196, (c) No.3242 and (d) No.3965.

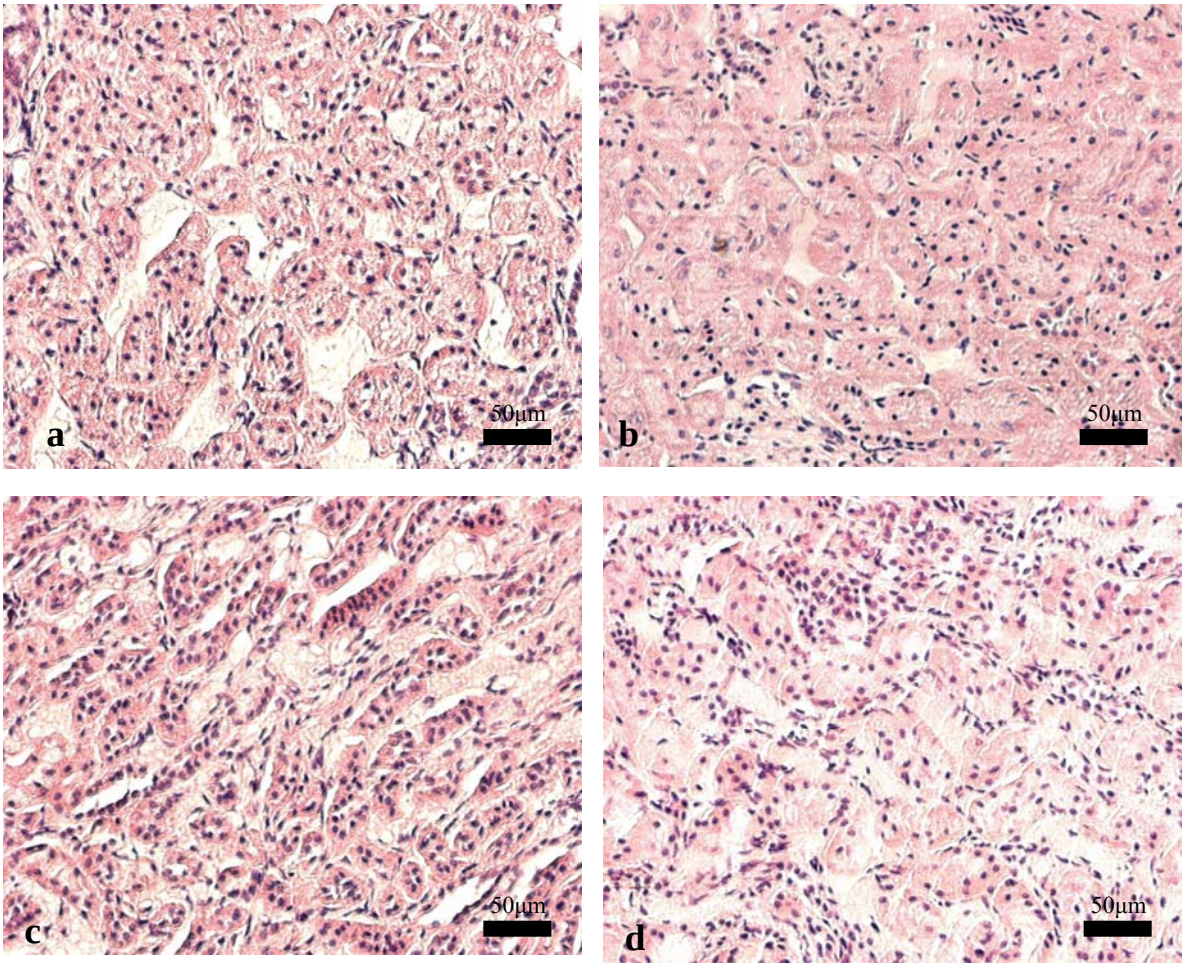


Figure 5.13: Medulla section of the rabbit kidney (a) control (loops of Henle and collecting tubules), (b) No.3196, (c) No.3242 and (d) No.3965 (H&E, x 20).

Compared with the photomicrography of the control liver, no significant changes were observed in the liver of the PVA-treated rabbits. The hepatocytes and portal areas in the PVA-treated liver show the similar morphology to the control liver. Inflammation infiltration, necrosis, or fibrous tissue proliferation cannot be detected in the liver of PVA-treated rabbits (Fig. 5.14, 5.15). Sinusoidal dilatation, central vein dilatation, enlargement of periportal area and mononuclear cell infiltration of serious hepatitis's changes cannot be viewed in PVA-treated liver tissue. But slight vacuolation of hepatocytes can be detected in PVA-treated No. 3242 rabbit (Fig. 5.15 (c)). This hepatocytes cytoplasmic degeneration did not show obviously in other two PVA-treated rabbits. The possibilities of the hepatocyte degeneration shown in PVA-treated No. 3242 rabbit could be the artefact of organ storage or slide preparation.

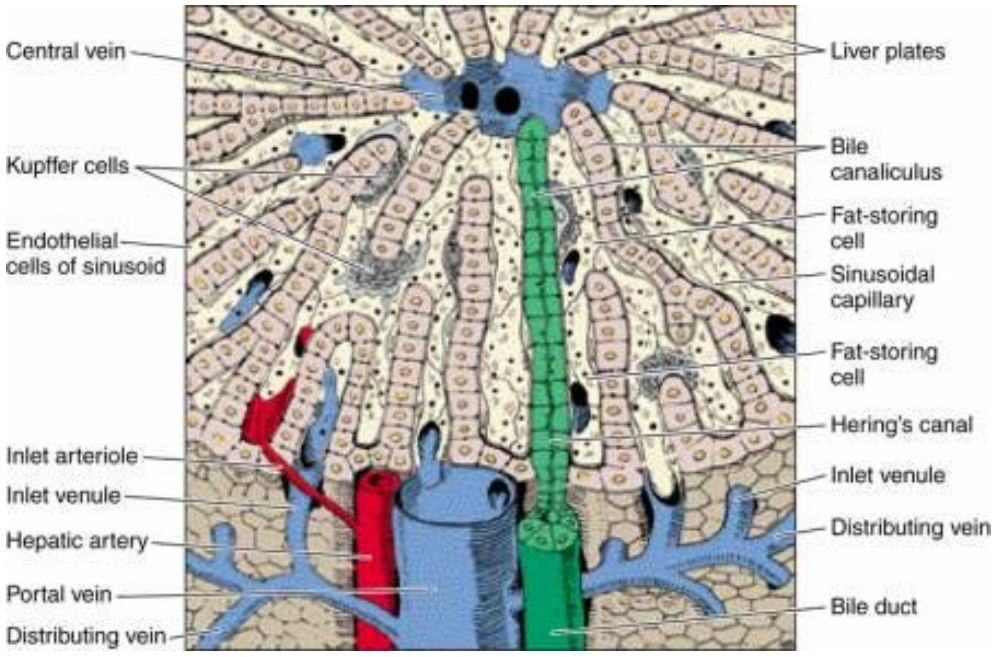


Figure 5.14: Presentation of arrangement of lobule of liver tissue. Blood in the branches of the hepatic artery and portal vein enters the sinusoids, between the cords of liver cells, and courses toward the central vein, which is a tributary of the hepatic vein. Bile flows in the opposite direction, from the center out, toward the tributaries of the bile duct.[185]

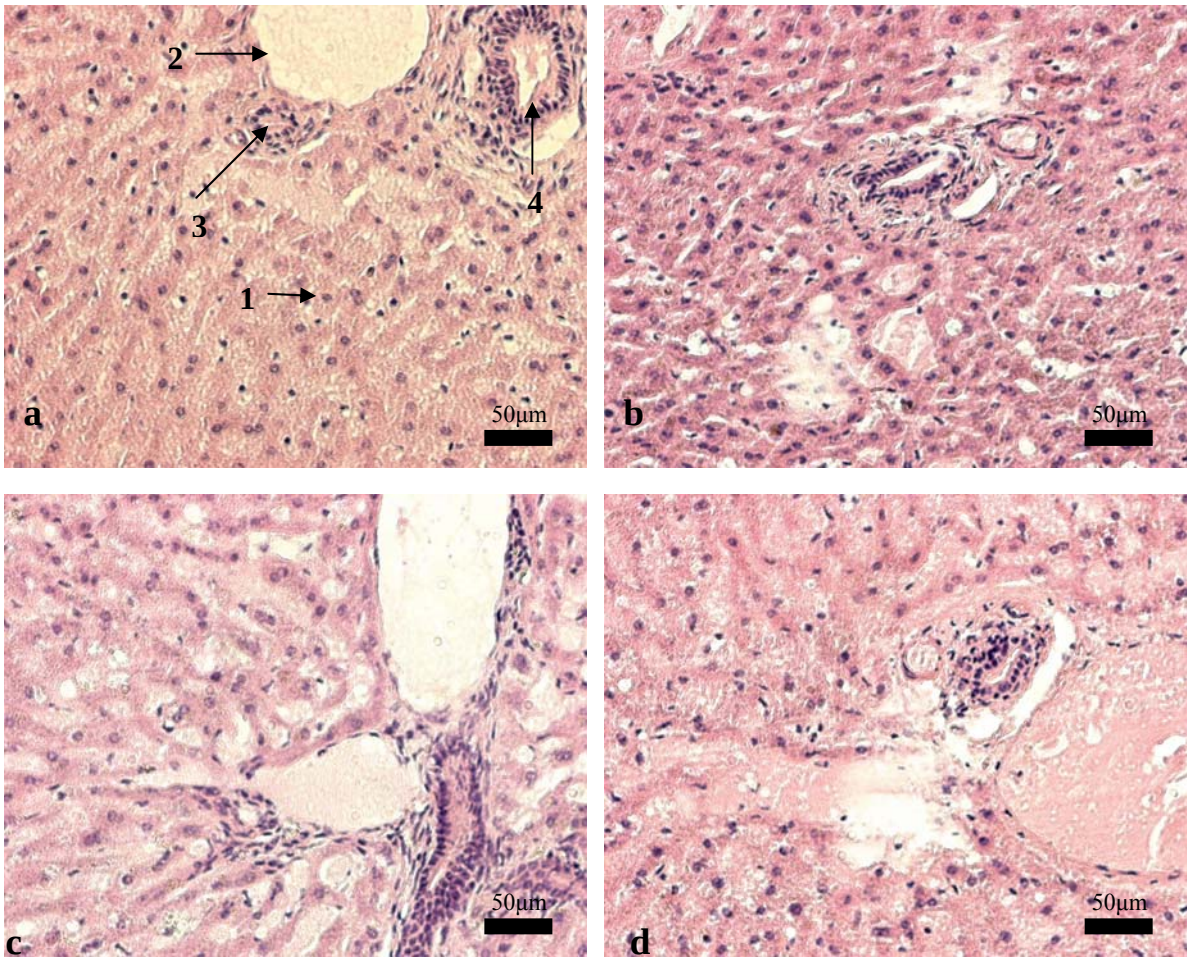


Figure 5.15: Histological appearance of rabbit liver (a) control (1 – normal hepatocyte, 2 - branch of the portal vein, 3 – branch of hepatic artery and 4 - bile duct), (b) No. 3196, (c) No.3242 and (d) No.3965 (H&E, x 20)

The urinary extracted polymer from PVA i.p administered rabbits shows the main spectral features of pure PVA in the investigations of FTIR and $^{1}$H-NMR spectroscopy. The characteristic signals represent PVA that can be detected in urinary extracted samples. Thermal gravimetric analysis (TGA) reveal that the urinary extracted sample has lower thermal stability than original PVA-195k. The obvious shift of the maximum rate of decomposition in DTG curves from 370 to 300 °C indicated the different pyrolysis property between renal excreted PVA and i.p administered PVA. GPC traces indicate that strong aggregation occurred between the extracted PVA and urine compounds. The aggregation can be broken under basic or acid condition. The GPC traces of base-treated urinary extracted samples exhibit multi-peak distributions. The peaks distribute in the same range of elution volume as original PVA that are supposed to represent the excreted PVA. These peaks show the different shape from the original PVA and shift slightly to lower molar masses. All the results mentioned above show that urinary extracted samples exhibit some obvious differences from the original PVA. Some

of them are caused by urine compounds that could not be separated from the collected PVA (e.g urobilin), such as IR bands at 1649, 1542 and 1237 $cm^{-1}$ and proton resonances at chemical shift of 1.2 and 0.8 ppm. Other differences still have no explanation as the detected functional groups (signals of IR band at 1373 $cm^{-1}$ and chemical shift of 1.8 ppm) and the decrease in the intensity of IR band at 850 $cm^{-1}$ and in the integral ratio of proton resonance of $CH_2$ to CH of the excreted PVA polymer.

The kidney as a main excretion gateway has selection criterions on the molecule size and molar mass of filtered substances. Molecules with r < 1.8 nm (molar mass < ca. 10,000 Dalton) can be filtered through glomerular membrane without any hindrance. Molecules with 1.8 nm< r < 4 nm are only partially filterable. Molecules with r > 4.4 nm (molar mass > 80,000 g/mol, e. g. globulin) usually cannot be filtered. Negative charged substances have lower filtration coefficients compared with neutral molecules with the same radius.[186] The reported critical cut-off of PVA in renal filtration is 30,000 g/mol.[171] The molar mass of PVA applied in the present study is 195,000 g/mol. Both of molar mass and molecule size ($R_h$ ~ 13 nm) of PVA-195k are far above the limits of glomerular filtration. Until now, PVA is usually regarded as a non-degradable polymer *in vivo*. This conclusion is based on the studies of pharmacokinetics and biodistribution of PVA. *In vivo* study on the chemical structure of excreted PVA has been reported rarely. The reason to the fact that the half-life of PVA in the circulation prolongs with the increase in the molar mass is also not so clear. I.p administered PVA-195k can be excreted gradually through kidney for months without damaging renal glomeruli. The endocytosis of PVA has been observed during PVA accumulation in liver.[172] Usually the reticuloendothelial system (e.g. monocytes, macrophages, lymph nodes, the spleen and Kupffer cells of the liver) plays an important role in scavenging foreign materials invading into the body. The participation of parenchymal, kuffer and endothelial liver cells was suggested in the clearance of PVA by the reticuloendotherial system.[187] In our histological test, slight vacuolation of hepatocytes can be detected in the live of PVA-treated rabbit (No. 3242). The biocompatibility of high molar mass PVA needs to be studied in more detail.

## *5.4 Conclusion*

With extensive investigation on urinary extracted polymers after intraperitoneal administering of high molar mass PVA (195,000 g/mol) by using FTIR spectroscopy, $^{1}$H-NMR spectroscopy, TGA, and GPC, it is confirmed that the brownish urinary extracted sample contains PVA. The results of FTIR spectroscopy and $^{1}$H-NMR spectroscopy are in good agreement with each other. FTIR spectroscopy, $^{1}$H-NMR spectroscopy, and GPC traces of urinary extracted samples show some differences from that of original PVA. The lower thermal stability of excreted PVA detected in TGA/DTG curves also show some difference from the administered PVA. The changes caused by urine components are identified by the spectroscopic results of the control sample and the urine pigment. Other changes compared to the IR and $^{1}$H-NMR spectra of the control sample and the urine pigment are assumed to be produced by modification of the excreted PVA (physically or chemically). In histological tests, the appearance of nephrotoxicity and hepatotoxicity cannot be observed in the histological sections of PVA-195k treated rabbits by comparing with the control rabbits (non-PVA-treated). However, the slight vacuolation of hepatocytes can be detected in the liver of PVA-treated No. 3242 rabbit.

# Chapter 6

# 6 Summary

Since poly(vinyl alcohol) PVA has been discovered in 1924, it has already become one of the largest, water-soluble synthetic polymers produced in the world based on volume. The simple chemical structure and the high hydrophilicity provide PVA many properties as a promising biomaterial, such as biocompatibility, nontoxicity and noncarcinogenicity. The present work is mainly focused on applying fully hydrolyzed PVA to produce postoperative anti-adhesion agents and on the urinary excretion of intraperitoneally administered PVA.

Due to the polyhydroxy groups of PVA, the concentrated PVA aqueous solutions tend to gelate through hydrogen bonding. The kinetic aging behavior of fully hydrolyzed PVA aqueous solution has revealed that it is dependent on the concentration and molar mass of PVA. The variation of hydrodynamic radii ($R_h$) and dynamic rheological characteristics of aged PVA solutions were determined by dynamic light scattering and rheological measurement, respectively. The dynamic light scattering results indicate that PVA polymer chains undergo two main aggregation processes due to strong intramolecular and intermolecular hydrogen bonding over time: weakly bound supermolecular aggregation and thermostable paracrystal formation. These thermostable paracrystal structures can be destroyed by thermal treatment at 60 °C. The dynamic behavior of PVA aqueous solutions can be classified into three regions by increasing the concentration of PVA. Two critical concentrations affected the aging behaviour of PVA solutions: minimum aggregation concentration ($C_{agg.}$) and the critical concentration of sol-gel transition ($C_{gel}$). Below $C_{agg}$, all polymer chains act as isolated coils, no intensive formation of supermolecular structures can be detected below this threshold concentration in aged PVA aqueous solutions. When the concentration is higher than $C_{gel}$, the paracrystal aggregates become dominant, and form the strongly joined matrix of PVA gel. In the range of these two critical concentrations, the size of aggregated PVA chains increased with increasing concentration. DLS results exhibit two relaxation modes denoted as the fast and slow modes from the individual PVA coils and aggregated PVA chains, respectively. High molar mass PVA exhibits higher $C_{agg}$ and lower $C_{gel}$ than low molar mass PVA. $C_{agg}$ of low molar mass PVA-26k is located in the range of 1 ~ 2 wt-%. $C_{agg}$ of high molar mass PVA-195k is located in the range of 2 ~ 3 wt-%. Below $C_{gel}$, the aging process has no obvious effects on the shear viscous behavior of PVA solutions.

PVA cryogel is a thermoreversible physical hydrogel, which undergoes a phase transition from polymer aqueous solutions to partial crystallized polymer hydrogel by freeze/thawing treatment. Characteristic parameters of PVA cryogel obtained by freeze/thawing cycles were studied by using rheometer, $^{1}H$ pulse NMR spectroscopy and SEM. An increase in the storage modulus G´ and a decrease in the loss angle tan δ (< 1) indicated that PVA cryogels became more elastic with increasing number of freeze/thawing cycles. The NMR spin-diffusion data indicate that the mobility of all molecules decreases with increasing number of freeze/thawing cycles, since the crystalline regions act as crosslinks which connect the molecules into a spanning network. With increasing the number of freeze/thawing cycles, more PVA crystallites are formed in the PVA-rich phase inducing the release of bound water that also promoted the growth of ice crystals. SEM images reveal that the pore size of freeze-dried PVA cryogel increases with repeated freeze/thawing cycles due to an increase of crystallinity of PVA. PVA solutions pass from the state of viscous liquid to crosslinked elastic gel at a critical point known as gel point. The gelling of a system near the gel point combines the surface-wetting property of liquids with the cohesive strength of solids which gives it advantageous properties in powerful adhesives and reaches the maximum tack at the gel point. Physically crosslinked PVA hydrogel at the gel point is more biocompatible when used as the postoperative anti-adhesion agent by avoiding chemical crosslinking agents which could be toxic. The practical difficulty for the production of reproducible PVA cryogels at the gel point is caused by the water supercooling phenomenon. This can be improved by adding L-aspartic acid as water nucleation agent. L-aspartic acid can nucleate water at around -5 °C, and exhibits better water crystallization activity than silver iodine and long-chain aliphatic alcohols. The critical concentration of water crystallization activity of L-aspartic acid in 8.3 wt-% PVA-195k aqueous solution is 0.5 g/100 ml. L-aspartic acid saturates at this concentration. The existence of L-aspartic acid crystals is essential to water crystallization. The lower freeze temperature is responsible for more elastic PVA cryogels. The complex moduli G* of PVA cryogels prepared from one freeze/thawing cycle tend to reach a stable state beyond a critical freeze time. The PVA cryogels with stable G* are studied in order to find out which PVA cryogel sample is the closest to the sol-gel critical transition point by comparing tan δ and complex viscosity $\eta^*$. The samples were produced by freezing 8.3 wt-% PVA-195k aqueous solution (added with 0.5 wt-% L-aspartic acid) at different freeze temperatures (-5, -10, -13, -15, -20, and -32 °C) for 2 h and thawing at 20 °C for 2 h. The divergence of frequency-independence of tan δ and $\eta^*$ indicated the sol/gel phase transition area of 8.3 wt-% PVA-195k between freeze temperatures of -13 to -15 °C after 2 h freezing.

PVA cryogel produced at -13 °C exhibits good adhesive ability on glass slides. PVA cryogels produced at -15 °C beyond the gel point exhibit an elastic gel and loose the surface wetting properties of liquids completely. The properties of PVA cryogel near the gel point can be reproduced by freeze 0.5 g L-aspartic acid/100 ml 8.3 wt-% PVA 195-k at -13 °C for 2 h.

Polymeric microspheres have a variety of applications in medical areas since they provide a large surface area and can be handled easily. The full-hydrolyzed PVA powders are expected to have a better solubility in water than the original PVA flakes, and could be sprayed directly on the surfaces of injured tissues to form a separating barrier. PVA particles ranging from nanometers to micrometers (0.03 – 200 μm) can be obtained by using the emulsion-diffusion method. The mechanism of formation of PVA particles is based on the diffusion of solvent from the emulsified PVA aqueous droplets towards the acetone phase. During this process PVA chains are converted from the dissolved state into undissolved state and finally PVA forms the PVA particles. This is a simple, economical and efficient way to produce PVA particles. SEM pictures revealed spherical and nonporous surface morphology of PVA particles. The size of the final PVA particles is determined by the production of PVA/MCT oil emulsions. Proper molar masses and concentrations of PVA aqueous solution, speed of homogenizer and concentration of surfactants are the main factors in controlling the droplet size of PVA emulsion. In the present study, Imwitor 600 is the most efficient surfactant to stabilize PVA/MCT oil emulsions. An increase in homogenization speed and the decrease in viscosities of disperse and continuous phases allow the reduction of particle size. Low viscosity MCT oil phase and low dispersed-phase volume induced broader size distributions. SEM photographs of PVA particles before and after humidity treatment show that PVA particles can absorb water at room temperature and merge to form a membrane on the surface after drying. The wetted PVA powders behave like hydrogel and form a high viscous liquid under stirring at room temperature. DSC measurements of the dissolution temperature of PVA in water indicate that PVA-195k powders exhibit better water solubility than the original PVA flakes. The dissolution temperature of PVA-195k powder is at 79 °C (heating rate 1 °C/min), and it is thus shifted to lower temperatures by comparing to the dissolution temperature of original PVA flakes at 88 °C (heating rate 1 °C/min). PVA particles are expected to act as drug delivery systems and anti-adhesion barrier at the same time. Hemostatic drugs entrapped in the PVA particles could be a more effective application in postoperative anti-adhesion.

The fate of PVA in the body is mainly dependent on the molar mass and the route of administering. The renal excretion of PVA in the blood circulation prolongs with the increase of molar mass. Although the molar mass and the molecular size of PVA are above the size

limitation of the glomerular filtration barrier (non-filtrable if molar mass > 80,000 g/mol, radius > 4 nm), i. p. administered high molar mass PVA can still be excreted through the kidney. This phenomenon is studied in the present work by investigation on the renal excreted PVA. Three rabbits were i.p. administered using PVA-195k. The urine of these rabbits was collected for 28 days. The brownish extracts from these urine samples show the spectral characteristics of PVA in the investigations of GPC, $^{1}$H-NMR and FTIR spectroscopy. However, several obvious differences can be detected in GPC traces, IR and $^{1}$H-NMR spectra of urinary extracted samples compared to pure PVA. IR bands at 1649, 1542 and 1237 $cm^{-1}$, the proton resonances at chemical shifts of 1.2 and 0.8 ppm and the GPC trace peak at $V_E$ of 12 ml are attributed to the brownish urine pigment. This is confirmed by the control sample and the urine pigment sample. TGA/DTG curves reveal that the thermal stability and degradability of urinary extracted samples are lower than original PVA and control sample. The shift in the maximum rate of decomposition in the temperature range from 370 to 300 °C indicates the differences in renal excreted samples and pre-administered PVA. The intensity of the IR band at 850 $cm^{-1}$ and the integral ratio of the proton resonance of the $CH_2$ / CH of the polymer backbone decrease in excreted PVA. The reduction of $CH_2$ group intensity might indicate some impurities in the samples collected from rabbit's urine or some chemical reaction of PVA. The disappearance of the band at 916 $cm^{-1}$ and the proton resonance at 1.8 ppm could be attributed to excreted PVA. Again this can be the results of chemical reaction of PVA or of impurities that could not be separated during the dialysis procedure of the urine. The histological tests show that nephrotoxicity and hepatotoxicity cannot be observed in the histological sections of PVA-195k treated rabbits. However, the slight vacuolation of hepatocytes can be detected in the liver of PVA-treated No. 3242 rabbit. Further purification of the urinary extracted PVA is required for more detailed investigations on the renal excretion of administered high molar mass PVA.

# Chapter 7

# 7 Zusammenfassung

Seit Poly(vinylalkohol) PVA im Jahre 1924 erstmalig synthetisiert wurde, ist es bereits zu einem der größten, wasserlöslichen, synthetischen Polymerprodukte der Welt geworden. Die einfache chemische Struktur und die starke Hydrophilie von PVA resultieren in vielen Eigenschaften eines viel versprechenden Biomaterials, z.B. Biokompatibilität, Nicht-Toxizität und nicht-karzinogene Eigenschaften. Die vorliegende Arbeit befasst sich mit der Anwendung von vollständig–hydrolysiertem PVA zur postoperativen Adhäsionsverhinderung und die Untersuchung der Ausscheidung i.p. appliziertem PVA über die Niere.

Aufgrund der vielen Hydroxylgruppen entlang der PVA Kette tendieren konzentrierte wässrige PVA Lösungen zur Bildung von physikalischen Hydrogelen durch Wasserstoffbrückenbindung. Die kinetischen Untersuchungen zur physikalischen Alterung von wässrigen PVA Lösungen haben gezeigt, dass das Verhalten der Alterung von der Konzentration und der Molmasse des PVA abhängt. Die Variation der hydrodynamischen Radien ($R_h$) und die dynamisch rheologischen Eigenschaften der gealterten PVA-Lösungen wurden durch dynamische Lichtstreuung und rheologische Messungen bestimmt. DLS Ergebnisse deuten darauf hin, dass die PVA Polymerketten durch starke intramolekulare und intermolekulare Wasserstoffbrückenbindungen im Laufe der Zeit zwei unterschiedliche Aggregationszustände durchlaufen können: i) schwach gebundene supramolekulare Aggregatbildung und ii) thermostabile Parakristalle. Diese PVA Parakristalle können durch Erhitzen auf 60 °C zerstört werden. Das dynamische Verhalten der Alterung von wässrigen PVA Lösungen als Funktion der Polymerkonzentration lässt sich in drei Regionen einteilen. Es gibt zwei kritische Konzentrationen, die den Alterungsprozess der PVA-Lösungen beeinflussen können: die minimale Aggregationskonzentration ($K_{agg.}$) und die kritische Konzentration des Sol-Gel-Übergangs ($K_{gel}$). Unterhalb von $K_{agg.}$, liegen alle PVA Ketten unkonjugiert vor und keine größeren Aggregate als die einzelnen Polymerketten werden in den gealterten PVA-Lösungen beobachtet. Wenn die Konzentration höher als $K_{gel}$ ist, erfolgt eine Vernetzung zu geordneten PVA-Parakristallen, die dann eine starke Matrix des PVA-Hydrogels bilden. Im Bereich dieser beiden kritischen Konzentrationen steigt die Größe der PVA-Aggregate mit zunehmender Konzentration. DLS Ergebnisse zeigen zwei unterschiedliche Dynamiken, eine schnelle und eine langsame Diffusion, die den Einzelketten und den Aggregaten entsprechen. PVA höherer Molmasse in wässriger Lösung besitzt eine

höhere $K_{agg.}$ und eine niedrigere $K_{gel}$ verglichen mit PVA niedrigerer Molmasse. $K_{agg.}$ des PVA mit niedriger Molmasse (PVA-26k) liegt im Bereich von 1 bis 2 Gew.-%. $K_{agg.}$ des PVA mit hoher Molmasse (PVA-195k) liegt im Bereich von 2 bis 3 Gew.-%.

PVA-Kryogel ist ein thermoreversibles physikalische Hydrogel, das aus wässrigen Lösungen durch Gefrier-/Auftauzyklen hergestellt wird. Dabei kommt es zur Kristallisation des PVA, das dann nicht mehr wasserlöslich ist. Die Eigenschaften der PVA-Kryogele wurden mit Rheometer, Puls-NMR Spektroskopie und SEM untersucht. Eine Erhöhung des Speichermoduls G' und ein Rückgang des Verlustwinkels tan $\delta$ (< 1) sind das Ergebnis der gestiegenen Elastizität des PVA-Kryogels mit zunehmender Anzahl der Gefrier-/Auftauzyklen. Wegen der kristallinen Regionen, die als physikalische Vernetzungspunkte dienen, nimmt die Beweglichkeit der Moleküle mit zunehmender Anzahl der Gefrier-/Auftauzyklen ab. Dies wird anhand der Spin-Spin-Relaxation-NMR-Daten ($T_2$) bestimmt. Mit zunehmender Anzahl der Gefrier-/Auftauzyklen bilden sich mehr PVA Kristalle in der PVA-reichen Phase aus. Das dabei freigesetzte Wasser fördert das Wachstum von Eiskristallen in der PVA-armen Phase. SEM-Bilder zeigen, dass sich die Poren von gefriergetrocknetem PVA-Kryogel aufgrund der Zunahme der Kristallinität von PVA vergrößern.

Der Sol-Gel-Übergang ist bekannt als der Punkt, bei dem aus einer Flüssigkeit ein elastisches Gel gebildet wird. Das System am Gel-Punkt verbindet die starke Oberflächenbenetzung von Flüssigkeiten mit der Kohäsion von festen Stoffen und erreicht die maximale Adhäsion (Klebrigkeit). Als Material zur postoperativen Adhäsionsverhinderung, hat das physikalisch vernetzte PVA-Hydrogel eine bessere Biokompatibilität als ein chemisch vernetztes Gel, da die Zugabe von chemischen Vernetzungsagenzien vermieden werden kann. Das Wasserunterkühlungs-Phänomen, d.h. die behinderte Kristallisation des Wassers auch bei Temperaturen unter 0 °C, resultiert in einer praktischen Schwierigkeit bei der reproduzierbaren Herstellung von PVA-Kryogel am Gel-Punkt. Dieses Problem wird durch die Verwendung des effektiven Keimbildners - L-Asparaginsäure behoben. L-Asparaginsäure kann Eiskerne bei etwa -5 °C im wässrigen PVA-System bilden, und zeigt eine bessere Nukleierungswirkung bei der Wasserkristallisation als Silberiodid und langkettige aliphatische Alkohole. Die Aktivität von L-Asparaginsäure in 8,3 Gew.-% PVA-195k wässriger Lösung ist nur bei einer Konzentration höher als 0,5 g/100 ml gegeben. L-Asparaginsäure ist an dieser kritischen Konzentration in 8,3 Gwt.-% PVA-195k wässriger Lösung gesättigt. Die Kristalle der L-Asparaginsäure sind erforderlich um das Wasser zu kristallisieren. Je niedriger die Temperatur beim Gefrieren ist, desto elastischer wird das

PVA-Kryogel. Die komplexen Moduli G* des PVA-Kryogels, das nur durch einen Einfrier-/Auftauzyklus hergestellt wurde, erreicht einen stabilen Zustand nach entsprechenden kritischen Zeiten des Einfrierens. Das PVA-Kryogel, das im stabilen Zustand ist, wurde durch den Vergleich des tan δ und der komplexen Viskosität $\eta^*$ beschrieben. Die Proben wurden durch Gefrieren 8,3 Gew.-% PVA-195k wässriger Lösung (plus 0,5 Gew.-% L-Asparaginsäure) bei verschiedenen Temperaturen (-5, -10, -13, -15, -20 und -32 °C) für 2 Stunden und Auftauen bei 20 °C hergestellt. Die Divergenz der Frequenz-Unabhängigkeit von tan δ und $\eta^*$ deutet darauf hin, dass der Gelpunkt im Bereich des Einfrierens von -13 bis -15 °C aufgetreten ist. Das PVA-Kryogel, das bei -13 °C produziert wird, weist eine sehr gute Klebrigkeit auf dem Objektträger auf. Das PVA-Kryogel, das bei -15 °C hergestellt wurde, ist bereits ein echtes elastisches Gel und verliert die Benetzungseigenschaften von Flüssigkeiten vollständig. Die Eigenschaften von PVA-Kryogel am Gelpunkt können durch Einfrieren der 0,5 g L-Asparaginsäure/100 ml 8,3 Gew.% PVA-195k Lösungen bei -13 °C für 2 Stunden reproduziert werden.

Da Polymer-Mikrokugeln eine große Gesamtoberfläche haben und leicht behandelt werden können, gibt es eine Vielzahl von Anwendungen im medizinischen Bereich. Vom vollständig hydrolysierten PVA Pulver wird erwartet, dass es eine bessere Löslichkeit in Wasser als das ursprüngliche PVA-Granulat besitzt. Somit sollte es möglich sein, die PVA-Mikrokugeln direkt auf die Oberfläche des verletzten Gewebes zu sprühen, um eine physikalische Barriere zwischen den verletzten Geweben zu formen. Die PVA-Partikel wurden erfolgreich durch Emulsion-Diffusions-Methode generiert. Die Größe der Partikel variiert im Nanometer- bis Mikrometerbereich (0,03 - 200 μm). Die Herstellung von PVA-Partikeln basiert auf der Diffusion von Wasser aus dem wässrigen Tröpfchen in die Acetonphase, wenn die PVA/MCT-Öl-Emulsion in Aceton dispergiert wird. Die PVA-Ketten werden dabei von einem gelösten Zustand in einen festen Zustand des PVA-Teilchens umgewandelt. Es ist eine einfache, kostengünstige und effiziente Methode, um PVA-Partikel zu produzieren. SEM-Bilder zeigen, dass die Morphologie der PVA-Partikel sphärisch und nichtporös auf der Oberfläche ist. Die Größe der PVA-Partikel wird hauptsächlich durch die Herstellung der PVA/MCT-Öl-Emulsionen bestimmt. Die Molmasse des PVA und die Konzentration der wässrigen PVA-Lösung, die Geschwindigkeit des Homogenisators und die eingesetzten Tenside sind die wichtigsten Faktoren bei der Kontrolle der Tröpfchengröße in PVA/MCT-Öl-Emulsionen. In der vorliegenden Arbeit, ist Imwitor 600 als das effizienteste Tensid bestimmt worden, um die PVA/MCT-Öl-Emulsionen zu stabilisieren. Eine Zunahme der Geschwindigkeit des Homogenisators und die Erniedrigung der Viskosität der dispersen und

kontinuierlichen Phasen ermöglichen eine Verringerung der Partikelgröße. Eine niedrigviskose MCT-Öl-Phase und ein kleines Volumen der dispergierten Phase induzieren eine breitere Partikelgrößenverteilung. SEM-Aufnahmen der PVA Partikel vor und nach der Feuchtigkeitsbehandlung zeigen, dass die PVA Partikel das Wasser bei Raumtemperatur absorbieren und zu einer Membran auf der Oberfläche des Probenhalters nach dem Trocknen verschmelzen können. DSC-Messungen der Lösungstemperatur von PVA deuten darauf hin, dass das PVA-195k Pulver eine bessere Wasserlöslichkeit als das Original-PVA-Granulat besitzt. Die Lösungstemperatur von PVA-195k Pulver ist bei 79 °C und verschiebt sich zu niedrigeren Temperaturen im Vergleich zur Lösungstemperatur des PVA-Granulats (88 °C). Von PVA Partikeln wird erwartet, dass sie als Drug-Delivery-System und postoperative Adhäsionsverhinderung gleichzeitig verwendet werden könnten. Die PVA-Partikel, die blutstillende Medikamente enthalten, können eine effektive Anwendung in der postoperativen Adhäsionsverhinderung darstellen.

Der Weg des PVA im Körper ist vor allem abhängig von der Molmasse und der Applikationsform. Die Ausscheidung von PVA über die Niere verlängert sich mit der Erhöhung der Molmasse. Obwohl die Molmasse und die Größe der einzelnen PVA-Ketten bereits über der Durchlässigkeit des glomerulären Filters (nicht filtrierbar, wenn Molmasse > 80000 Dalton und Molekülradius r > 4,4 nm) liegt, ist zu beobachten, dass das hochmolekulare PVA nach intraperitonealer Applikation noch durch die Nieren ausgeschieden wird. Dieses Phänomen wird in der vorliegenden Arbeit durch die Untersuchung der PVA-Proben erforscht, die über die Nieren ausgeschieden wurden. Drei Kaninchen wurden mit intraperitonealer Applikation von 20 ml 10 Gew.-% PVA-195k Proben behandelt. Die Urine der behandelten Kaninchen wurden über 28 Tage hinweg gesammelt. Die bräunlichen Auszüge aus diesen Kaninchen-Urinen zeigen ähnliche Eigenschaften verglichen mit dem originalen PVA in den Ergebnissen von GPC, $^{1}$H-NMR- und FTIR-Spektroskopie. Allerdings gibt es einige offensichtliche Unterschiede in den GPC-Messungen und den FTIR- und $^{1}$H-NMR-Spektren. Die IR-Banden bei 1649, 1542 und 1237 $cm^{-1}$, die $^{1}$H-NMR-Spektren bei 0,8 und 1,2 ppm und die GPC-Messungen bei einem Elustionsvolumen von 12 ml sind das Ergebnis der bräunlichen Urinpigmente. Dies konnte durch Kontrollproben und dem Einsatz von Bilirubin (Das Urinpigment Urobilin ist nicht kommerziell verfügbar) festgestellt werden. Die Intensität der IR-Band bei 850 $cm^{-1}$ und das Integral der Protonenresonanz $CH_2$ zu CH haben sich in den über die Niere ausgeschiedenen Proben geändert. Die Verringerung der Intensität der $CH_2$-Gruppe deutet darauf hin, dass die dialysierten Proben nicht rein sind oder dass es zu einer chemischen Reaktion am PVA

gekommen ist. TGA/DTG-Kurven deuten darauf hin, dass die thermische Stabilität von Proben, die aus dem Urin erhalten wurde, niedriger ist als die des ursprünglichen PVA. Die Verschiebung der höchsten Geschwindigkeit der Zersetzung im Temperaturbereich von 370 bis 300 °C zeigt die Unterschiede zwischen dem Nieren-ausgeschiedenem PVA und dem originalen PVA auf. Die Signale der IR-Bande bei 1377 $cm^{-1}$ und der chemischen Verschiebung im NMR-Spektrum bei 0,8 ppm sind einer $CH_3$-Gruppe zuzuordnen. Diese $CH_3$-Gruppe stammt offensichtlich aus dem braunen Farbstoff des Urins. Die histologischen Untersuchungen zeigen, dass keine Nephrotoxizität und Hepatotoxizität in den histologischen Proben der mit PVA-195k behandelten Kaninchen beobachtet werden können. Jedoch ist eine leichte Vakuolisierung der Hepatozyten in der Leber von dem mit PVA-behandelten Kaninchen Nr. 3242 zu beobachten. Weitere detaillierte Untersuchungen der Urinausscheidungen erscheinen notwendig, um einen exakten Mechanismus der Ausscheidung von hochmolekularem PVA über die Niere zu identifizieren.

## Literature


[1] Haehnel W., Herrmann W. O., (to Consortium für Elektrochen. Ind. GmbH), Ger. Pat., **1924**, 450: 286

[2] Herrmann W. O., Haehnel W., Ber., **1927**, 60: 1658

[3] Staudinger H., Frey K., Stark W., Ber., **1927**, 60: 1782

[4] Finch C.A., Polyvinyl Alcohol—Properties and Applications, John Wiley & Sons, London, **1973**; Finch, C. A. Polyvinyl Alcohol—Developments, John Wiley& Sons, London, **1992**

[5] Tubbs R. K., Sequence distribution of partially hydrolyzed poly(vinyl acetate), J. Polym. Sci. A1 **1966**, 4: 623

[6] Nord F. F., Bier M., Timasheff S. N., Investigations on proteins and polymers. IV.1 Critical phenomena in polyvinyl alcohol-acetate copolymer solutions, J. Am. Chem. Soc., **1951**, 73: 289

[7] Ibrahim F. W., Correct determination of Staudinger's index (intrinsic viscosity) and of Huggins' constant, J. Polym. Sci., Part A, **1965**, 3: 469

[8] Schulz G. V., Blaschke F., Eine Gleichung zur Berechnung der Viscositätszahl für sehr kleine Konzentrationen, [Molekulargewichtsbestimmungen an makromolekularen Stoffen, IX], J. prakt. Chem., **1941**, 158: 130

[9] Sakurada I., Polyvinyl Alcohol Fibers, Marcel Dekker, New York and Basel, **1985**

[10] Thorpe F. G., 'Chemical modification of preformed polymers', in Newer Methods of Polymer Synthesis, edited by J. R. Ebdon, Blackie, Glasgow and London, Ch. 5, **1991**

[11] Lobova A. B., Goncharova N. A., Shamolina I. I., Volf L. A., Acetalization of polyvinyl alcohol fibres with glutaraldehyde, Fibre Chemistry, **1985**, 16:439

[12] Peppas N. A., 'Hydrogels of poly(vinyl alcohol) and its copolymers', in Hydrogels in Medicine and Pharmacy, Vol. 2, Polymers, CRC Press, Boca Raton, Fla., Ch.1, **1986**

[13] Hidber P. C., Graule T. J., Gauckler L. J., Competitive adsorption of citric acid and poly(vinyl alcohol) onto alumina and its influence on the binder migration during drying, J Am. Ceram. Soc., **1995**, 78: 1775

[14] Ochiai H., Shimizu S., Tadokoro Y., Murakami I., Complex formation between poly(vinyl alcohol) and borate ion, Polymer, **1981**, 22:1456

[15] Takamura T., Takayama G., Ukida G., Ultraviolet-induced crosslinking of poly(vinyl alcohol) in the presence of sensitizers , J. Appl. Polym. Sci., **1965**, 9: 3217

[16] Tanabe T., Nambu M., Medical material of polyvinyl alcohol and process of making, U.S. Patent no. 4,734,097, March 29, **1988**

[17] Peppas N. A., Hydrogels in Medicine and Pharmacy II, CRC Press, Boca Raton. FL **1987**

[18] Watanabe Y., Hamada N., Morita M., Tsujisaka Y., Purification and properties of a polyvinyl alcohol-degrading enzyme produced by a strain of *Pseudomonas*, Archiv. Biochem. Biophys. **1976**, 174: 575

[19] Peppas N. A., Turbidimetric studies of aqueous poly (vinyl alcohol) solutions, Makromol. Chem., **1975**, 176: 3433

[20] Lozinsky V. I., Cryotropic gelation of poly(vinyl alcohol) solutions, Russ. Chem. Rev., **1998**, 67: 573

[21] Lozinsky V. I., Galaev I. Y., Plieva F. M., Savina I. N., Jungvid H., Mattiasson B., Polymeric cryogels as promising materials of biotechnological interest, Trends Biotechnol. **2003**, 21: 445

[22] Lozinsky V. I., Korotaeva G. F., Vainerman E. S., Rogozhin S. V., Study of cryostructurization of polymer systems III. Cryostructurization in organic media, Colloid Polym. Sci., **1984**, 262: 617

[23] Wu K. A., Wisecarver K. D., Cell immobilization using PVA crosslinked with boric acid, Biot. Bioeng., **1992**, 39: 447

[24] Yokoyama F., Masada I., Shimamura K., Ikawa T., Monobe K., Morphology and structure of highly elastic poly(vinyl alcohol) hydrogel prepared by repeated freezing-and-melting, Coll. Poly. Sci., **1986**, 264: 595

[25] Lozinsky V. I., Domotenko L.V., Vainerman E. S., Mamtsis A. M., Rogozhin S. V., On the possibility of mechanodestruction of poly(Vinyl Alcohol) molecules under moderate freezing of its concentrated water solutions, Polym. Bull., **1986**, 15: 333

[26] Lozinsky V. I., Damshkaln L. G., Study of cryostructuration of polymer systems. XVII. Poly(vinyl alcohol) cryogels: Dynamics of the cryotropic gel formation, J. Appl. Polym. Sci., **2000**, 77: 2017

[27] Hassan C. M., Peppas N. A., Structure and applications of poly(vinyl alcohol) hydrogels produced by conventional crosslinking or by freezing/thawing methods, Adv. Polym. Sci. **2000**, 153: 37

[28] Peppas N. A., In: Peppas, N. A., (ed) Hydrogels in medicine and pharmacy, Polymers. CRC, Boca Raton, FL, **1987**, 2: 1–48

[29] Varfolomeev S. D., Rainina E. I., Lozinsky V. I., Cryoimmobilized enzymes and cells in organic synthesis, Pure Appl. Chem., **1992**, 64: 1193

[30] Lozinsky V. I., Plieva F. M., Poly(vinyl alcohol) cryogels employed as matrices for cell immobilization. 3. Overview of recent research and developments, Enzyme Microb. Technol., **1998**, 23: 227

[31] Peppas N. A., Stauffer S. R., Reinforced uncrosslinked poly(vinyl alcohol) gels produced by the cyclic freezing-thawing processes. J Cont. Rel., **1991**, 16: 305

[32] Kobayashi M., Oka M., Characterization of a polyvinyl alcohol-hydrogel artificial articular cartilage prepared by injection molding, J Biomat. Sci., Polym. Edi., **2004**, 15: 741

[33] Suzuki M., Hirasa O., An approach to artificial muscle using polymer gels formed by micro-phase separation, Adv. Polym. Sci., **1993**, 110: 241

[34] Paradossi G., Cavalieri F., Chiessi E., Spagnoli C., Cowman M. K., Poly(vinyl alcohol) as versatile biomaterial for potential biomedical applications, J Mater. Sci. Mater. Med., **2003**, 14: 687

[35] Oka M., Naguchi T., Kumar P., Ikeuchi K., Yamamuno T., Hyon S. H., Ikada Y., Development of an artificial articular cartilage, Clinical Materials, **1990**, 6:361

[36] Yamaoka T., Tabata Y., Ikada Y., Comparison of body distribution of poly(vinyl alcohol) with other water-soluble polymers after intravenous administration, J Pharm. Pharmacol., **1995**, 47: 479

[37] Noguchi T., Yamamuro T., Oka M., Kumar P., Kotoura Y., Hyon S. H., Ikada Y., Poly(vinyl alcohol) hydrogel as an artificial articular cartilage: Evaluation of biocompatibility, J Appl. Biomater., **1991**, 2: 101

[38] Kaetsu I., Radiation synthesis of polymeric materials for biomedical and biochemical applications, Adv. Polym. Sci., **1993**, 105: 81

[39] Nambu M., US Patent 4,472,542, **1984**

[40] Hyon S.H., Ikada Y., US Patent 4,663,358 **1987**

[41] Hassan C. M., Peppas N. A., Cellular PVA hydrogels produced by freeze/thawing, J Appl. Polm. Sci., **2000**, 76:2075

[42] Peppas N.A., Yang W.H., Polymer structural effects on the oxygen permeation of soft contact lens materials, Proc. IUPAC, **1980**, 27: 28

[43] Hyon S. H., Cha W. I., Ikada Y., Kita M., Ogura Y., Honda Y., Poly(vinyl alcohol) hydrogels as soft contact lens material, J Biomater. Sci. Polym. Ed, **1994**, 5: 397

[44] Devlin B.G., Tena, M.; Medina, N.A. U.S. Pat. Appl. Publ., **2005**, US 2005056954 A1 2005031.

[45] Kobayashi M., Chang Y. S., Oka M., A two year in vivo study of polyvinyl alcohol-hydrogel (PVA-H) artificial meniscus, Biomaterials, **2005**, 26: 3243

[46] Bray J. C., Merril E. W., PVA hydrogels for synthetic articular cartilage material, J Biomed. Mater. Res., **1973**, 7: 431

[47] Bao Q. B., Higham P. A., **1991** US Patent 5,047,055

[48] Sharma C. P., Surface modification: tissue compatibility towards the development of artificial skin, ICMR Project Report **1989**

[49] Peppas N. A., Benner R. E. Jr., Proposed method of intracopdal injection and gelation of poly (vinyl alcohol) solution in vocal cords: polymer considerations, Biomaterials, **1980**, 1: 158

[50] Mallapragada S. K., Peppas N. A., Colombo P., Modification of drug release profiles and swelling behavior in poly(vinyl alcohol) due to the presence of a crystalline phase, Polym. Mater. Sci. Engin. Proc., **1996**, 74: 416

[51] Takamura A., Ishii F., Hidaka H., Drug release from poly(vinyl alcohol) gel prepared by freeze-thaw procedure, J Contr. Rel., **1992**, 20: 21

[52] Peppas N. A., Scott J. E., Controlled Release from poly(vinyl alcohol) gels produced by freezing-thawing processes, J Contr. Rel., **1992**, 18: 95

[53] Qiu Y. , Park K., Environment-sensitive hydrogels for drug delivery, Adv. Drug Del. Rev., **2001**, 53: 321

[54] Langer R., Folkman J., Polymers for the substained release of proteins and other macromolecules, Nature, **1976**, 263:797

[55] Peppas N. A., Mongia N. K., Ultrapure poly(vinyl alcohol) hydrogels with mucoadhesive drug delivery characteristics, Eur. J Pharm. Biopharm., **1997**, 43: 51

[56] Weis C., Odermatt E., Kressler J., Funke Z., Wehner T., Freytag D., Poly(vinyl alcohol) membranes for adhesion prevention, J Biomed. Mater. Res. B, **2004**,70: 191

[57] Lozinsky V. I., Plieva F. M., Galaev I. Y., Mattiasson B., The potential of polymeric cryogels in bioseparation, Bioseparation, **2001**, 10: 163

[58] Chase H. A., Purification of proteins by adsorption chromatography in expanded beds Trends Biotechnol., **1994**, 12: 296

[59] Maeda H., Kawai T., Sekii S., Intra- and intermolecular hydrogen bonds in polyvinyl alcohol solutions, J. Polym. Sci., **1959**, 35: 288

[60] Ruiz J., MANTECO A., Cadiz V., States of Water in Poly(vinyl alcohol) Derivative Hydrogels, J Polym. Sci. : Part B: Polym. Phys., **2003**, 41: 1462

[61] Komatsu M., Takashi, T., Miyasaka K., Light-scattering studies on the sol-gel transition in aqueous solutions of poly(vinyl alcohol), J. Polym. Sci., Part B: Polym. Phys. **1986**, 24, 303

[62] Mrkvičková L., Prokopová E., Quadrat O., An investigation of aging poly(vinyl alcohol) solutions by the light scattering method, Colloid. Polym. Sci., **1987**, 265: 978

[63] Takigawa T., Urayama K., Masuda T., Critical behavior of the intrinsic viscosity of poly(vinyl alcohol) solutions near the gelation point. J. Chem. Phys., **1990,** 93: 7310

[64] Peppas N. A., Hansen P. J., Crystallization kinetics of poly(vinyl alcohol), J. Appl. Polym. Sci., **1982**, 27: 4787

[65] Frisch H. L., Simha R., In: F.R. Eirich Editor, Reology theory and applications Academic Press, New York **1956**

[66] Prichard J. G., (ed), Polyvinyl Alcohol, Basic properties and Uses, Gordon & Breach, London **1970**

[67] Gruber E., Soehendra B., Schurz J., Ordering in solutions of poly (vinyl alcohol) in water as detected by light scattering, J. Polym. Sci.: Polym. Symp., **1974**, 44: 105

[68] Mrkvičková L, Koňák, Č, Sedláček B In: Sedláček B (ed), Physical Optics of Dynamic Phenomena and Processes in Macromolecular Systems, Walter de Gruyter Co, Berlin New York P 353 **1985**

[69] Klenin V. J., Klenina O. V., Shvartsburd B. I., Frenkel S. Ya., Thermodynamic nature of supermolecular order in the aqueous solutions of poly (vinyl alcohol), J. Polym. Sci.: Polym. Symp., **1974**, 44: 131

[70] Liu M, Cheng R, and Wu C, Laser light scattering study of intrachain and interchain associations of poly(vinyl alcohol) in aqueous solution, Euro. Polym. J, **1999**, 35: 1907

[71] Peppas N. A., Turbidimetric studies of aqueous poly(vinyl alcohol) solutions, Makromol Chem., **1975**, 176: 3433

[72] Braun D., Walter E., Zur Alterung von wäßrigen Polyvinylalkohollösungen, Coll. Polym. Sci., **1980**, 258: 376

[73] Crowther N. J., Eagland D., The volumetric behaviour of poly(vinyl alcohol) in aqueous solution, J. Chem. Soc., Faraday Trans., **1986**, 82: 2791

[74] Kolnibolotchuk N. K., Klenin V. J., Frenkel S. Y., Formation of supermolecular order in aqueous solutions of poly(vinyl alcohol) in a turbulent flow, J. Polym. Sci.: Polymer Symposia, **1974**, 44: 119

[75] Kawai T., Freezing point depression of polymer solutions and gels, J Polym. Sci., **1958**, 32: 425

[76] Fletcher N. H., Nucleation and growth of ice crystals upon crystalline substrates, J. Phys., **1958**, 13: 409

[77] Budhlall B., Landfester M. K., Sudol E. D., Dimonie V. L., Klein A., El-Aasser M. S., Characterization of Partially Hydrolyzed Poly(vinyl alcohol). Effect of Poly(vinyl alcohol) Molecular Architecture on Aqueous Phase Conformation, Macromolecules, **2003**, 36: 9477

[78] Gavish M., Popovitzbiro R., Lahav M., Leiserowitz L., Ice nucleation by alcohols arranged in monolayers at the surface of water drops, Science, **1990**, 250: 973

[79] Damas C., Leprince T., Viet Ngo T. H., Coudert R., Behavior study of polyvinyl alcohol aqueous solution in presence of short chain micelle-forming polyols, Colloid. Polym. Sci., **2008**, 286: 999

[80] Liakakos T., Thomakos N., Finec P. M., Dervenis C., Young R. L., Peritoneal adhesions: etiology, pathophysiology, and clinical significance, Dig. Surg., **2001**, 18: 260

[81] Ellis H., The cause and prevention of post-operative intraperitoneal adhesions, Surg. Gynecol. Obstet., **1971**,133: 497

[82] Cheong Y. C., Laird S. M., Li T. C., Shelton J. B., Ledger W. L., Cooke I. D., Peritoneal healing and adhesion formation/reformation, Hum. Reprod. Update., **2001**, 7: 556

[83] diZerega G. S., Campeau J. D., Peritoneal repair and post surgical adhesion formation, Hum. Reprod. Update., **2001**, 7: 547

[84] Ellis H., Moran B. J., Thompson J. N., et al., Adhesion-related hospital readmissions after abdominal and pelvic surgery: a retrospective cohort study, Lancet, **1999**, 353: 1476

[85] Diamond M. P., Freeman M. L., Clinical implications of postsurgical adhesions, Hum. Reprod. Update., **2001**, 7: 567

[86] Hirsh J., Dalen J. E., Fuster V. et al, Aspirin and other platelet-active drugs: the relationship between dose, effectiveness and side effects, Chest., **1992**, 102: 327

[87] Becker J. M., Dayton M. T., Fazio V. W., et al; Prevention of postoperative: Abdominal adhesions by a sodium hyaluronate-based bioresorbable membrane: A prospective, randomized, double-blind multicenter study, J Am. Coll. Surg., **1996**, 183: 297

[88] Revuelta J. M., Garcia-Rinaldi R., Val F., Expanded polytetrafluoroethylene surgical membrane for pericardial closure: An experimental study, J Thorac. Cardiovasc. Surg., **1985**, 89: 451

[89] Li T. C., Cooke I. D., The value of an absorbable adhesion barrier, Interceed(R), in the prevention of adhesion reformation following microsurgical adhesiolysis, Obstet. Gynecol. Surv., **1995**, 50:190

[90] De Cherney A. H., di Zerega G. S., Clinical problem of intraperitoneal postsurgical adhesion formation following general surgery and the use of adhesion prevention barriers, Surg. Clin. North. Am., **1997**, 77: 671

[91] Enkins T. E., Stovall T. G., Warren J., Ling F. W., Meyer N. L., A histological evaluation of peritoneal injury and repair: implication for adhesion formation, Obstet. Gynecol., **1987**, 70: 225

[92] Waleed S. W., Shalaby Shalaby W., Chap. 13 Postoperative adhesion prevention, Absorbable and biodegradable Polymers, Page:191-204, **2004** by CRC Press LLC.

[93] Kobayashi M., Toguchida J., Oka M., Development of the shields for tendon injury repair using polyvinyl alcohol - hydrogel ( PVA-H), J Biomed. Mater. Res., **2001**, 58: 344

[94] Huang M. H., Yang M. C., Evaluation of glucan/poly(vinyl alcohol) blend wound dressing using rat models, International journal of pharmaceutics, **2007**, 346: 38

[95] Willcox P. J., Howie D. W., Jr., Schmidt-Rohr K., Hoagland D. A., Gido S. P., Pudjijanto S., Kleiner L. W., Venkatraman S., Microstructure of poly(vinyl alcohol) hydrogels produced by freeze/thaw cycling, J Polym. Sci., Part B: Polym. Phys., **1999**, 37: 3438

[96] Lozinsky V. I., Damshkaln L. G., Study of cryostructuration of polymer systems. XVII. Poly(vinyl alcohol) cryogels: dynamics of the cryotropic gel formation, J Appl. Polym. Sci. **2000**, 77: 2017

[97] Lozinsky V. I., Plieva F. M., Galaev I. Y., Mattiasson B., The potential of polymeric cryogels in bioseparation, Bioseparation, **2002**, 10: 163

[98] Lozinsky V. I., Galaev I. Y., Plieva F. M., Savina I. N., Jungvid H., Mattiasson B., Polymeric cryogels as promising materials of biotechnological interest, Trends Biotechnol. **2003**, 21: 445

[99] Ricciardi R., Mangiapia G., Lo Celso F., Paduano L., Triolo R., Auriemma F., De Rosa C., Lauprêtre F., Structural organization of poly(vinyl alcohol) hydrogels obtained by freezing and thawing techniques: A SANS study, Chem. Mater., **2005**, 17: 1183

[100] Auriemma F., De Rosa C., Triolo R., Slow crystallization kinetics of poly(vinyl alcohol) in confined environment during cryotropic gelation of aqueous solutions, Macromolecules, **2006**, 39: 9429

[101] Hassan C. M., Peppas N. A., Structure and morphology of freeze/thawed PVA hydrogels, Macromolecules, **2000**, 33: 2472

[102] Guenet J. M., Thermoreversible Gelation of Polymers and Biopolymers, Academic Press: San Diego, **1992**

[103] Stauffer D., Coniglio A., Adam M., Gelation and critical phenomena, Adv. Polym. Sci., **1982**, 44: 103

[104] Martin J. E., Adolf D., Wilcoxon J. P., Viscoelasticity of near-critical gels, Phys. Rev. Let., **1988**, 61: 2620

[105] Winter H. H., Mours M., Rheology of polymers near liquid-solid transitions, Adv. Polym. Sci., **1997**, 134: 165

[106] Barnes H. A., Hutton J. F., Walters K., An introduction to Rheology. Elsevier, Amsterdam, **1989**

[107] Bafna S. S., The precision of dynamic oscillatory measurements, Polymer engineering and science, **1996**, 36: 90

[108] Ross-Murphy S. B., Biophysical methods in food research, Critical Reports on Applied chemistry, vol. 5, ed. H. W.-S. Chan. SCI Blackwell, Oxford, **1984**, pp. 138

[109] Mezger T. G., The Rheology Handbook, 2nd Edition, Vincentz Network **2006**

[110] Mueller G. M., Wolber P. K., Warren G . J., Clustering of ice nucleation protein correlates with ice nucleation activity, Cryobiology, **1990**, 27: 416

[111] Mishima O., Stanley H. E., The relationship between liquid, supercooled and glassy water. Nature, **1998**, 396: 329

[112] Vali G., Principles of ice nucleation. In "Biological Ice Nucleation and its Applications" (Lee R. E., Jr., Warren G. J., and Gusta L. V., Eds.), pp. 1–28. APS Press, St. Paul **1995**

[113] Knight C. A., The Freezing of Supercooled Liquids, Van Nostrand, New York, **1967**

[114] Mutaftschiev B., *Handbook on Crystal Growth* (North–Holland, Amsterdam, **1993**), p. 187.

[115] Liu X. Y., Boek E. S., Briels W. J., Bennema P., Prediction of crystal growth morpholoy based on structural analysis of the solid-fluid interface, Nature, **1995**, 374: 342

[116] Debenedetti P. G., Metastable liquids: concepts and principles, Princeton Univ Pr, 1996 P

[117] Ning D., Liu X. Y., Controlled ice nucleation in microsized water droplet, Appl. Phys. Lett., **2001**, 81: 445

[118] Knight C. A., Ice nucleation in the atmosphere. Adv. Coll. Int. Sci., **1979**, 10: 369

[119] Zachariassen K. E., Kristiansen E., Ice nucleation and antinucleation in nature. Cryobiology, **2000**, 41: 257

[120] Vali G., Ice nucleation – theory. A tutorial, Presentation at the 1999 NCAR/ASP Summer Colloquium,. http://www-das.uwyo.edu/vali/.

[121] Fanks F., Nucleation of ice and its management in ecosystems, Phil. Trans. R. Soc. Lond. A, **2003**, 361: 557

[122] Mason B. J., Van den Heuvel A. P., The properties and behaviour of some artificial ice nuclei, Proc. Phys. Soc., **1959**, 74: 744

[123] Edwards G. R., Evans L. F., Effect of surface charge on ice nucleation by silver iodine. Transations of the Faraday Society, **1962**, 58: 1649

[124] Vonnegut B., The nucleation of ice formation by silver iodine, J Appl. Phys., **1947**, 18: 593

[125] Bryant G. W., Hallett J., Mason B. J., The epitaxial growth of ice on single-crystalline substrates, J Phys. Chem. Solids, **1960**, 12: 189

[126] Maki L. R., Gaylan E. L., Chang-Chien M., Caldwell D. R., Ice nucleation induced by Pseudomonas syringae, Appl. Microbiol., **1974**, 28: 456

[127] Gavish M., Popovitzbiro R., Lahav M., Leiserowitz L., Ice nucleation by alcohols arranged in monolayers at the surface of water drops. Science, **1990**, 250: 973

[128] Power B. A., Power R. F., Some Amino-Acids as Ice Nucleators, Nature, **1962**,194: 1170

[129] Gavish M., Wang J. L., Eisenstein M., Lahav M., Leiserowitz L., The role of crystal polarity in alpha-amino acid crystals for induced nucleation of ice. Science, **1992**, 256: 815

[130] http://msds.chem.ox.ac.uk/AS/l-aspartic_acid.html

[131] Winter H. H., Mours M., Rheology of polymers near liquid-solid transitions, Adv. Polym. Sci., **1997**, 134: 165

[132] Li L., Aoki Y., Rheological images of poly(vinyl chloride) gels. 1. The dependence of sol-gel transition on concentration, Macromolecules, **1997**, 30:7835

[133] Choi J. H., Ko S. W., Phase behavior and physical gelation of high molecular weight syndiotactic poly(vinyl alcohol) solution, Macromolecules, **2001**, 34: 2964

[134] Ohta S., Nitta N., Takahashi M., Murata K., Tabata Y., Degradable gelatin microspheres as an embolic agent: an experimental study in a rabbit renal model, Korean J Radiol. **2007**, 8: 418

[135] Edlund U., Albertsson A. C., Degradable polymer microspheres for controlled drug delivery, Adv. Polym. Sci., **2002**, 157: 67

[136] Flandroy P., Grandfils C., Daenen B., Snaps F., Dondelinger R. F., Jerome R., Bassleer R., Heinen E., In vivo behaviour of poly(D,L)-lactide microspheres designed for hemoembolization, J Contr. Rel., **1997**, 44:153

[137] Flandroy P., Grandfils C., Jerome R., Clinical applications of microspheres in embolization and chemoembolization: Comprehensive review and perspectives. In: Rolland A, editor. Pharmaceutical particulate carriers: Therapeutic applications. New York: Marcel Dekker. **1993**, pp 321.

[138] Jain J. A., The manufacturing techniques of various drug loaded biodegradable poly(lactide-co-glycolide) (PLGA) devices, Biomaterials, **2000**, 21: 2475

[139] Bodmeier R., Mcginity J. W., The preparation and evaluation of drug-containing poly(DL-lactide) microspheres formed by the solvent evaporation method, Pharma. Res., **1987**, 4: 465

[140] Quintanar-Guerrero D., Allémann E., Doelker E., Fessi H., A mechanistic study of the formation of polymer nanoparticles by the emulsification-diffusion technique, Coll. Polym. Sci., **1997**, 275: 640

[141] Clarke N., O'Connor K., Ramtoola Z., Influence of formulation variables on the morphology of biodegradable, Drug Devel. Indus. Pharm., **1998**, 24: 169
microparticles prepared by spray drying. Drug Development and Industrial Pharmacy 24: 169

[142] Giunchedi P., Conte U., Spray-drying as a preparation method of microparticulate drug delivery systems: An overview, STP Pharma. Sci., **1995**, 5: 276

[143] Cho J. S., Kwon A., Cho C. G., Microencapsulation of octadecane as a phase-change material by interfacial polymerization in an emulsion system, Colloid Polym. Sci., **2002**, 280: 260

[144] Nakashima T., Shimizu M., Kukizaki M., Particle control of emulsion by membrane emulsification and its applications, Adv. Drug. Deliv. Rev., **2000**, 45: 47

[145] Li J. K., Wang N., Wu X. S., Poly(vinyl alcohol) nanoparticles prepared by freezing-thawing process for protein/peptide drug delivery, J Contr. Rel., **1998**, 56: 117

[146] Pandolfe W. D., Homogenizers, in Encyclopedia of Food Science and Technology, John Wiley & Sons, New York, **1991**, 1413

[147] McCarthy W. W., Ultrasonic emulsification, Drug and Cosmetic Industry, **1964**, 94: 821

[148] Dickinson E., Stainsby G., Emulsion stability, in Advances in Food Emulsions and foams, Dickinson E. and Stainsby G., Eds., Elsevier Applied Science, London, **1988**, chap. 1.

[149] Loncin M., Merson R. L., Food Engineering: Principles and selected applications, Academic Press, New York, **1979**

[150] Kandori K., Applications of microporous glass membranes: Membrane emulsification, in Food Processing: Recent Developments, Gaonkar A. G., Ed., Elsevier Science, Amsterdam, **1995**

[151] Dickinson E., Stainsby G., Colloids in Foods, Applied Science Publishers, London, **1982**

[152] Walstra P., Emulsion stability, in Encyclopedia of Emulsion Technology, Vol. 4, Becher, P., Ed., Marcel Dekker, New York, **1996**a, chap. 1.

[153] Walstra P., Disperse Systems: Basic considerations, in Food chemistry, 3rd ed., Fennema, O. R., Ed., Marcel Dekker, New York, **1996**b, chap. 3.

[154] McClements D. J., Food emulsions: Principles, practice, and techniques, **1998**, CRC Press

[155] Cosmetic Ingredient Review (CIR), Final report on the safety assessment of polyvinyl alcohol, Inter. J Toxi., **1998**, 17: 67

[156] Weis C., Odermatt E. K., Kressler J., Funke Z., Wehner T., Freytag D., Poly(vinyl alcohol) membranes for adhesion prevention, J Biom. Mate. Res. Part B: Appl.Biom., **2004**, 70: 191

[157] Weis C., Odermatt E. K., A-Part Gel-an efficient adhesion prevention barrier, J Biom. Mate. Res. Part B: Appl.Biom., **2007**, 82: 174

[158] DeMerlis C. C., Schoneker D. R., Review of the oral toxicity of polyvinyl alcohol ( PVA ), Food Chem. Toxi., **2003**, 41: 319

[159] Hall C.E., Hall O., Polyvinyl alcohol nephrosis: relationship of degree of polymerization to pathophysiological effects, Proc. Soc. Biol. Med., **1963**,112: 86

[160] Tanaka T., Fujishima Y., Hanano S., Kaneo Y., Intracellular disposition of polysaccharides in rat liver parenchymal and nonparenchymal cells, Inter. J Pharm., **2004**, 286: 9

[161] Lukas G., Brindle S., Greengard P., The route of absorption of intraperitoneally administrated compounds, J Pharmacol. Exp. Ther., **1971**, 178: 562

[162] Lochhart R. D., Hamilton G. F., Fyfe F. W., Anatomy of the human body, J. B. Lippincott Company, Philadelphia, **1960**

[163] Romanes G. J., Editor: Cunningham's Textbook of Anatomy, Oxford Universit Press, London, **1964**

[164] Yamaoka T., Tabata Y., Ikada Y., Fate of water - soluble polymers administered via different routes, J Pharma. Sci., **1995**, 84: 349

[165] Tabata Y., Murakami Y., Ikada Y., Tumor accumulation of poly(vinyl alcohol) of different sizes after intravenous injection, J Control. Rel: official journal of the Controlled Release Society, **1998**, 50: 123

[166] Yamaoka T., Tabata Y., Ikada Y., Body distribution of intravenously administered gelatin with different molar masss, J Control. Rel., **1994**, 31: 1

[167] Besheer A., Maeder K., Kaiser S., Kressler J., Weis C., Odermatt E. K., Tracking the urinary excretion of high molar mass poly(vinyl alcohol), J Biomed. Mater. Res. Part B: App. Biomat., **2007**, 82: 383

[168] Venturoli D., Rippe B., Ficoll and dextran vs. globular proteins as probes for testing glomerular permselectivity: Effects of molecular size, shape, charge and deformability, Am J Physiol. Renal. Physiol., **2005**, 288: 605

[169] Bohrer M. P., Deen W. M., Robertson C. R., Troy J. L., Brenner B. M., Influence of molecular configuration on the passage of macromolecules across the glomerular capillary wall. J Gen. Physiol., **1979**, 74: 583

[170] Ohlson M., Sorensson J., Lindstrom K., Blom A. M., Fries E., Haraldsson B., Effects of filtration rate on the glomerular barrier and clearance of four differently shaped molecules, Am J Physiol. Renal. Physiol., **2001**, 281:103

[171] Yamaoka T., Tabata Y., Ikada Y., Comparison of body distribution of poly(vinyl alcohol) with other water-soluble polymers after intravenous administration, J Pharm. Pharmaco., **1995**, 47: 479

[172] Kaneo Y., Hashihama S., Kakinoki A., Tanaka T., Nakano T., Ikeda Y., Pharmacokinetics and biodisposition of poly(vinyl alcohol) in rats and mice. Drug Metabol. Pharmacok., **2005**, 20: 435

[173] Matsumura S., Steinbüchel A., Miscellaneous Biopolymers and Biodegradation of Synthetic Polymers, Weinheim, Germany: Wiley–VCH; **2003** Ch.15 Biodegradation of poly(vinyl alcohol) and its Copolymers, Vol. 9 p. 329

[174] Kawai F., Xenobiotic polymers. In: Imanaka T., editor. Great development of microorganisms. Tokyo:NTS. Inc; **2002**. p. 865

[175] Matsumura S., Tomizawa N., Toki A., Nishikawa K., Toshima K., Novel poly (vinyl alcohol) - degrading enzyme and the degradation mechanism, Macromolecules, **1999**, 32: 7753

[176] Chiellini E., Corti A., D'Antone S., Solaro R., Biodegradation of poly (vinyl alcohol) based materials, Prog. Polym. Sci., **2003**, 28: 963

[177] Watson C. J., Recent studies of the urobilin problem, J Clin. Pathol. **1963**, 16: 1

[178] http://en.wikipedia.org/wiki/Urobilin

[179] Yang Z., Si S., Fung Y., Bilirubin adsorption on nanocrystalline titania films, Thin Solid Films, **2007**, 515: 3344

[180] Yang B., Taylor R. C., Morris M. D., Wang X., Wu J., Yu B., Xu G., Soloway R. D., Normal coordinate analysis of bilirubin vibrational spectra: effects of intramolecular hydrogen bonding, Spectrochimica Acta, Part A: Molec. Biomo. Spect., **1993**, 49A:1735

[181] Wang Y., Ono H., Ikeda A., Hori N., Takemura A., Yamada T., Tsukatani T., 1H NMR and 13C NMR investigations of sequence distribution and tacticity in poly(vinyl alcohol-co-vinyl levulinate), Polymer, **2006**, 47: 7827

[182] Marstokk O., Roots J., Synthesis and characterization of hydrophobically modified poly(vinyl alcohol), Polymer Bulletin, **1999**, 42: 527

[183] http://academic.kellogg.cc.mi.us/herbrandsonc/bio201_McKinley/Urinary%20System.htm

[184] http://www.healthandage.com/html/res/primer/kidney.htm in Urinary System Accessed 2/3/2006.

[185]http://www.mc.vanderbilt.edu/histology/labmanual2002/labsection3/PancreasLiverGallbladder03.htm

[186] Silbernagl S., Despopoulos A.: Taschenatlas der Physiologie. Thieme: **2007**. Ch. 7. Kidney, P 148

[187] Praaning-van Dalen D. P., Brouwer A., Knook D. L., Clearance capacity of rat liver Kupffer, endothelial, and parenchymal cells, Gastroenterology, **1981**, 81: 1036

# Resume

## Personal Details

| | |
|---|---|
| First name, Surname | Yanjiao Jiang |
| Date and place of birth | Dec. 5th, 1978 in Nei Mongol, China |
| Nationality | Chinese |

## Education and employments

| | |
|---|---|
| March 2005- Present | Promotion in physical chemistry of polymer<br>Martin-Luther-Universität Halle-Wittenberg, Germany |
| 2002 - 2004 | Master of Biomedical Engineering<br>Martin–Luther University Halle-Wittenberg & FH Anhalt, Germany |
| 2001 - 2002 | Physician assistant in Jingang Clinic, Dalian, China |
| 1996 - 2001 | Bachelor of science in medicine<br>Dalian University, China |

## Statement

I hereby declare that this submission is my own work. I also certify that, to the best of my knowledge any help received in preparing this work, and all sources used, have been acknowledged in this Thesis.

**Yanjiao Jiang**